

Development of Flame Retardant Synthetic Fibres Using Novel Technologies

**Submitted by:
Ahilan Sitpalan**

A thesis submitted to the University of Bolton in partial fulfilment of the
requirements for the degree of Doctor of Philosophy

Institute for Material Research and Innovation,
University of Bolton,
Deane Road, Bolton, BL3 5AB,
United Kingdom

May 2014

Declaration of Authorship

I declare that the work described in this PhD thesis has not previously been presented in any form to the University or to any other institutional body, whether for assessment or for other purposes. Save for any express acknowledgements, references and / or bibliographies cited in the work, I confirm that the intellectual content of the work is the result of my own effort and of no other person.

Signed.....

Date.....

Acknowledgements

I would like to express my sincere thanks and gratitude to Professor Baljinder Kandola, my Director of Studies, for her guidance, enthusiasm and encouragement throughout this research project. I would also like to thank Professor Richard Horrocks for his valuable advice and support. Special thanks go to, Dr. John Milnes, Dr. Gill Smart, Mr. Akbar Zarei and Mr. Shahram Shafie for their overall support with the experimental procedure. I would also like to thank my colleagues and friends.

I am finally grateful to my loving family for the encouragement and unending support they have given me.

Finally, I would like to thank my wife, for her faith in me.

Abstract

The dispersion of clays at the nanometer level is known to induce a significant improvement in mechanical properties, flame resistance and barrier properties, compared with pure polymer. Application of ultrasound in polymer processing can be used to improve additive dispersion in polymer melts and solutions but may also initiate chemical reactions and modify the rheological and mechanical properties.

This thesis studies the effects of applying ultrasound to the molten fibre-forming polymers, polypropylene (PP) and polyamide 6 (PA6) containing nanoclay and flame retardant additives in order to assess whether improved dispersion generates improved flame retardant properties of derived fabrics.

Initially, ultrasound was applied to polypropylene during compounding with up to 5 wt% of ammonium polyphosphate (APP) as flame retardant and 2 wt% of Nanomer 1.3T (Nanocor Inc) as nanoclay. Two ultrasonic probes were used having a power of 50 W at 10, 30, 50 and 100% amplitude and 100W at amplitudes of 20 and 90%. For polyamide 6, the additive selected as flame retardant was aluminium phosphinate (Al-Phos) (Exolit OP 935, Clariant) and the nanoclays, Nanomer 1.3T and Cloisite 25A (Southern Clay Products, USA). Compounded polymer chips of the various formulations were extruded into filaments and tapes by using the Labline extruder and filaments were knitted into fabrics, where possible. Nanoclay dispersion was studied by optical imaging, scanning electron microscopic and electron dispersive scattering or SEM-EDS imaging in terms of silicon or Si-dot mapping for selected tape sample areas using the Datacell software. This calculated the number of Si dots and hence clay particles within a given area and a reduction in Si dot intensity following ultrasound exposure was taken as a measure of increased dispersion in that dispersed particles at the nanolevel were now no longer visible because they are beyond the resolution of the SEM instrument. Results indicated that the 100 W probe with 90% amplitude (ie 90 W power) showed greatest dispersion, so this power was selected for further study. Flammability of the PP tape samples was studied by limiting oxygen index and a modified UL-94 test. Results showed that, in the case of polypropylene, LOI values of samples containing clay and / or flame retardant were not significantly affected by additive or the presence of ultrasound. However, the modified UL-94 test showed that presence of nanoclay and / or flame retardant decreased burning rate which further decreased with

ultrasonification. Knitted fabrics were tested for vertical flame spread using the sample ignition test rig described in BS 5438 and results showed rate of burning and burning drips reduced for the ultrasonicated samples. In the case of PA6, the same 100W ultrasonic probe with 90% amplitude was used in the compounding stage. Of particular note was that the LOI of the PA6/25A(2 wt%)/Al-Phos(5 wt%) sample increased more than others and the same sample showed reduced flammability in the vertical flame spread test. However, quality of the filaments was poor due to the extrusion process and some of the samples failed to extrude using the Labline extruder. Subsequent work used the recently acquired Fibre Extrusion Technology (FET) extruder.

Based on the above results, PA6 containing 2 wt% of nanoclay and 10 wt% of same flame retardant was used with and without presence of 100 W ultrasonic power at 90% amplitude. Compounded samples were extruded into filaments and tapes and filaments were knitted into fabrics. Properties were characterised as above and the PA6/25A(2%)/AlPhos(10%) sample showed superior performance compared to the others in terms of reduced flammability and this performance was enhanced by ultrasonification during compounding. In order to assess whether chemical degradation had occurred during ultrasonification, the relative viscosity of these samples was measured using a ASTM D 445 Ubbelohde viscometer. The results indicated that chemical degradation is negligible or absent at the probe power used. Differential scanning calorimetry (DSC) was used to determine the degree of crystallinity and values decreased with the addition of clay and flame retardant and further decreased in samples exposed to ultrasound.

To extend this PA6 study, ammonium sulphamate (2.5 wt% AS) and dipentaerythritol (1 wt% DP) were selected as flame retardants and various nanoparticles including fumed silica were added. Samples were compounded and extruded into filaments and knitted into fabrics. Of special note is that the PA6/AS(2.5 wt%)/DP(1 wt%)/25A(2 wt%) combination was found to have superior tensile properties as filaments and significantly reduced flame spread in fabric form.

In the final part of the thesis, the effect of ultrasound during compounding on core-sheath bicomponent fibres containing combinations of nanoclays and flame retardants was considered. Results showed that the addition of nanoclay or flame retardant to either the core (C) or sheath (S) of the fibres slightly reduced their tensile modulus and elongation-

at-break values with respect to a control PA6-C/PA6-S yarn and there was little improvement observed with the ultrasound-exposed samples. The result of vertical flame spread testing showed that the PA6-C / PA6/25A(2 wt%)/Al-Phos (10 wt%)/90W-S sample was superior to all others in terms of their reduced flammability properties defined as minimal burn time, although its values of burn length, flame spread rate and number of drops were not the lowest values.

Table of Contents

Declaration of Authorship.....	ii
Acknowledgements.....	iii
Abstract.....	iv
Table of Contents.....	vii
List of Figures.....	xiv
List of Tables.....	xvii
Chapter 1: Introduction.....	1
1.1 General.....	1
1.2 Aim and objectives of the project.....	2
Chapter 2: Review of Literature.....	4
2.1 Introduction.....	4
2.2 Structure and properties of polypropylene.....	4
2.3 Structure and properties of polyamide 6.....	6
2.4 Role of flame retardants.....	8
2.5 Flame retardant mechanisms.....	9
2.5.1 Physical mechanism.....	9
2.5.1.1 By cooling.....	9
2.5.1.2 By forming protective layer.....	10
2.5.1.3 By dilution.....	10
2.5.2 Chemical mechanisms.....	10
2.5.2.1 Gas phase reactions.....	10
2.5.2.2 Condensed phase mechanisms.....	11
2.6 Reactive versus additive flame retardants.....	12

2.6.1 Typical FR additives for polypropylene fibres.....	12
2.6.2 Typical FR additives for PA6 fibres.....	13
2.7 The role of nanoclays as possible flame retardants.....	15
2.7.1 Nanoclay and nanocomposite structures.....	15
2.7.2 Potential of clay additives as flame retardants.....	17
2.7.2.1 Nanocomposite polypropylene studies.....	18
2.7.2.2. Nanocomposite polyamide 6 studies.....	19
2.8 Methods of improving nanoclay dispersion polymers.....	20
2.9 Ultrasound induced nanoclay dispersion.....	21
2.9.1 Aim and outline of ultrasound properties.....	21
2.9.2 Cavitation.....	22
2.9.3 Effects of ultrasound on polymers.....	22
2.10 The effects of ultrasound on nanoclay / polymer dispersions....	23
2.11 Bicomponent fibres.....	25
2.11.1 Bicomponent fibre configurations.....	25
2.11.2 Core - sheath bicomponent fibre spinning.....	26
2.11.3 Uses of core-sheath bicomponent fibres.....	26
2.11.4 Properties of core / sheath bicomponent fibres by incorporating additives.....	27

Chapter 3: Optimisation and Effects of Ultrasound on Polypropylene

(PP) Filament / Fabric Properties.....	28
3.1 Introduction.....	28
3.2 Experimental.....	28
3.2.1 Materials.....	29
3.2.2 Sample matrix.....	29
3.2.3 Compounding.....	31
3.2.4 Melt extrusion in to filaments / tapes.....	32
3.2.5 Fabric production.....	33
3.3 Characterisation for physical, mechanical and flammability properties	33
3.3.1. Morphology of tapes.....	33
3.3.2. Tensile properties.....	34
3.3.3 Thermal analysis.....	34
3.3.4 Limiting oxygen index of extruded strands and tapes.....	34
3.3.5 UL-94 of strands.....	34
3.3.6 Fabric testing.....	35
3.4 Results and discussion.....	36
3.4.1. Optimisation of ultrasonification conditions so as to achieve improved levels of nanodispersion and relate them to polymer performance.....	36
3.4.1.1 Characterisation of tapes.....	36
3.4.1.2 Quantification of particulate dispersion.....	41
3.4.1.3 Transmission electron microscopy.....	45
3.4.2 Thermal stability.....	46
3.4.3 Effect of ultrasonification on fibre properties.....	49

3.4.4 Effect of ultrasonification on flammability of strands and tapes	50
3.4.4.1 Limiting oxygen index	50
3.4.4.2 Flame spread and melt dripping of strands	52
3.4.5 Effect of ultrasonification on flammability of fabrics	54
3.5 Conclusions.....	56

Chapter 4: Optimisation and Effects of Ultrasound on Polyamide

6 (PA6) Filament / Fabric Properties.....	57
4.1 Introduction.....	57
4.2 Experimental.....	57
4.3 Samples.....	58
4.3.1 Materials.....	58
4.3.2 Sample matrix.....	58
4.3.3 Melt extrusion into filament / tapes and fabric production...	60
4.4 Results and discussion.....	60
4.4.1 Tensile properties.....	60
4.4.2 Characterisation of tapes.....	62
4.4.3 Limiting oxygen index	67
4.4.4 UL-94.....	69
4.4.5 Fabric flame spread.....	71
4.5 Conclusions.....	73

Chapter 5: Effects of Ultrasound on Polyamide 6 (PA6) Filament / Fabric

Properties.....	75
5.1 Introduction.....	75
5.2 The flame retardant potential of nanoclays dispersed with aluminium diethyl phosphinate in PA6.....	75
5.2.1 Materials.....	76
5.2.2 Sample matrix.....	76
5.2.3 Melt extrusion in to filaments / tapes.....	76
5.2.4 Fabric production.....	80
5.2.5 Characterisation of filaments/ Tapes / Fabric samples.....	80
5.3 Results and discussion.....	80
5.3.1 Tensile properties.....	80
5.3.2 Characterisation of tapes by SEM and EDS.....	81
5.3.3 Limiting oxygen index.....	88
5.3.4 UL-94 testing.....	89
5.3.5 Vertical fabric strip testing and flame spread.....	93
5.3.6 Effect of ultrasound on PA6 degradation.....	98
5.3.6.1 Relative viscosity measurements.....	98
5.3.7 Crystallinity.....	100
5.4 Conclusions.....	102

Chapter 6: Effects of Nanoparticles on the Flameretardancy of

Ammoniumsulphamate (AS) and Dipentaerythritol (DP)

Flame-Retardant System in Polyamide 6 (PA6)..... 103

6.1 Introduction.....	103
6.2 Experimental.....	104

6.2.1 Materials.....	104
6.2.2 Sample preparation.....	104
6.2.3 Melt extrusion in to filaments.....	106
6.2.4 Fabric production.....	106
6.2.5 Characterisation of samples.....	107
6.3 Results and discussion.....	107
6.3.1 Thermal stability of compounded samples.....	107
6.3.2. Limiting oxygen index of plaques and strands.....	109
6.3.3. UL 94 results for plaques.....	111
6.3.4. Tensile properties of filaments yarns.....	112
6.3.5 Fabric flame spread.....	114
6.4 Conclusions.....	121
Chapter 7: Bicomponent Filament / Fabric Properties.....	122
7.1 Introduction.....	122
7.2 Experimental.....	122
7.3 Samples.....	122
7.3.1 Materials.....	122
7.3.2 Sample matrix.....	123
7.3.3 Melt Extrusion into filaments.....	124
7.4 Results and Discussion.....	126
7.4.1 Morphology of bicomponent filaments.....	126
7.4.2 Tensile properties.....	131
7.4.3 Vertical fabric strip testing and flame spread.....	134
7.5 Conclusions.....	146

Chapter 8: Overall Conclusions.....	148
8.1 Ultrasonic exposure of fibre-forming polymers.....	148
8.1.1 Effects of ultrasound on clay dispersion and properties of polypropylene (Chapter 3)	148
8.1.2 Effects of ultrasound on the properties of polyamide 6 tapes and filaments (Chapter 4).....	150
8.1.3 Effects of ultrasound on the properties of Polyamide 6 filaments extruded using the FET extruder (Chapter 5)...	151
8.2 Effects of nanoparticles on the flame retardancy of the ammoniumsulphamate (AS) and dipentaerythritol (DP) flame-retardant system in polyamide 6 (PA6).....	153
8.3 Effect of dispersed nanoclays and flame retardants in Bicomponent fibres (Chapter 6).....	154
8.4 Suggestions for future work.....	156
References.....	157

List of Figures

Figure 2.1: Chemical structure of polypropylene	4
Figure 2.2: Crystalline and amorphous structure of polypropylene	5
Figure 2.3: Model of micro fibrillar arrangement of extended polymer chains in a fibre after drawing.....	6
Figure 2.4: Synthesis of polyamide 6 from caprolactum	7
Figure 2.5: Gas phase mechanism of flame retardant	10
Figure 2.6: Flame retardant mechanism of condensed phase	11
Figure 2.7: Layered structure of montmorillonite	16
Figure 2.8: Probable polymer / layered silicate structures.....	17
Figure 2.9: Organoclay dispersion and exfoliation during melt Processing.....	21
Figure 2.10: A variety of cross-sections for bicomponent fibres are possible.	26
Figure 3.1: The 50W Hielscher ultrasonic probe assembly fitted to the end of the Prism Eurolab Compounder barrel.....	32
Figure 3.2: Optical microscopic image of PP and PP/1.3T(2 wt%).....	37
Figure 3.3: SEM of PP and PP/1.3T(2 wt%).....	39
Figure 3.4: SEM of PP/APP(5 wt%) and PP/1.3T(2 wt%)/APP.....	40
Figure 3.5:EDS images representing Si dots of PP and PP/1.3T tapes, where clusters are circled.....	41

Figure 3.6: Si dots quantification using small area for measurement at one time (averaging the results for 12 samples) and using whole sample area.....	45
Figure 3.7: which indicates that nanoclay fundamental platelets are more separated, i.e., intercalated, in the presence of ultrasonification...	45
Figure 3.8: DTA and TGA curves of PP/1.3T and PP/1.3T/APP without/with ultrasonification.....	47
Figure 4.1: SEM images for PA6 tapes with PA6/1.3T(2 w%)/90W andPA6/Al-Phos(5 wt%).....	63
Figure 4.2: EDS images representing Si, P and Al dots.....	65
Figure 4.3: TEM micrographs of Cloisite 25A clay particles in polyamide6(PA6/25A(2wt%)) formulations without and with ultrasonification.....	66
Figure 4.4: Vertical flame test result for fabric at 0, 10 and 20 seconds after Ignition.....	73
Figure 5.1: Photographic, labelled diagrams of FET extruder.....	79
Figure.5.2: SEM images for compounded PA6 samples.....	83
Figure 5.3: EDS silicon dot images alongside their respective SEM images for PA6containing clay only (Si dots).....	84
Figure 5.4: EDS images phosphorus dots for PA6 samples containing Al-Phos (P dots).....	85
Figure 5.5: EDS images for aluminium dots for PA6 samples containing Al-Phos (Al dots).....	86

Figure 5.6: Snap shots of the flame spread experiment in 10s time interval	97
Figure 5.7: Volumetric pipette and Ubbelohde viscometer.....	98
Figure 6.1: Vertical flame test result for fabric in 5 seconds time interval after ignition.....	120
Figure 7.1: Symmetric diagram of bicomponent spinneret (Core / Sheath)	125
Figure 7.2: Optical images (40 x) of PA6 in sheath and PA6 / Al-Phos (10wt%) core bicomponent fibre.....	127
Figure 7.3: SEM and EDS images PA6 in sheath and PA6 / Al-Phos (10 wt%) Core bicomponent fibre.....	128
Figure 7.4: SEM and EDS images 20 µm Sheath (edge) of PA6 in sheath and PA6 / Al-Phos (10 wt%) bicomponent fibre.....	129
Figure 7.5: SEM and EDS images of 20 µm Core (Center) of PA6 in sheath and PA6 / Al-Phos (10 wt%) bicomponent fibre.....	130
Figure 7.6: Snap shots of the flame spread experiment to the samples not exposed to ultrasound during compounding.....	141
Figure 7.7: Snap shots of the flame spread experiment to the samples after exposure to ultrasound during compounding.....	145

List of Tables

Table 3.1: Polypropylene sample matrix.....	30
Table 3.2: Si dots quantification using small area of a sample and average of 12 separate areas.....	43
Table 3.3: Si dots quantification for whole sample area.....	44
Table 3.4 (a): DTA analysis of PP matrix samples.....	48
Table 3.4(b): TGA analysis of PP matrix samples.....	49
Table 3.5: Tensile properties for PP matrix samples.....	50
Table 3.6: LOI values of compounded PP strands.....	51
Table 3.7: LOI values of extruded tapes.....	51
Table 3.8: Details of UL94 result of strands.....	53
Table 3.9: Flame spread results of PP fabrics.....	55
Table 4.1: Sample matrix for PA6.....	59
Table 4.2: Tensile properties of PA6.....	61
Table 4.3: LOI result for PA6.....	68
Table 4.4: Flame spread UL94 result for compounded PA6 strands....	70
Table 4.5: Fabric flame spread.....	72
Table 5.1: Sample matrix for PA6.....	76
Table 5.2 Tensile properties for PA6 filament yarns.....	81
Table 5.3: Si dot quantitative analysis.....	87
Table 5.4: P dot quantitative analysis.....	87
Table 5.5: Al dot quantitative analysis.....	88
Table 5.6: Limiting oxygen index values of PA6 tapes.....	89
Table 5.7: Flame spread results after UL-94 testing in the	

vertical orientation.....	91
Table 5.8: Flame spread results after UL-94 testing in the horizontal orientation.....	92
Table 5.9: Flame spread results of PA6 fabrics.....	94
Table 5.10: Relative viscosity of PA6.....	99
Table 5.11: Relative crystallinities of PA6 formulations.....	101
Table 6.1: Composition of PA6 samples with AS, DP, nanoclays and silica.....	105
Table 6.2: Selected samples for the extrusion into filaments and knitting	106
Table 6.3: TGA-DTA data of PA6 blended with 2.5 wt% AS, 1 wt % DP and with nanoparticles (1 and 2 wt %).....	109
Table 6.4: Limiting oxygen index values of PA6 plaques and strands..	110
Table 6.5: Flame spread UL94 result for PA6 plaque samples.....	111
Table 6.6: Physical properties of undrawn filament yarn samples.....	113
Table 6.7: Physical properties of filament yarn after drawing with cool draw ratio of 1:2.....	113
Table 6.8: Fabric flame spread.....	115
Table 7.1: Sample matrix for PA6 bicomponent samples without application of ultrasonic energy.....	123
Table 7.2: Sample matrix for PA6 bicomponent samples with 100 W, 90% amplitude application of ultrasonic energy.....	123
Table 7.3: Extruder conditions.....	124
Table 7.4: Tensile properties of bicomponent fibres without application	

of ultrasound.....	132
Table 7.5: Tensile properties of bicomponentfibres with application of Ultrasound.....	133
Table 7.6: Flame spread results of bicomponent fabricswithout exposure to ultrasound.....	137
Table 7.7: Flame spread results ofbicomponent fabricsexposedto ultrasound during compounding.....	138
Table 7.8: Changes in the more importantburning parameters of samples in Table 7.7 compared with those of the PA6-C/PA6-S sample in Table 7.6.....	147

Chapter 1: Introduction

1.1 General

The expanding use of engineering, fibre-forming polymers in a wide variety of applications results in continued demand for improved thermal and mechanical properties. Many plastic materials have a tendency to start burning if they are exposed to fire. Fire kills and injures people and destroys materials. To prevent a fire from starting and continuing so called flame retardants are often used in polymers and textiles. It is clear that fire retardants are an important part of polymer formulations [1].

Of the conventional fire retardants, halogen-based compounds are both economical and effective in that they can enhance the fire retardancy of polymers without significantly degrading their physical properties, such as strength. However, it has been claimed that toxic species, which are generated during the combustion of halogen-containing polymers, could cause serious environmental contamination [2]. Therefore, developing halogen-free, low-smoke, and environmentally-friendly fire retardant polymers has become increasingly important in recent years [3]. However, the high levels of loading (15 wt% - 30 wt%) required can lead to processing difficulties and a decrease in physical properties of the polymers used in fibre applications. (In this whole thesis additives loading are in the weight percentage and denoted as %). Hence the development of newer and preferably more highly effective, fire retardants has prompted much attention during the last decade [4]. Fire retardants with very small particle size appear to offer significant advantages over conventional formulations because they offer the chance of improved dispersion, increased specific surface area, and in the case of fibre-forming applications, lower likelihood of blocking spinnerette orifices. Recently nano-scale layered metal materials, such as montmorillonite clays and layered double hydroxides (LDHs) have been shown to form so-called nanocomposite structures when dispersed in polymers which show certain superior properties [5-7]. In layered material / polymer systems, for example, improvements across multiple properties are typically achieved, such as flammability in terms of reduced heat release rates and also improved tensile behaviour, principally as increased modulus [8-9]. These improvements of polymer nanocomposites usually

originate from the change of the polymer structural nature surrounding the additive particle and depend strongly on the dispersion of these additives in the polymers [10-12]. Melt processing of the high viscosity, molten polymer / nanoclay mixtures is assisted by high shear mixing in the screw extruder [13-19] and internal static mixer, if fitted [17, 20-23]. Melt processing methods have environmental advantages as they are solvent-free processes. While organic chemical functionalization of the inorganic nanoparticles is used to enhance the dispersion of nanoclays in the polymer matrix, plasma processing has been shown to be similarly effective [24]. In-situ polymerization may also be utilized to keep the nanoclay particles dispersed in the polymer matrix as the viscosity changes from a low value for the molten monomers to the higher values associated with the final polymer [25]. Some other methods have been attempted for enhancing dispersion, like in-situ production melt intercalation extruders, ball milling techniques used but found limited success [26].

Recently, the use of high power ultrasound in extrusion processes has been proposed for improving dispersion of nanosize fillers [27] and increasing the levels of intercalation and exfoliation of nanoclays [28-29] in polymers with a residence time of ultrasonic treatment of only a few seconds. Ultrasound technology is considered not easy to use in industrial processes, since devices providing high sonic energy are not easy to manufacture [27]. However, based on research work already carried out and referred to in this work there are industrial processes, where low energy ultrasound is used [29, 30].

1.2 Aim and objectives of the project

The aim of this project is to develop novel methods of enhancing dispersion of nano / micro particulate flame retardants in polymers melts in order to enhance their flame retardant efficiency and so enable lower-than-conventional levels to be realised for achieving acceptable levels of flame retardancy in derived fibres and fabrics. To achieve this aim the following objectives were identified:

- (i) to investigate the effectiveness of applying ultrasound to the compounding stage in synthetic fibre-forming polymers, principally polypropylene (PP) and polyamide 6 (PA6), in order to define ultrasonification conditions which achieve optimal levels of nanodispersion of selected organically-modified nanoclays and conventional flame retardant additives;

- (ii) to determine the effects of ultrasonification on the resulting extruded filament tensile properties;
- (iii) to determine the flammability properties of extruded tapes, films and filaments as knitted fabrics;
- (iv) to correlate the ultrasonic variables with possible observed changes in flammable properties; and to extend the work to extrude bi-component fibres containing nanoclays and flame retardant particulates in core or sheath, each separately or together and assess the effects of flame retardant additive / nanoparticle location within the respective filaments.

Chapter 2: Review of Literature

2.1 Introduction

A considerable amount of research has addressed the preparation and properties of polymer–clay nanocomposites, which have been prepared by dispersing clay minerals into polymers. The incorporation of organoclays in a polymer promotes improvements in the properties of nanocomposites compared with virgin polymer. Several research groups have reported the effect of organoclays on the structural, mechanical and thermal properties of polyamide 6 (PA6) and polypropylene (PP) clay nanocomposite materials [31–36]. In recent years, parallel to the advances in polymer nanocomposite production, PA6 and PP organoclay nanocomposite filaments have also been investigated for their structural, mechanical and thermal properties. During fibre production, thermoplastic polymers have been preferentially treated with modified clay minerals at low concentrations of less than 5 wt% or even 2 wt% [37–38] and their level of dispersion help to improve properties, such as mechanical, thermal and flame retardant behaviour. To achieve the dispersion, several methods have been used, including the application of ultrasound to both polymer solutions and melts [39].

2.2 Structure and properties of polypropylene

Polypropylene is prepared by polymerisation of propylene ($\text{CH}_2=\text{CH}-\text{CH}_3$) [40] and belongs to the group of olefinic polymers, which can generally be described by the chemical structure as Figure 2.1.

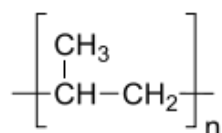


Figure 2.1: Chemical structure of Polypropylene [40].

Here n reflects the degree of polymerisation and the position of the methyl pendant group must be carefully controlled so as to yield an isotactic geometry in which the methyl

groups are attached on the same side of the polymer backbone otherwise the resulting material will not have acceptable mechanical properties [40].

The use of polypropylene (PP) materials in a wide range of applications is increasing rapidly, due to a favourable combination of processability, properties and price. A large fraction of the PP homo polymer production is converted into fibres by various melt spinning processes [40]. The relatively low melting point of polypropylene (160-170 °C) is an advantage and below this, PP fibres can be softened sufficiently to bond to one another without destroying fibre properties. Polypropylene fibres are composed of crystalline and non-crystalline regions [41]. Under slow cooling conditions, spherulites develop from a crystallizing nucleus and these can range in size from fractions of a micrometer to centimeters in diameter depending on the exact cooling conditions. The axis of the crystal unit cell is aligned radially and the chain axis is homogeneously distributed in planes perpendicular to this radial direction (Figure 2.2). Each crystal is surrounded by non-crystalline material [40]. Fibre spinning and drawing may cause the orientation of both crystalline and amorphous regions. If the extension is less than 0.5%, the spherulite deformation is elastic and no disruption of the structure occurs, otherwise spherulites are sheared apart and their component crystallites become highly oriented in the direction of the force and finally are converted to microfibrils (Figure 2.3). The degree of orientation achieved by drawing influences the mechanical properties of the filaments [41].

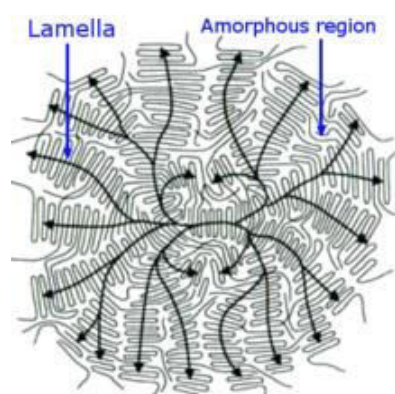


Figure 2.2: Crystalline and amorphous structure of polypropylene [40].

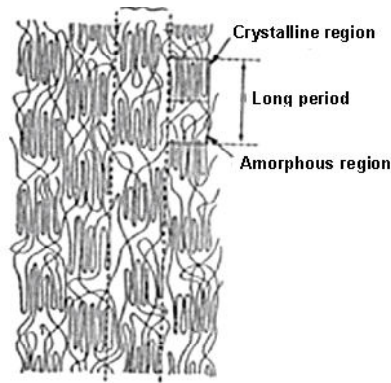


Figure 2.3: Model of micro fibrillar arrangement of extended polymer chains in a fibre after drawing [42].

PP fibres have many useful textile properties; however, one key disadvantage is that they are flammable. Fire hazard is a combination of many factors, including; ignitability, ease of extinction, flammability of the volatile products generated, rate of heat released, flame spread, smoke obstruction and smoke toxicity [43, 44]. The challenges of reducing the flammability of polypropylene are discussed in Sections 2.3, 2.4 and 2.5.

2.3 Structure and properties of polyamide 6

Polyamides, also known as nylons, are essentially man-made fibre. Polyamides were invented by Wallace Carothers in 1935 and gave rise to the commercial development of the world's first synthetic fibre, polyamide 6.6 (PA6.6) [45]. Later by 1939, the simpler polyamide 6 (PA6) was similarly developed in Germany, although was little known until the end of World War 2 [46]. Polyamides usually exhibit high modulus, toughness and strength, low creep [47]. Solid Polyamide 6 (PA6) is widely used in manufacturing of gears, fittings, bearings, electrical switches, bobbins, and connectors, power tool housings, wheelchair wheels and automotive cooling fans as well as being a significant fibre [48]. Polyamides or nylons 6.6 and 6 fibres are used in many applications, including fabrics, carpets, musical strings, and rope [48].

Polyamides consist of methylene segments $(CH_2)_n$ separated by amide units $(-CO-NH-)$ and are packed either parallel or antiparallel in their structure [49]. They are identified by means of a numerical system according to the number of carbon atoms present in the monomer structure [50] which may either comprise a single linear ω - amino acid (or its

lactam derivative) or a diacid and diamine. For PA6 the monomer would ideally be considered to be the 6 carbon-containing monomer $\text{NH}_2(\text{CH}_2)_5\text{CO.OH}$, but this tends to self react to form caprolactam $\text{[NH}(\text{CH}_2)_5\text{CO.O]}$.

Polyamide 6 is synthesized by a step-growth mechanism following the ring-opening polymerization of caprolactam as shown in Figure 2.4. This bulk polymerization process of polyamides is said to be a step-growth polymerization because each bond in the polymer is formed independently of the others [49, 50]. In the synthesis of polyamide 6, caprolactam is allowed to react with water, hydrolyzing a few percent of the caprolactam to ϵ -aminocaproic acid. Ring-opening polymerization of the caprolactam is initiated by the NH_2 groups of the ϵ -aminocaproic acid, and is followed by a polycondensation reaction of the NH_2 and COOH end groups of the low molecular weight product of the ring-opening polymerization reaction, resulting in a high molecular weight product. During the final step water is eliminated [51].

The most effective applications of polymers as engineering materials often require a better understanding and control of their surface mechanical properties. This is particularly relevant in the polymer fibre industry. The fibre-forming process controls the structure and the mechanical and thermal properties of the fibre [52]. Moreover, the mechanical properties of polyamides are dependent on the presence of water in the environment [53]. The decrease in the mechanical properties of polyamide fibres is due to the diffusion of water molecules into the amorphous regions of the semi-crystalline polymer leading to plasticisation and the rupture of intermolecular hydrogen bonds. Therefore, the environment has to be controlled [54].

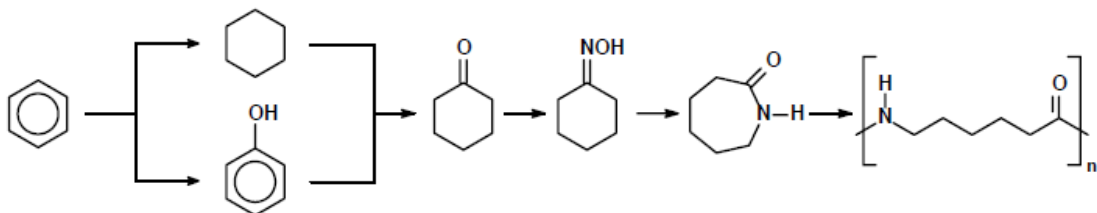


Figure 2.4: Synthesis of polyamide 6 from caprolactam [50].

2.4 Role of flame retardants

While the importance of textiles in domestic fires has been well-documented and discussed especially in the UK, in particular the hazard of flammable home furnishings and textile materials, their ease of ignition and their contribution to the development of a dwelling fire has been recognised for over 30 years [55]. These materials are considered as the main fire risks in dwellings and are often the first ignited materials [56].

To prevent polymers, whether in bulk or in fibre / textile forms, from burning, the presence of a flame retardant is one of the most effective methods, which improves resistance to ignition, reduces flame propagation rate, elevates ignition temperature and prevents continuous burning [57]. The major aim of using flame retardants is not to render the polymer completely non-flammable but to reduce flammability sufficiently to provide more time for people to escape from a fire and reduce death and injuries.

Using flame retardants for textiles goes back to historical times and, for example, in 1735 the use of where borax, vitreol and some other substances were patented for use in England for canvas and linen fabric [57]. Later, cotton was treated with boric acid to impart flame resistance. Around 1821, ammonium phosphate was introduced for linen and hemp [58]. Most flame retardant chemical formulations and additives were invented between 1950 and 1980 [59]. Since this time, new systems and many kinds of products were invented and developed for the rapidly growing and developing textile industry [58]. Since the 1990s, concerns over the toxicological and environmental consequences of using such chemicals on textile materials have been a major barrier to the development and application of flame retardant chemistry [59]. Nevertheless, flame retardants still continue to have a significant role as a consequence of upgrading additives and advanced chemicals to produce the most effective fire retardant material possible [58].

Today, one of the major concerns for textile industry is to meet the current flammability standards which determine regulations for fabric flammability and, because of environmental concerns during the last decade, extensive research has been going on to develop new products that balance the required level of flame retardancy with acceptable levels of environmental sustainability. For some textile applications, durability against water is another concern for manufacturers. While large volumes of FR chemicals used in

the textile industry are non-durable, which wash off completely after washing [60], if a fabric can survive water soaking to various degrees this creates a so-called a semi-durable flame retardant property. This type of treatment usually loses its effectiveness with alkaline detergent or hard water washing [61]. If fabrics can maintain their basic properties after multiple laundering cycles, these are called durable flame retardant fabrics [61]. An ideal FR fabric for textile applications must be comfortable, eco-friendly, durable and cost effective.

In 1912, the stannic oxide FR process was founded, and claimed that garments treated with stannic oxide can with stand two years of regular usage [62]. In the 1950s, research was undertaken to obtain durable FR cotton using various organophosphorus chemical procedures [62]. While the chemistries and technologies are outside the scope of this thesis, the development of these treatments for cotton has created a level of fabric flame retardancy which is used to compare flame retardant synthetic fibre and usually rely on additives introduced during the polymerisation or extrusion processes as explained in Section 2.5 below.

2.5 Flame retardant mechanisms

Flame retardant materials interfere with the combustion process during one or more of the stages of heating, pyrolysis, ignition or flame spread [63]. Flame retardants can act via physical or chemical mechanisms, and within these two general mechanisms, there are various potential ways in which flame retardants can react.

2.5.1 Physical mechanisms

2.5.1.1 By cooling

Here the FR additives can degrade endothermally which cools the substrate to a temperature which is below the temperature required for ignition and sustaining, pyrolysis and ultimately combustion [63, 64].

Typical examples are metal hydroxides such as aluminum hydroxide and magnesium hydroxide which on heating lose water thereby absorbing energy and also releasing water vapour into the flame thereby diluting the active species present.

2.5.1.2 By forming protective layer

These additives can form a physical shield with low thermal conductivity so reducing the heat transfer from the igniting source to the polymer surface thus reducing the degradation rate of the polymer and hence the fuel flow that feeds the polymer flame [64]. Typical examples here include borates which melt to form glassy surface layers and physical intumescent such as expandable graphite.

2.5.1.3 By dilution

The incorporation of inert substances like (fillers, such as talc and chalk) and additives dilutes the fuel in the solid and sometimes in the gaseous phases if water is given off, for example, so that the lower ignition limit of the gas phase is not reached [64].

2.5.2 Chemical mechanisms

Essentially, these mechanisms either involve the flame chemistry and so are termed gas phase retardants or influence the pyrolysis chemistry occurring in the polymer and so are referred to as condensed phase retardants.

2.5.2.1 Gas phase reactions

The radical mechanism of gas phase chemistry occurring within the polymer flame during combustion may be inhibited by use of suitable FR materials, therefore stopping the exothermic processes occurring in the flame and cooling down the system [65]. Typically, a flame retardant RX or HX may release X· radicals into the flame which then react with the highly reactive radicals HO· and H· responsible for the flame exothermic chain reactions (see Figure 2.5(a) and (b)) [65]. Typical of such flame retardants are the so-called halogen-containing ones in which either a chlorine (Cl·) or bromine (Br·) radical is released when heated [66].

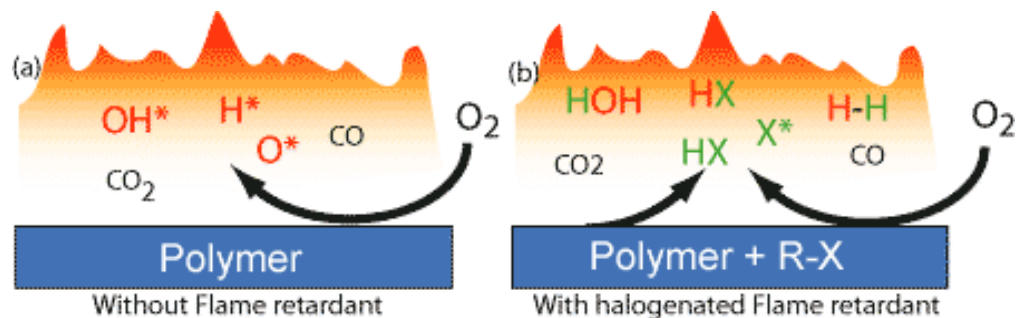


Figure 2.5: Gas phase mechanism of flame retardant [65].

2.5.2.2 Condensed phase mechanisms

Flame retardants can transform the polymer to a carbonaceous char (ie, charring) on the polymer surface in the first instance and then throughout its bulk are referred to as condensed phase flame retardants [67]. They act often by exerting a dehydrating action on the polymer chemical structure, especially if the polymer contains functional groups like –OH. These processes can also include or give rise to cross-linking processes which transform the polymer chains to a three-dimensional network. The char barrier acts as an insulating layer to reduce the heat transfer from the flame to the underlying polymer (see Figure 2.6) as well as reducing the concentration of volatile fuels [65, 68].

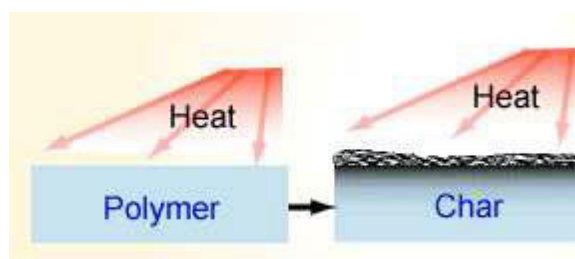


Figure 2.6: Flame retardant mechanism of condensed phase [65].

Typical examples include salts and organic derivatives of phosphorus which release phosphorus-containing acids on heating. These then can promote dehydration as well as cross-linking reactions which are often enhanced if nitrogen-containing species are also present. This phosphorus-nitrogen synergism is well-documented in the literature [67]. In polymers without pendant groups like –OH, condensed phase activity is more difficult to achieve. In polyamides, for example, which have a tendency to cross-link when exposed to temperatures above their melting points, condensed phase activity would result if the flame retardant increased this cross-linking tendency. Currently there are very few effective condensed phase flame retardants for polymers like PA6 and PA6.6 [59]. Polymers lacking any functional groups such as polypropylene may only be flame retarded with intumescent additives which comprise a char - forming component [59].

2.6 Reactive versus additive flame retardants

Chemical flame retardants are either additive or reactive. Reactive flame retardants are added during the polymerisation process and become an integral part of the polymer. The result is a modified polymer with flame retardant properties and a different molecular structure compared to the original polymer molecule. This enables the polymer to keep the flame retardant properties intact over time with very low emissions to the environment [68]. Reactive flame retardants are used mainly in thermosets, especially polyester, epoxy resins and polyurethanes (PUR) in which they can be easily incorporated [68].

Additive flame retardants are incorporated into the polymer prior to, during, or more frequently after polymerisation. They are used especially in thermoplastics. If they are compatible with the plastic they act as plasticizers, otherwise they are considered as fillers. Additive flame retardants are monomer molecules that are not chemically bound to the polymer. They may therefore be released from the polymer and thereby also discharged to the environment [69]. However, additive flame retardants are preferred for most thermoplastic polymers, including polypropylene and polyamides because of their ease of introduction and minimal effects on physical properties.

2.6.1 Typical FR additives for polypropylene fibres

Flammability of polypropylene polymer can be reduced by introducing flame retardants into the polymer [70-72]. Since there are environmental concerns about the use of halogenated compounds, halogen-free flame retardants are becoming increasingly popular. Ammonium polyphosphate (APP) is a conventionally-used phosphorous flame retardant and reacts to form the char as an insulating protective layer in polypropylene only if a char-forming additive is also present (eg dipentaerythritol) unless present at very high concentrations >30 wt% [73]. Magnesium hydroxide ($Mg(OH)_2$) is a widely used metal hydroxide flame retardant for non-charring polymers like PP but again require very high concentrations >50 wt%. It provides effective flame retarding effects by endothermically producing a residual insulating layer and releases water at about 360 °C which dilutes the flame [70]. Boron compounds such as zinc borate (Zb) decompose to release water at about 320 °C in a similar manner and create a glassy, insulating barrier [74]. Again, high concentrations are required.

Because of its wholly aliphatic hydrocarbon structure, polypropylene by itself burns very rapidly with a relatively smoke-free flame and without leaving a char residue unless one of the above flame retardant types is present [74].

Wang *et al.* looked into improving the fire retardancy of polypropylene (PP) using ammonium polyphosphate (APP) as a flame retardant additive [75]. The addition of 25 wt% of ammonium polyphosphate (APP) improve the flame retardancy but did not make any significant positive improvements in tensile properties [75]. While the introduction of conventional flame retardants into polypropylene is possible, as discussed above, high concentrations are required even for quite modest levels of flame retardancy in comparison with other fibre-forming polymers. Consequently for PP fibres, the only successful commercial flame retardants are based on bromine-containing agents although the currently most successful one is tris(tribromoneopentyl) phosphate manufactured by ICL Products as FR-370 [75]. An alternative system that can minimise the presence of bromine and remove the need for antimony III synergist is the Ciba hindered amine compound NOR 116 which is present only at about 5 wt% together with a conventional bromine-containing FR at concentrations below 10 wt% [75].

However, notwithstanding these problems, the challenge of flame retarding synthetic fibres in general is significantly higher than for bulk polymers because of their high surface area to volume ratio and the low acceptance to high filler loadings in the fibre production process.

2.6.2 Typical FR additives for PA6 fibres

A number of articles on flame retardant finishing of nylon fabrics based on various formulations have been published [76]. One difficulty in flame retardant addition to polyamide 6 is the high reactivity of the nylon melt which usually results in thermal degradation and difficulty of extrusion into filaments having the desired tensile properties. Both halogenated flame retardants, such as brominated flame retardants, formaldehydes and cyclic phosphoryl chloride derivatives have been used on nylon fabrics due to their effective flame retardancy although few have been commercially successful [76-78]. However, because of the increasing concerns about the possible hazard caused to the environment, phosphorus-based and intumescent flame retardant systems have attracted more recent attention for flame retardant treatment of nylon textiles [79-81].

Metal salts of dialkylphosphinates have been known to be effective flame retardants since the late 1970s [82]. More recently, Clariant investigated a wide spectrum of zinc, aluminum and calcium salts of dialkylphosphinates as flame retardants [83]. Aluminium diethyl phosphinates that were originally developed for polyamides, achieved UL 94-V0 ratings with, < 20 wt% additive [84].

Some of the key aspects of metal phosphinates are their high phosphorus content (~17%), good thermal stability (up to 320 °C) and lower affinity to moisture. Hydrolytic stability is especially important, since the release of phosphoric acids will promote degradation during extrusion. Schartel *et al.* investigated the mechanism of aluminium diethyl phosphinate as a flame retardant in poly(butylene terephthalate) [85]. The results indicate that diethyl phosphinic acid is released in the gas phase during the decomposition of the polymer and a UL 94-V0 rating could be achieved with a combined flame retardant loading of 20 wt%. It has been reported that metal phosphinates are also effective in polyamides [86]. To reach the desired effect, high loadings are sometimes necessary (up to 40 wt%), which often have a negative impact on the material and mechanical properties of the polymer [87].

Lewin *et al.* showed that small weight percentage (< 2 wt%) of ammonium sulphamate (AS) and dipentaerythritol (DP) yield high levels flame retardancy of polyamide 6 with V-0 ratings being achieved even at such low concentrations [88, 89]. High LOI values of 30 - 37 vol% were also observed [89]. These authors suggested that in the AS - DP system, the decomposition of the PA6 during the combustion is very rapid due to the strong, hydrolyzing, oxidizing and carbonizing action of the sulphuric acid formed from the AS during pyrolysis [88-91]. Furthermore, they explain this behaviour in terms of the very effective sulphation reactions with polyamide chains that can lead to both chain scission and char formation. Above 275 °C the AS can release ammonia and water. Also, AS can react with amine groups of PA6 and promote PA6-AS-DP cross-links and char formation. Introduction of 1 wt% of an organomontmorillonite clay (Cloisite 25A, Southern Clays Inc.) reduced LOI by 4 units while maintaining V-0, but on increasing to 3 wt%, the LOI reduced about 10 LOI units and reduced V-2 rating was recorded. This reduction in the FR performance was attributed to the large surface area of the exfoliated clay adsorbing and thus deactivating a part of the combined AS and DP flame retardant. Inclusion of an unfunctionalized clay (Cloisite Na⁺) did not exert the same effect because of its poorer dispersion and hence lower interaction with the FR system. Very recent work

undertaken at Bolton by Dr Jai Dahyia, assisted by myself, undertook a further study of this PA6-AS-DP system in order to confirm the results of Lewin *et al.* and provide a basis for the possible exploitation of this system for producing flame retardant PA6 fibres. This work has been published [92] and is more fully described and extended in Chapter 6.

2.7 The role of nanoclays as possible flame retardants

Most of the literature concerning layered materials as additives to polymers has focused on nanocomposites of two types of nanomaterials: (a) montmorillonite (MMT), a cationic clay [93-94] (b) layered double hydroxides (LDHs), sometimes referred to as hydrotalcite-like anionic clays [95-99]. Of relevance to this thesis are the montmorillonite clays and so these will be discussed in detail below.

Such nanoclays are derived from montmorillonite mineral deposits known to have “platelet” structures with average dimension of 1 nm thick and 70 to 150 nm wide [100]. They are known to enhance properties of many polymers when present only at low concentrations (eg 1-5 wt%), including polyamide 6 and PP, leading to better stiffness, thermal stability, barrier properties (to moisture, solvents, vapours, gases and flavours), reduced static generation and UV transmission in film and bottles; improved chemical, flame, abrasion resistance, and dimensional stability in injection moulded products [101]. Furthermore, polymers comprising nanoclays have higher heat distortion temperatures and improved fire performance in terms of reduced heat release rates [94, 101].

2.7.1 Nanoclay and nanocomposite structures

Cationic clay possess a 2:1 layered structure with an octahedral alumina layer located between two silicon tetrahedral layers (Figure 2.7). Its particles are essentially bundles of nanoclay sheets that are roughly 1 nm in thickness and 100–1000 nm in breadth [102]. For example, 8 μm clay particles has approximately 3000 nanoclay sheets of 1 nm thick and 20–200 nm in diameter [103]. Layered smectite-type MMT possesses a negative surface charge which is compensated by exchange of cations, such as Na^+ or Ca^{2+} . The adjacent layers are separated by a regular van der Waals gap. As organic cations exchange for exchangeable ions on the mineral surfaces, the cations are released into the solution. The organic cations may also enter into ion-exchange reactions with exchangeable cations

between the layer surfaces of the clay and hence may be modified to make the clay more compatible with a given polymer [104].

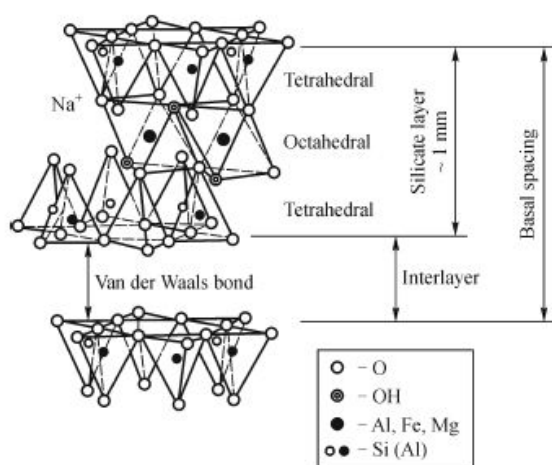


Figure 2.7: Layered structure of montmorillonite [104].

It is not easy to disperse nanolayers in most polymers due to the high face-to-face stacking of layers in aggregated platelets and their intrinsic hydrophilicity which make them incompatible with hydrophobic polymers [105]. Modification of clay layers with hydrophobic agents is necessary in order to render the clay layers more compatible with polymer chains. This is a surface modification which causes to the reduction of surface energy of clay layers and match their surface polarity with polymer polarity [105].

The surface modification of clay layers can be achieved through a cation exchange process by the replacement of sodium and calcium cations present in the interlayer space or clay galleries by alkylammonium or alkylphosphonium cations [106, 107]. In addition to the surface modification and increasing the hydrophobicity of clay layers, the insertion of alkylammonium or alkylphosphonium cations into the galleries causes an increase in the interlayer spacing which promotes so-called intercalation of polymer chains into the galleries during nanocomposite preparation (see Figure 2.8) [108]. Also the alkylammonium or alkylphosphonium cations can provide functional groups which interact with polymer chains and therefore increase the interfacial interactions.

The efficiency of organic modification by an ion exchange process in the increasing of interlayer spacing depends also on the surface charge of clay layers. The structure of the

organoclays and their effect on interlayer spacing also depends on the molecular size of organic cations [109]. Full separation of layers leads to exfoliation of the individual clay platelets and the formation of a stable nanocomposite, clay-polymer system as shown in Figure 2.8. [108]. Generally when the polymer chains cause an increase of interlayer spacing more than 80-100 Å (8-10 nm), the exfoliated structure is obtained [110,111].

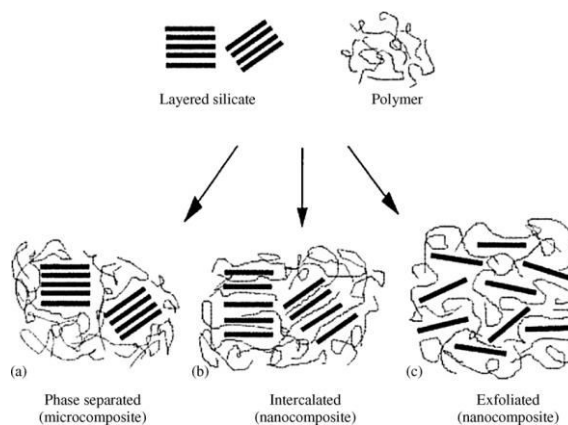


Figure 2.8: Probable polymer / layered silicate structures [108].

2.7.2 Potential of clay additives as flame retardants

The disadvantages of the additive flame retardant approach may be reduced with nano-level dispersion of the additive and due to high specific surface of a nanoclay particle and nano-scale interactions with the polymer matrix, even at very low concentrations, the often remarkable improvement of mechanical, thermal properties and flame retardancy compared to virgin polymer may be explained [112]. In recent years, great attention has been paid to clay nano-additives due to their low cost and large available quantity. The action of nanoclay when exposed to heat in a polymer is not simple but it is known that particles migrate to the molten polymer surface to form an excellent heat barrier and due to their catalytic effect on charring, they can reinforce the char structure [113].

Another mechanism proposed to explain the effects of layered materials on polymer combustion is the formation of a multilayered carbonaceous-layered structure on the surface of nanocomposites during the combustion [114]. The carbonaceous char may be reinforced by clay crystalline layers, creating an excellent physical barrier which protects

the substrate from heat and oxygen, and slows down the escape of flammable volatiles generated during polymer degradation [115].

The use of organoclays as precursors to nanocomposite formation has been extended into various polymer systems (thermoset and thermoplastic) including epoxy [116, 117], polyamides [118, 119], polyolefins [120-121], polystyrene [122] and others. While for true nanocomposite structures, the clay nanolayers must be uniformly dispersed and fully exfoliated in the polymer matrix, the dispersion of nanoparticles into the liquid matrix such as a polymer melt is a significant challenge.

2.7.2.1 Nanocomposite polypropylene studies

Several authors have reported the spinnability and mechanical properties of melt-spun nanocomposite fibres from polymer matrices of polypropylene [123, 124] and polyamide [125, 126].

Melt intercalation of polypropylene was studied in the past by many researchers, first in Toyota Research Center [127-129] and later by others [130-137]. In several of those papers [133-137] the achievement of partial or full exfoliation of montmorillonite (MMT) platelets was claimed. For example, Sharma and Nayak [138] obtained 95% enhancement in tensile strength and 152% in tensile modulus of clay modified polypropylene. Shariatpanahi *et al.* [139] observed improvements in tensile modulus and impact strength by 15 and 22%, respectively, with the addition of montmorillonite clay into polypropylene matrix via direct melt mixing method. Baniasadi *et al.* [140] reported the improvement of thermomechanical properties of nanocomposites by introducing small amount of clay into polymer matrix. Zhang *et al.* [141] successfully prepared polypropylene (PP) / organomontmorillonite (OMMT) nanocomposites via melt intercalation by using a conventional twin screw extrusion technique, and dispersed organoclay layers were observed in the PP polymer at the nanometre level. Wenyi *et al.* [142] investigated the dispersion of OMMT in a polypropylene matrix and observed an increase in melting and crystallinity point of the nanocomposites. Joshi *et al.* [143] characterized monofilaments which contain polypropylene / clay, and obtained improved tensile strength, modulus, thermal stability, and reduced elongation at break.

In terms of their potential as flame retardants in extruded filaments, Horrocks *et al.* [144] successfully produced polypropylene filaments that contained Cloisite 20A nanoclay, and observed that filament modulus was increased to some degree although flame retardant effects were minimal when present alone [144-145]. Subsequently, attempts were made to produce fire retardant polypropylene fibres and tapes by melt extrusion using different nanoclays i.e. Cloisite 20A, Cloisite 30B and Bentonite 107 alone [144] and in the presence of flame retardants [145]. To improve the efficiency of flame retardant systems in PP, other work has been undertaken to study the combined effects of certain fire retardants and some nanoclays [146] and these workers report that together they enhance the flame retardancy and mechanical properties at relative low clay loadings, generally less than 5 wt%, which make nanoclays ideal candidates for potential flame retardants [147].

2.7.2.2. Nanocomposite polyamide 6 studies

Over 20 years ago, researchers at Toyota have reported that nylon 6 / clay nanocomposites with good property could be prepared by using Na⁺-montmorillonite slurry without organic treatment [148], which provided an economical route to prepare nylon-6 / clay nanocomposites. The researchers observed a significant improvement in mechanical properties with clay loading of 4.2 wt%, with a 100% increase in modulus and more than 50% increase in strength properties. Further, an improvement in thermal properties was observed, with the increase of heat distortion temperature (HDT) by 80 °C compared to the pure polyamide 6. Vlasveld *et al.* observed that PA6 nanocomposites absorb water at a slower rate than the unfilled PA6 specimens [149]. The diffusion coefficients of the nanocomposites are reduced to approximately 1/3rd of the original value at the highest silicate loading. The conditioning temperature strongly influenced the time needed to reach saturation. The degree of exfoliation influenced the properties of PA6 nanocomposites. The modulus of the PA6 nanocomposites increased continuously with increasing silicate content and at around 10 wt%, the moduli of the Cloisite® and Nanomer® nanocomposites were twice that of the unfilled PA6 [149]. Maiti *et al.* studied the crystallization behaviour of nylon 6 nanocomposite, about 3.7 wt% of clay was enough to nucleate bulk sample. They reported 80 °C higher heat of distortion temperature (HDT) of nylon 6-clay composite more than that of control nylon 6 [150].

The flammability improvements for nanoclay addition are less advantageous when the more common empirical regulatory (pass / fail) flammability tests are conducted such as UL94 and standard national / international flammability tests) [151-153]. In specific cases, the nanoparticle addition can result in reduced flammability rating due to the melt viscosity increase preventing dripping as a mechanism of flame extinction (e.g, change UL94 rating from V-2 to HB (a fail)) [153]. The primary advantage for nanoclay addition for these tests generally involves reduction in the flame retardant additives that need to be incorporated to pass the specific test [153-155]. This has been observed in various nanoparticle modified composites including exfoliated clay with halogen-based flame retardants [156]. Studies involving polyamide 6 [157, 158] and polypropylene [159] yielded similar observations with regard to observed reductions peak heat release rate by cone calorimetry but no change in the total heat release with exfoliated clay addition.

A significant component to achieving these improvements in properties lies in the proper dispersion of the nanoparticles in the polymer matrix which is dependent upon a number of factors including the particle type, any functionalizing group, the polymer matrix and the method of processing used (and especially related shear present) [160].

2.8 Methods of improving nanoclay dispersion polymers

As stated above, optimising the dispersion and preferably fully exfoliating the layered structure of the nanoclay within a given matrix is crucial to improving the properties of a polymer. There is evidence that poorly dispersed clay more typical of microcomposite structures would not significantly improve flame retardancy [161]. Techniques such as in-situ polymerization, solution mixing, or sonication have been widely used to disperse nanoparticles in a liquid and the latter technique in particular seems to be relatively effective in obtaining an exfoliated structure [162, 163]. In this way the cluster structures are broken down, exfoliated and distributed homogeneously throughout the polymer. Stacked nanoclay platelets can also be sheared apart into smaller pieces and the interlayer spacing increased during extrusion process (Figure 2.9). In this study, ultrasonication was used to disperse the nanoclay in order to assess whether improvements in flame retardancy would result.

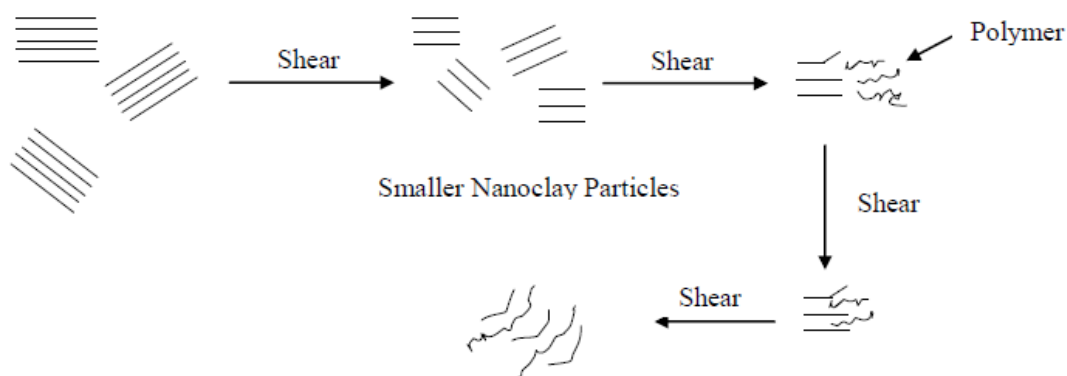


Figure 2.9: Organoclay dispersion and exfoliation during melt processing [164].

2.9 Ultrasound induced nanoclay dispersion

The attraction forces both within the clay layers as well as between adjacent layered particles must be overcome in order to break up and disperse the particles in the polymer melt. To overcome this problem, ultrasonic dispersion has been suggested and developed [165-167].

2.9.1 Aim and outline of ultrasound properties

Sound passes through an elastic medium as a longitudinal wave, i.e. as a series of alternating compressions and rarefactions. This induces the medium, in this case a polymer melt, to be displaced parallel to the direction of motion of the wave. Ultrasound is a sound wave with a frequency typically in the range of 20 kHz up to approximately 500 MHz [168]. Based on the applied frequency, the use of ultrasound can be broadly divided into two areas:

- Low intensity, high frequency ultrasound (2-500 MHz, $0.1-0.5 \text{ W/cm}^2$)
- Power ultrasound with a high intensity and a low frequency (20-900 kHz, $>10 \text{ W/cm}^2$)

The first type of ultrasound does not alter the state of the medium through which it travels and is commonly used for non-destructive evaluation and medical diagnosis [169]. This type of ultrasound cannot be used for inducing chemical reactions. Higher power

ultrasound uses the energy to create cavitation, which involves the formation, growth, and implosive collapse of microscopic bubbles in a liquid [170].

2.9.2 Cavitation

Ultrasound, when passing through a liquid medium causes not only mechanical vibration of the liquid but also generation of acoustic streaming within the liquid. If the liquid medium contains dissolved gas nuclei, which will be the case under normal conditions, they can be grown and collapse by the action of the ultrasound. The phenomenon of growth and collapse of microbubbles under an ultrasonic field is known as “acoustic cavitation” [171]. During the positive-pressure cycle the distance between molecules decreases, while during the negative pressure period the distance increases. At a sufficiently high intensity a critical distance between the molecules is exceeded during the negative pressure period, and a cavity is formed [168]. The acoustic pressure amplitude determines the growth of a cavitation bubble and consequently the nature of any chemical effects upon collapse [172]. When cavitation bubbles oscillate and collapse, several physical effects are generated such as the increased dispersion and ultimate exfoliation of clay particles [173]. Consequently, ultrasonication has been used as a technique to disperse nano-materials in different matrices [174-180].

It is usually achieved using an ultrasonic bath or an ultrasonic probe / horn also known as a sonicator. Standard laboratory sonicators run at 20–30 kHz with a power less than 100 W. The probe is usually made of an inert metal such as titanium. Most probes are attached with a base unit and then tapered down to a tip with a diameter from 1.6 to 12.7 mm [181]. This means that the energy from the wide base is focused on the tip, thus giving the probe high intensity.

2.9.3 Effects of ultrasound on polymers

The effects of ultrasound on polymers can be both physical and chemical. In recent years, there has been growing interest in using high intensity ultrasound in chemistry, for which the term sonochemistry is defined. Early chemical applications were in organic and organometallic synthesis [182, 183], but more recently it has been used for the modification and processing of polymers [184], nanoparticles [185] and other materials [186]. High intensity (or *power*) ultrasound has a number of effects which may be used to

control polymerization reactions or for post-synthesis modification and dispersion of particles.

Sonochemical effects can primarily be attributed to the generation in liquids of cavitation as discussed above. A typical cavity or bubbles grows to 50 – 100 μm in size before collapsing explosively as the sound wave propagates through the polymer. This can result in extreme conditions of temperature ($> 2000\text{ K}$) and pressure ($> 500\text{ bar}$) being generated [187, 188] over a micro second time scale. Moderately high concentrations of reactive intermediates such as radicals can be formed, either from breakdown of solvent or of added reagents [189]. The region of liquid around the bubble has high gradients of temperature, pressure and strain. The motion of fluid around the bubbles is rapid resulting in very efficient mixing and the formation of liquid jets due to shock waves emitted after final collapse. This rapid motion can result in effective strain degradation of polymer chains in the vicinity of cavitation bubbles [190] as long as they are over a certain molecular weight.

2.10 The effects of ultrasound on nanoclay / polymer dispersions

Dispersion is improved when shear is present and improvements in mechanical properties, for instance, have been widely cited for a number of polymer-nanoclay injection moulded and melt-spun fibre systems [191].

Some of the most commonly used methods for dispersing nanoparticles in polymers include mechanical mixing, magnetic stirring and sonication. Mechanical stirring, which is often applied to improve the homogeneity of the dispersion [192], cannot prevent the particles from reaggregating. Additional external forces are required [193, 194] and for several applications ultrasound has been proved suitable for dispersing particles homogeneously in a polymer [195]. Sanchez *et al.* applied ultrasonic waves with a frequency of 40 kHz, 100 V amplitude, and 300 W powers to intumescent / PP formulations [196]. They showed that processes involving a single screw extruder attached with the ultrasonic probe improved particle dispersion, with average particle sizes of around $1\mu\text{m}$ such that lower concentrations of additives could be used to obtain a V-0 rating according to the UL94 test. Improved thermal stability, flame retardant properties and mechanical properties were also achieved [196]. Swain SK and Isayev AI studied the

effect of continuous ultrasonic treatment during the melt intercalation of montmorillonite clay into high density poly(ethylene), HDPE, on the structural, mechanical, rheological and oxygen barrier properties. The authors evaluated the effect of the clay at different content (2.5, 5.0 and 10.0 wt%) and the nanocomposites were prepared using a single screw extruder attached with a ultrasonic slit die, operating at a frequency of 20 kHz and amplitudes of 5, 7.5 and 10 μm . High dispersion of clay in the HDPE matrix and higher complex viscosity due to ultrasonic treatment were reported. Mechanical properties were improved and oxygen permeability was substantially decreased after ultrasonic treatment [197]. Isayev *et al.* continuously attempt to improve nanoclay dispersion during melt processing of clays in polypropylene [198] and PA6 [199]. The last two works showed improvements by using ultrasonic power on various functionalized Cloisite® (Southern Clay Products Ltd, Austin, USA) montmorillonite clays, and while observing improvements in mechanical and barrier properties, they did not mention thermal behaviour and flammable properties.

In previous work at the University of Bolton, work with PA6 and PA6.6 produced films containing dispersed nanoparticles acting as char forming layers [153] demonstrated that interactions between nanoclays and flame retardants were influenced by the level of dispersion achieved. This work was extended to include melt compounded polypropylene / clay combinations in which it was observed that multiple compounding improved dispersion as observed by TEM and fibre physical properties [144, 145]. Application of compatibilised clay-graft PP mixtures and their dilution during melt extrusion also improved dispersion resulting in slight improvement of fire properties and reduced peak heat release rates of knitted fabric samples. However, the poor reproducibility of flammability of polypropylene filaments containing a clay and ammonium polyphosphate was related to poor dispersion [145]. While the above work and literature does not provide concrete evidence for the advantages of nano-level versus micro-level dispersion on thermal and flammability improvements, this study has a major aim to investigate further the effects of dispersion following ultrasonic application for both polypropylene and PA6 polymers derived filaments in the presence of clays and flame retardants.

The slight improvements that nanoclays in the presence of small amounts of flame retardants have on the flammability of polymers like polypropylene [59, 145, 153] and polyamide 6, these are insufficient to promote acceptable flame retardant properties. This

current study will hopefully demonstrate whether or not improved dispersion following ultrasonification can raise the levels of flame retardancy in PP and PA6 fibres containing both clays and flame retardants at combined levels < 10 wt%.

2.11 Bicomponent fibres

2.11.1 Bicomponent fibre configurations

Bicomponent fibre technology combines two polymers by co-extruding them to form a single filament with a designed cross-sectional arrangement [200]. Figure 2.10 shows common cross sections, which include side-by-side, sheath and core, segmented-pie, tipped trilobal and islands-in-the sea [201]. In this way, bicomponent fibres synergistically combine the properties of two individual polymers which is an attractive option for a variety of applications and provide significant flexibility in product design. Their unique characteristics are valuable for applications including sound and temperature insulation, fluid holding capacity, substrates for functional materials, sensors, tissue scaffolds, fuel cells, filters and drug delivery devices [202, 203].

Side-by-side is one of the common bicomponent cross-sectional configurations as depicted in Figure 2.10. This cross-section is separated into two hemispheres, where each hemisphere is a distinct polymer type, and there is an interface formed between the two immiscible components. Sometimes the side-by-side bicomponent fibres can be split into two fibres as well, So-called “segmented-pie” fibres are another type and made of segments of two polymers as in a “pie diagram”. The fibres with an 8-segmented pie or 16-segmented pie are the popular ones used as precursors for producing micro fibres of very fine denier [203]. To improve visual performance, especially in carpets where soil hiding properties are desirable, fibres with multiple lobes such as cross and the trilobal cross-section are possible. “Islands-in-the-sea” bicomponent fibres are another type and technically this is a complicated structure to make and use. In cross-section, they are areas of one polymer in a matrix of a second polymer. These types of bicomponent structure facilitate the generation of micro-denier fibres. Sheath-core bicomponent fibres are those fibres where one of the components (core) is fully surrounded by the second component (sheath) [203]. A highly contoured interface between sheath and core can lead to mechanical interlocking that may be desirable in the absence of good adhesion. Among these types of bicomponent structures the core-sheath is dominant in the tensile properties.



Figure 2.10: A variety of cross-sections for bicomponent fibres are possible. [203]

2.11.2 Core - sheath bicomponent fibre spinning

The most common way of production of core-sheath fibres is a technique, where two polymer liquids are separately led to a position very close to the spinneret orifices and then extruded in core - sheath form [204]. In the case of a concentric fibre cross-section, the orifice supplying the "core" polymer is in the center of the spinning orifice outlet and flow conditions of core polymer fluid are strictly controlled to maintain the concentricity of both components when spinning [205, 206]. Other methods of fibre production are based on several approaches which may give rise to either a symmetrical or asymmetrical cross-section. These include eccentric positioning of the inner polymer channel and controlling of the supply rates of the two component polymers [207], introducing a varying element near the supply of the sheath component melt [208], introducing a stream of single component merging with concentric core - sheath component just before emerging from the orifice and deformation of spun concentric fibre by passing it over a hot edge [209]. Other techniques to produce core - sheath fibres include coating of spun fibre by passing through another polymer solution [210] and spinning of copolymer into a coagulation bath containing another polymer [211]. Modifications in spinneret orifices enable one to obtain different shapes of core or / and sheath within a fibre cross-section. There requires to be considerable understanding and control of liquid polymer surface tensions, viscosities and flow rates of component melts during melt spinning of these fibres.

2.11.3 Uses of core-sheath bicomponent fibres

The first commercial application of core - sheath bicomponent fibre [212] has been used in carpets and upholstery fabrics. It appears that concentricity of the core plays an important role if the final product strength is the major concern, but if yarn bulkiness or texture is required at the expense of strength, the eccentric type of the fibre is used [213]. Other uses of core - sheath fibres derive from characteristics of the sheath helping to improve the

overall fibre properties. One core-sheath fibre has been reported [214] whose sheath is made of a polymer having high absorptive power for water, thereby having obvious advantages for use in clothing. Other core - sheath fibres showed better dyeability [215], soil resistance [216], heat-insulating properties [217], adhesion [217] etc. Production of ceramic core - sheath bicomponent fibres is another application utilizing the difference of sheath and core [218].

2.11.4 Properties of core / sheath bicomponent fibres by incorporating additives

Properties can be changed of core / sheath bicomponent fibres by incorporating additives to either core or sheath. The patent literature has many examples of the use of additives to modify fiber properties and this literature is outside the scope of this thesis although some examples will be given below.

The addition of carbon black produces conducting fibres that can be used for antistatic or current carrying purposes [219]. One early patent covers an antistatic core / sheath fibre with core containing carbon black and this fibre has been used in nylon carpeting to control static charges [220]. Addition of silica particles improved water repellency. Flame resistance has been obtained by addition of decabromobiphenyl ether and tin oxide [204]. Finally, a flame retardant fabric comprising bicomponent fibres having a sheath and a core, in which the sheath comprises a fully aromatic thermoplastic polymer with a Limited Oxygen Index of at least 26 and the core comprises a polypropylene has been reported [217].

There appears to be no literature regarding the addition of flame retardant and / or nanoclay in the core or sheath and their combined effect on fabrics comprising such the core-sheath bicomponent fibres. In this study, we develop a process to introduce them and use ultrasonic to improve additive dispersion. Flammable and tensile properties will be compared with the location of nanoclay and / or flame retardant with and without application of ultrasonic wave.

Chapter 3: Optimisation and Effects of Ultrasound on Polypropylene (PP) Filament / Fabric Properties

3.1 Introduction

In recent years, polymers with micro dispersed size particles have attracted attention by both academic and industrial researchers. Significantly improvement in the desired properties of nano-dispersed particles in polymers; such as their mechanical properties, optical properties, thermal properties and flame resistance has been reported [221]. With regards to flame retardance, wide ranges of flame retarding additives are used to improve the fire resistance of the polymer system. The most commonly used ones include bromine-containing species in combination with the synergist antimony III oxide and aluminium hydroxide (or aluminium trihydrate). However a large number of different kinds of phosphorus containing inorganic and organic flame retardants are available. In a previous preliminary study at Bolton, ammonium polyphosphate (APP) in the presence of a nanoclay was used as a flame retardant system for polypropylene fibres [145]. In this chapter, this work is extended to study the effects of ultrasound on improving the dispersion of both clay and APP flame retardant.

3.2 Experimental

Previous experience has shown that clay levels of 2 wt% are ideal to provide improved fire performance, but there were difficulties observed in extruding filaments and or knitting them into fabrics because of poor clay dispersion in the non-polar PP [145, 153, 222]. Due to these reasons, Nanomer 1.3T, a clay recommended by the company Nanocor Inc as nanoclay functionalised suitably for dispersion in polypropylene, and ammonium polyphosphate (APP) as flame retardant were selected for this study. Generally 25-30 wt% of APP gives a positive flame retardant effect on polypropylene but a negative effect on tensile properties, specially where filaments are concerned. In this work flame retardant (FR) levels have been maintained at 5 wt% where it is likely that only marginal levels of flame retardancy, such as reduced burning rates, will be achieved. In doing so, not only is

it anticipated that any degree of nanoclay-FR synergy present would be observed but also the total additive content will be < 10 wt% and so have minimal effect on tensile properties.

Furthermore, since the compounded polymer is to be extruded into filaments, it is essential to maintain all additives present at 10 wt% or less if their tensile properties are not to be compromised.

3.2.1 Materials

Filament grade polypropylene (PP), Moplen HP561R (LyondellBasell Polymers) having a melt flow index (MFI) 25 g / 10 min (230 °C / 2.16 kg) was used.

The nanoclay selected was Nanomer 1.3 T, (NanocorInc).

The grade of ammonium polyphosphate (APP) chosen was C60 from Budenheim having an average diameter of 7 µm, which is the finest particle size available commercially for this material.

3.2.2 Sample matrix

Table 3.1 shows the samples used for this work and their compositions as explained above. On the basis of above explanations, a nanoclay level of about 2 wt% is sufficient to improve fire performance.

Each formulation in Table 3.1 was compounded into polymer strands (St) for pelletising as chips (Ch). These chips were extruded into tapes (Tp) and filaments (Fil). Filaments were knitted into fabrics (Fab) if their strength allowed this to occur.

Table 3.1: Polypropylene sample matrix.

Sample	Without ultrasonic probe	50W Ultrasonic probe			100W Ultrasonic probe	
		20%, 10W	60%, 30W	100%, 50W	20%, 20W	90%, 90W
PP	Ch, St, Tp, Fil, Fab					
PP/1.3T (2 wt%)	Ch, St, Tp, Fil, Fab	Ch, St, Tp, Fil	Ch, St, Tp, Fil	Ch, St, Tp, Fil	Ch, St, Tp, Fil	Ch, St, Tp, Fil,Fab
PP/APP(5 wt%)	Ch, St, Tp, Fil, Fab					
PP /1.3T(2 wt%)/APP (5 wt%)	Ch, St, Tp, Fil, Fab					Ch, St, Tp, Fil,Fab

Notes: Ch=Compounded chips, St= Strands, Tp=Tape, Fil=Filaments, Fab=Fabric.

3.2.3 Compounding

Polypropylene and additives were hand-mixed in a plastic container for compounding in the Thermo electron Prism Eurolab 16 twin screw extruder, with or without application of ultrasound. The extruder having a 16 mm screw diameter, L/D = 24 both with and without ultrasound generation was used to compound different polymer mixture as shown in Table 3.1. Two ultrasound generators of 50 and 100 W, both at 30 kHz frequency were used. The internal diameters of probes were of 7 and 10 mm respectively. To introduce the probe into the molten zone of the twin-screw extruder, modification of the extruder was undertaken. A home-made head was made from a pressure transducer port drilled out to a 13 mm diameter hole to a depth sufficient to leave 0.5 mm thickness at the end and the top face drilled and tapped for 4 M4 blind holes. These were to be used to secure a stainless steel inverted top hat insert into which the probe could be introduced. The Figure 3.1 shows a photograph of the assembly. Two Hielscher 30 kHz ultrasonic generators having respectively 50 W and 100 W maximum outputs were used with 7 and 10 mm probes. Each generator / probe assembly was fitted into the specially machined plug located within the compounder housing at the end of the twin-screw high pressure region. The floor of the plug was 0.5 mm thick through which ultrasonic waves were transmitted into the polymer melt at the high pressure end of the barrel. Silicone oil was used to fill excess space between the plug interior and the probe and so maximise ultrasound transmission to the compounder.

To optimise the conditions for this experiments, the PP + Nanomer 1.3T (PP/1.3T) formulation was studied with 100 W and 50 W ultrasonic probes at varying intensities between 20 and 100%. The following conditions were used with assumed net beam wattages given in bold and in brackets:

- 50 W Probe, 20% amplitude (**10 W**)
- 50 W Probe, 60% amplitude (**30 W**)
- 50 W Probe, 100% amplitude (**50 W**)
- 100 W Probe, 20% amplitude (**20 W**)
- 100 W Probe, 90% amplitude (**90 W**)

Based on results discussed in a later section, the 100 W probe at 90% amplitude was used as an optimised condition for rest of the formulated PP samples.

The compounding extrusion rate for polypropylene was kept between 27.3 and 44.3 g/min. Temperatures in the six zones of the compounder were 150, 200, 205, 205, 200, and 200 °C. Samples were extruded as strands (diameter 1.8 ± 0.2 mm) into the water bath and pelletised into chips.

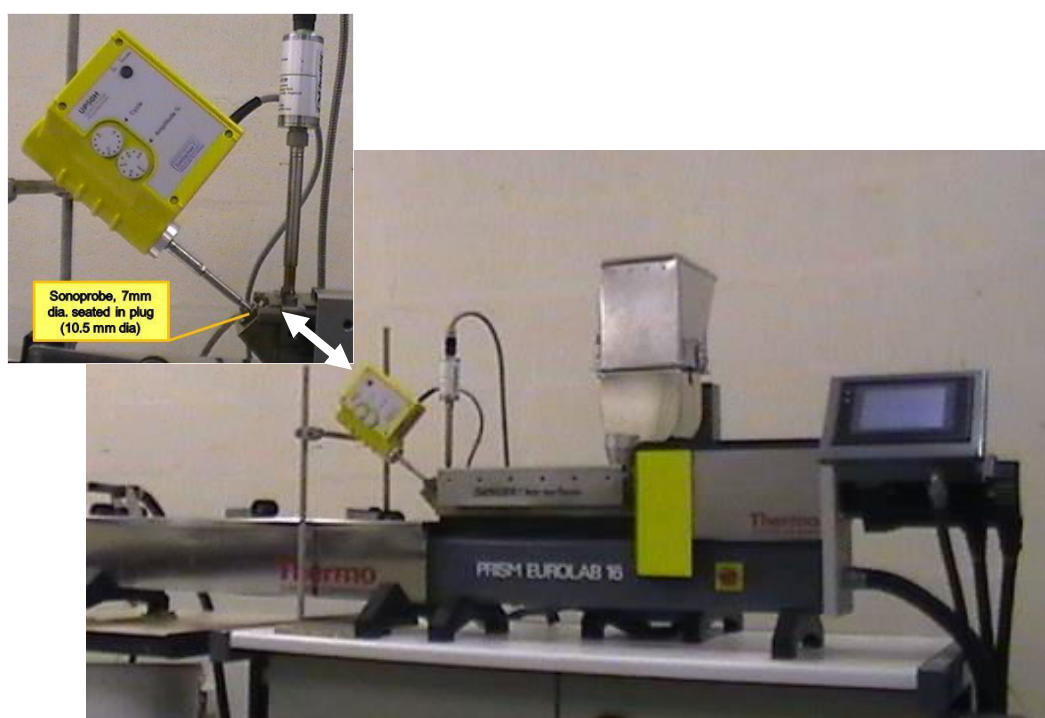


Figure 3.1: The 50W Hielscher ultrasonic probe assembly fitted to the end of the Prism Eurolab Compounder barrel.

3.2.4 Melt extrusion in to filaments / tapes

Compounded polymer pellets were extruded into filaments using a laboratory-sized Labline MK 1 single screw melt laboratory extruder. The screw has an internal diameter of 22 mm and three zones, a feed zone, a compression zone and a metering zone. The polymer is melted in the barrel as it is carried along by the screw through three different barrel temperature zones. Finally polymer is passed through the 40 hole spinneret to extrude into filaments. The filaments are passed through a set of six rollers, the first two of which are heated prior to traversing the faster drawing rolls. Finally these filaments are wound onto a cardboard cylinder. Following barrel region temperature conditions were used for polypropylene, barrel region 1: between 165 and 175 °C, barrel region 2: 190 °C,

barrel region 3: 200 °C, adaptor: 220 °C, die: 220 °C. Screw rotation was 20 rpm and extruded filaments were drawn at a draw ratio 1:3.

Polymer tapes (40 mm width, 0.6 ± 0.2 mm) were extruded by using a tape die in place of the spinnerette. These samples were used for microscopic investigation.

3.2.5 Fabric production

Filaments were knitted into fabrics using a small, hand, circular knitting machine, gauge E7. Fabric area densities of knitted fabrics depended on the gauge of the knitting machine. Some of the PP filaments were difficult to knit in to fabric due to coarse and brittle nature of filaments. Area densities of PP fabric ranged between 70 and 120 g/m².

3.3 Characterisation for physical, mechanical and flammability properties

3.3.1. Morphology of tapes

A Nikon Labophot 2 optical microscope with image capture by a JVC TK - C1381 video camera was used to capture microscopic images of the extruded tape samples. These images were captured at different magnification (10X to 300,000X) and were used to compare the morphologies of tapes. A Hitachi Technologies (Model 3400) SEM with 100 nm resolution was used for scanning electron microscopic imaging. All images were obtained at 15 kV. Secondary electron and X-ray detectors were used to get EDS images of silicon, phosphorus, and aluminium containing particulates. Quantitative analysis of the EDS images was carried out by Datacell software. A selected area on the EDS image of each sample was for the quantitative analysis and colour coding on the software was used to select Si dots on the image. This helped to measure area of the dots, number of dots and selected area of the sample.

Transmission electron microscopy (TEM) of selected samples was undertaken at the Department of Material Science, University of Oxford using a JEOL JEM-2000 FX Analytical instrument with a beam voltage of 200 kV on samples of 100 nm thick with a maximum resolution of 0.3 nm was used to obtain transmission electron microscopic (TEM) image.

3.3.2. Tensile properties

Tensile testing of the filaments was conducted using a Textechnic Statimat M test with a gauge length of 100 mm, load cell 10 N and test speed of 300 mm/min. The reported values of linear density, modulus, tenacity and elongation-at break are the respective average values taken from ten tests.

3.3.3 Thermal analysis

Thermal stabilities of samples were investigated using thermogravimetric analysis (TGA) and differential thermal analysis (DTA). Combined TGA-DTA was performed using a TA system STD 2690 instrument under air atmosphere (gas flow 100 ml/min) and heating rate of 10 °C/min, using a sample size of 10-15 mg.

3.3.4 Limiting oxygen index of extruded strands and tapes

Limiting oxygen index (LOI) is the minimum concentration of oxygen, defined in a flowing mixture of oxygen and nitrogen just support flaming combustion of the material. The oxygen concentration of the mixture used in each test is increased or reduced by a small amount until the required concentration is reached. All the tests were carried out by using Fire testing technology Limiting Oxygen Index apparatus on extruded strands and tapes using the standard ASTM 2863 test procedure by using a Fire Testing Technology (FTT) digital oxygen Index testing equipment. LOI values for each sample were measured. In addition to the standard LOI measurement, time to extinguish the flame and burnt length of the samples were also noted, from which burning rate could be calculated.

3.3.5 UL-94 of strands

UL-94 is the most commonly used test for measuring the ignitability and flame spread of a sample, exposed to a small flame [224]. The standard UL-94 test is performed on a polymer sample (125 mm x 13 mm, with various thicknesses up to 13 mm) suspended vertically above a cotton patch. The sample is subjected to two 10 s flame exposures with a calibrated flame in a unit which is free from the effects of external air currents. After the first 10 s exposure, the flame is removed, and the time for the sample to self-extinguish is recorded. Cotton ignition is noted if polymer dripping ensues; dripping is permissible if no cotton ignites. Then the second ignition is performed on the same sample, and the self-extinguishing time and dripping characteristics recorded. If the plastic self-extinguishes in less than 10 s after each ignition, with no dripping, it is classified as V-0. If it self-

extinguishes in less than 30 s after each ignition, with no dripping, it is classified as a V-1, and if the cotton ignites then it is classified as V-2. If the sample does not self-extinguish before burning completely, it is classified as failed (F).

In the horizontal version of UL-94, a specimen is supported in a horizontal position and is tilted at 45°. A flame is applied to the end of the specimen for 30 seconds or until the flame reaches the 10 mm mark. If the specimen continues to burn after the removal of the flame, the time for the specimen to burn between the 10 and 40 mm marks and burnt length are recorded. If the specimen stops burning before the flame spreads to the 40 mm mark, the time of combustion and damaged length between the two marks is recorded.

In this work a modified UL-94 test method was used. The samples used are in the form of strands (125 mm long, ~2 mm diameter), and tapes (125 mm x 5 mm x ~0.4 mm). In both cases flame is applied to the bottom of the specimen while the top of the burner is located 10 mm away from the bottom edge of the specimen. The flame is applied for 10 s and removed. The after flame time as T_1 (the time required for the flame extinguish) is measured. After extinction, the flame is applied for another 10 s and the after flame time T_2 is then measured. At the end of experiment the total burn length is also measured for the calculation of burning rate.

3.3.6 Fabric testing

Fabric samples were mounted on the vertical strip sample holder for flame spread test using the test rig describe in test 1 (190 x 70 mm) of BS 5438. The fabric was marked at 10, 60, 120 and 180 mm intervals. On ignition of the sample, the first 10 mm sample burning was not taken in to account and a time of burning was recorded from the 10 mm point onwards. The standard flame was applied for 10 s as specified in the test to the bottom edge of the fabric. A video film recorded the whole burning process. Times to reach 60, 120 and 180 mm marks and / or flame out were noted. Molten drops were collected and their masses were measured. The values were used to interpret how much mass of sample has burnt. Three replicates of each sample were tested and results averaged.

3.4 Results and discussion

3.4.1 Optimisation of ultrasonification conditions so as to achieve improved levels of nanodispersion and relate them to polymer performance

As mentioned in Section 3.2.3, to optimise the ultrasonification conditions, the PP + Nanomer 1.3T (PP/1.3T) formulation was used with the 100 W and 50 W ultrasonic probes at varying intensities between 20 and 100%.

Holes / microvoids were observed in the films of all polypropylene samples, including the control PP. The formation of such holes in cast or extruded films has not been mentioned in the literature but they appeared to form at the boundaries of large spherulitic crystallites. Generally in commercial polypropylene film extrusion, rate of extrusion and cooling rates are many times faster than in these experiments; so they would contain very small spherulites which would be easily sheared during any subsequent drawing. The holes suggest that in these thin samples significantly-sized spherulites were formed and stresses arising at their boundaries could cause the observed hole formation. A brief reference to this condition is also mentioned in the literature [223]. However, the frequency of holes seemed to be change with change in ultrasonic probe power. At higher magnifications the clay particles could be observed.

3.4.1.1 Characterisation of tapes

Figure 3.2 shows optical microscopic images for control PP and PP/1.3T(2 wt%) samples. The holes are clearly seen as black spots in the lowest magnification (40X) films and the spherulitic structures present are evident in the higher magnification micrographs. Figure 3.3 and 3.4 show SEM images for all PP samples. These images do not show any specific detail apart from the inter-spherulite holes and spherulitic structures. These two features were observed in all formulated films.

Figure 3.5 shows EDS images of samples as Si maps in defined areas. Si dots seemed to be more uniformly distributed when the ultrasound probe was used. For the PP/1.3T(2 wt%) unsonicated sample, there are some clusters observed, which decrease in frequency with ultrasonic probe usage. At the 50 W probe condition, the frequency of clusters decreased with increasing amplitude. No clusters were observed when the 100 W ultrasonic probe is used. It must be emphasised that as particle dispersion improves, so the

average particle size will reduce and at a critical level reduce below the resolution of the SEM, the resolution of the SEM is greater than 100 micron. Thus improved dispersion will be accompanied by an observed reduction in particle dimension and a reduction in number of observed particles per unit area.

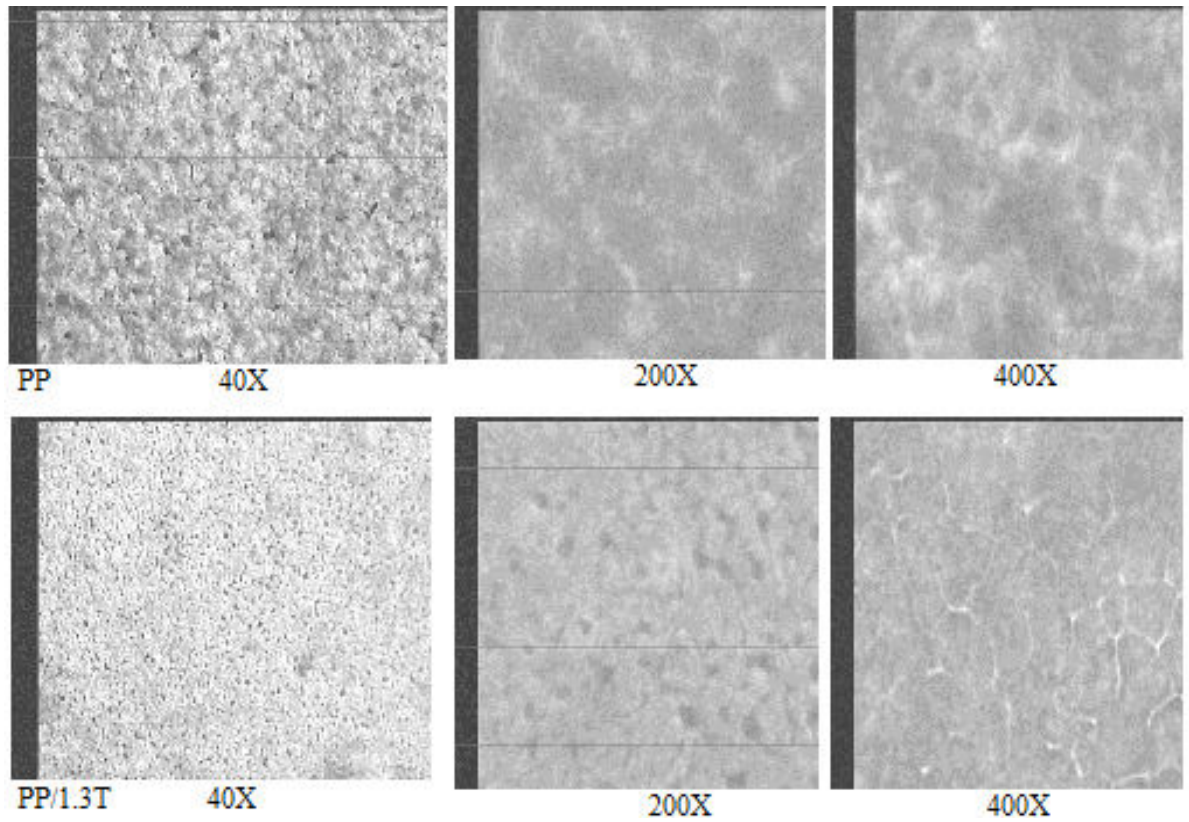
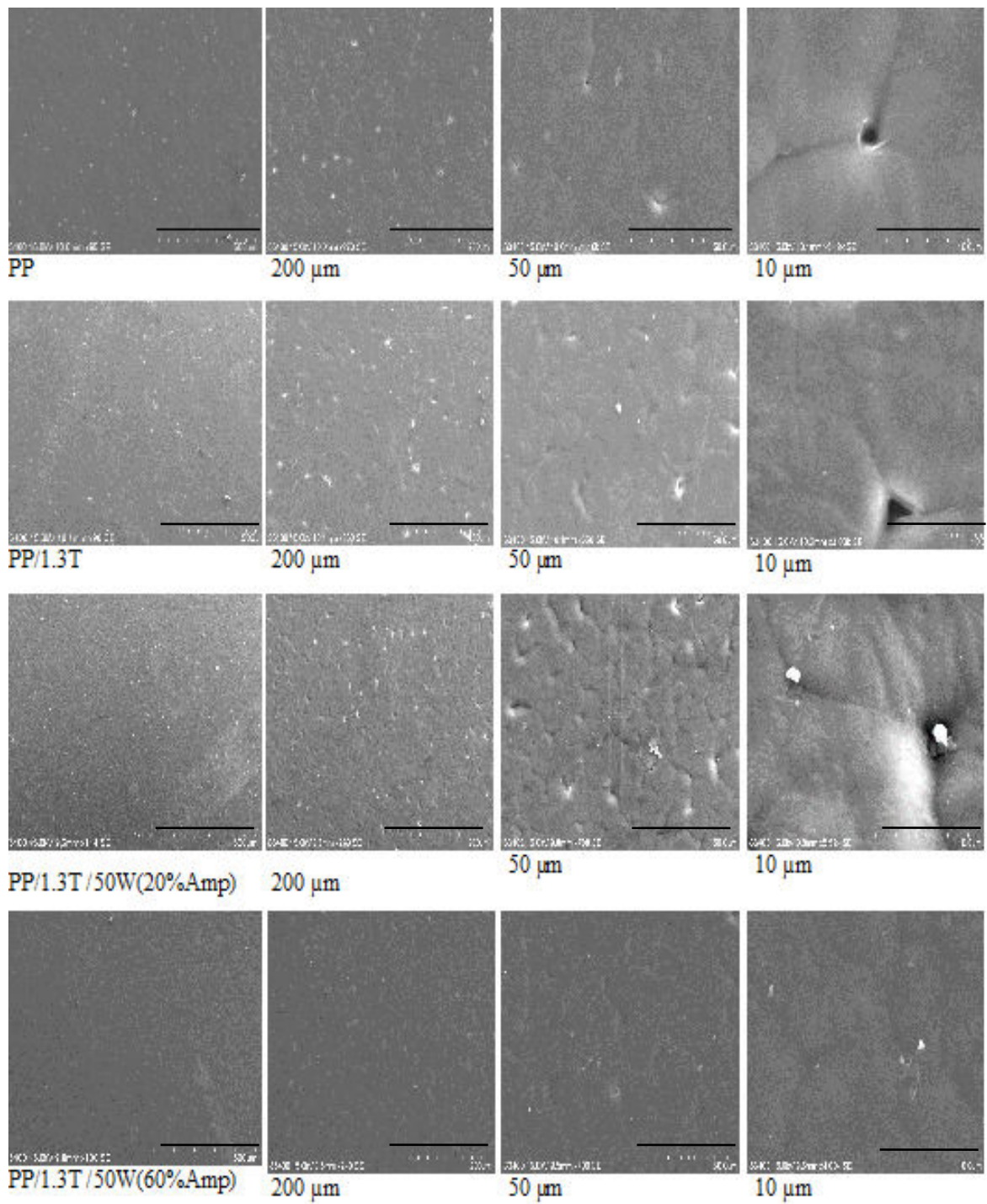


Figure 3.2: Optical microscopic image of PP and PP/1.3T(2 wt%) tape.



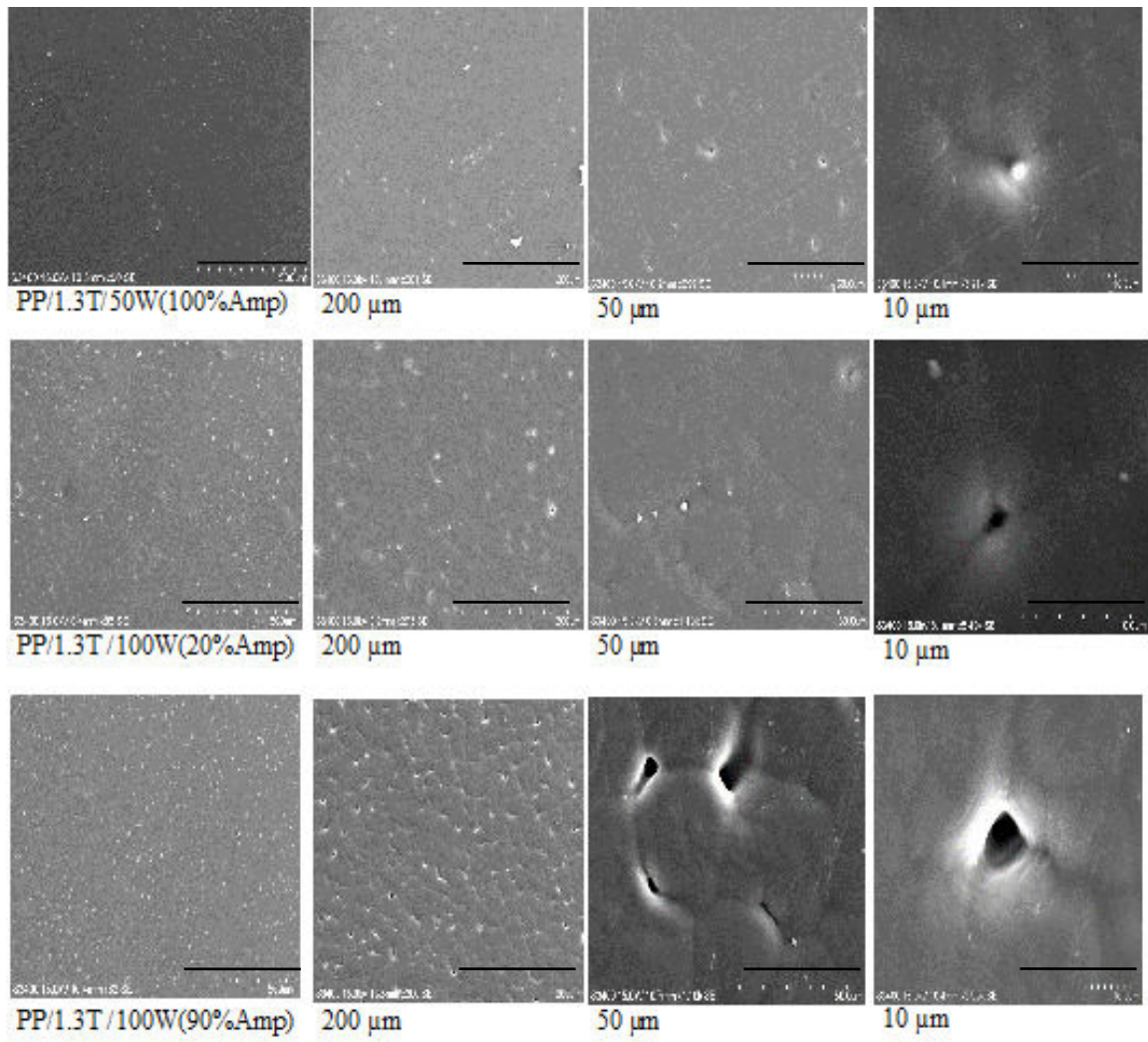


Figure 3.3: SEM of PP and PP/1.3T(2 wt%); note that the horizontal bar in each micrograph relate to the length dimensions shown.

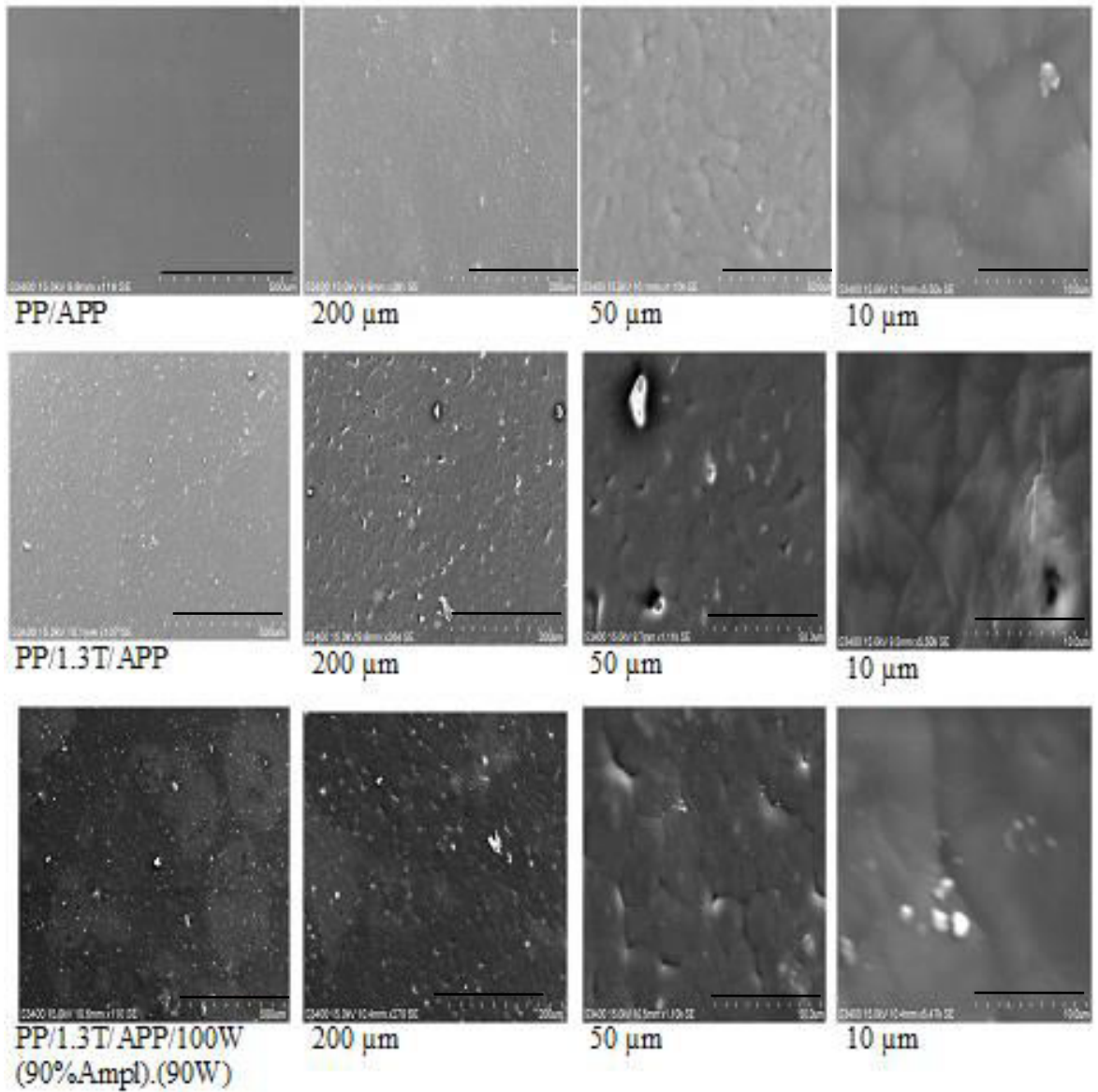


Figure 3.4: SEM of PP/APP(5 wt%) and PP/1.3T(2 wt%)/APP(5 wt%); note that the horizontal bar in each micrograph relates to the length dimensions shown.

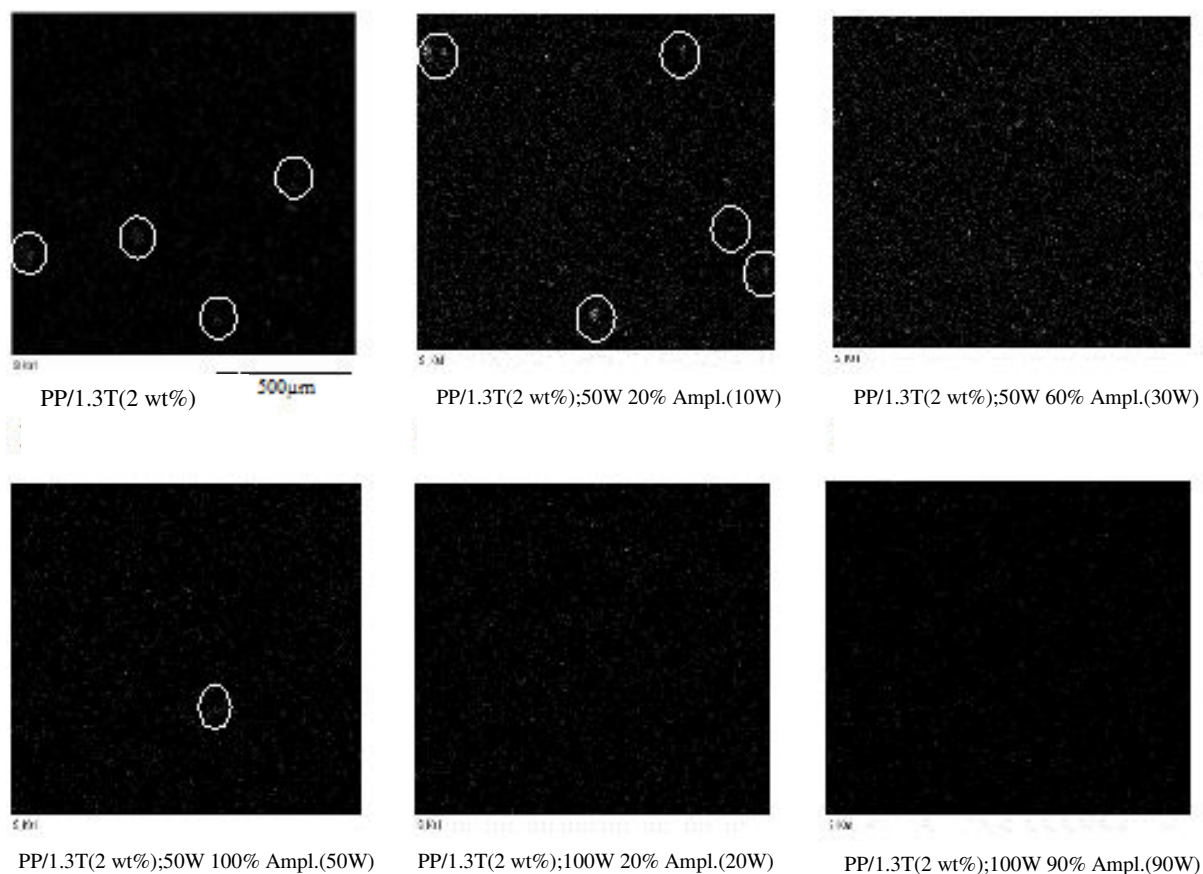


Figure 3.5: EDS images representing Si dots of PP and PP/1.3T(2 wt%) tapes, where clusters are circled.

3.4.1.2 Quantification of particulate dispersion

Datacell software was used to quantify the incidence of Si dots from SEM-EDS images and the data produced as shown in Tables 3.2 and 3.3. For each sample a specified pre-calibrated area was selected on the EDS image. Using the colour coding on the software, Si dots were selected and counted by the software. The software also measured area of the dots, number of dots for both selected areas (see Table 3.2) and the total area of the sample (see Tables 3.3). Table 3.2 shows that the number of Si dots and Si dot density (as dots per unit area) are reduced with the addition of nanoclay and further more reduced with the application of ultrasound. Surprisingly, the PP control appears to have more dots (166) than those which contain the added nanoclay. There is no simple explanation for this, however, because this control was the first sample to be extruded, it is possible that because there had been previous work under taken using nanoclays as additives in the extruder, some contamination had occurred. Table 3.3 shows that the Si dot number and

density for the whole sample under observation increases following the addition of nanoclay as expected and then reduces following the application of ultrasound. In Figure 3.6 the number of particles within a defined area (average of 12 results) as a function of ultrasonic power has been plotted for all samples. The results do not closely follow the qualitatively observed trend (compare Figure.3.5 and Table 3.2).Therefore, the whole sample area was selected and the results plotted as a function of ultrasonic power still do not follow closely the qualitatively observed trend in Figure 3.5. However, in spite of the possible error within the experimental data, from Table 3.3 it can be seen that the number of clusters was very low when the 100 W probe was used and so based on this study it was decided, therefore, to use the 100 W probe at 90% amplitude.

Table 3.2: Si dots quantification using small area of a sample and average of 12 separate areas.

Sample	Area of the sample (mm ²)	Si dot Area (mm ²)	Si dot Ratio	N ^o of Si dots	Si dots per unit Area (Dots/mm ²)	Power of Ultra sonification (W)
100% PP	0.0342	0.0007	0.9805	166	4859	0
PP/1.3T(2 wt%)	0.0241	0.0003	0.9897	50	2067	0
PP/1.3T(2 wt%)/50W(20%Ampl.)	0.0231	0.0003	0.9867	34	1489	10
PP/1.3T(2 wt%)/50W(60%Ampl.)	0.0215	0.0009	0.9586	214	9952	30
PP/1.3T(2 wt%)/50W(100%Ampl.)	0.0221	0.0002	0.9902	49	2240	50
PP/1.3T(2 wt%)/100W(20%Ampl.)	0.0231	0.0003	0.9867	34	1489	20
PP/1.3T(2 wt%)/100W(90%Ampl.)	0.0239	0.0002	0.9937	20	833	90

Table 3.3: Si dots quantification for whole sample area.

Sample	Area of the sample (mm ²)	Area of Si Dots (mm ²)	Si Dot Ratio	Number of Si Dots	Si Dots per unit Area (Dot/mm ²)	Power of Ultra sonification (W)	N ^o of Clusters	Cluster varification with number of dots
PP/1.3T(2 wt%)	0.7289	0.0070	0.9905	1690	2319	0	11	7-small 4- Large
PP/1.3T(2 wt%)/50W(20% Ampl.)	0.7053	0.0258	0.9647	6051	8579	10	9	4-small 5-Large
PP/1.3T(2 wt%)/50W(60% Ampl)	0.7086	0.0206	0.9718	4938	6969	30	12	8-Small 4-Large
PP/1.3T(2 wt%)/50W(100% Ampl.)	0.7287	0.0072	0.9903	1720	2360	50	7	3-Small 4-Large
PP/1.3T(2 wt%)/100W(20% Ampl.)	0.7301	0.0058	0.9921	668	915	20	5	5- Small
PP/1.3T(2 wt%)/100W(90% Ampl.)	0.7211	0.0057	0.9921	1352	1875	90	5	5-Small

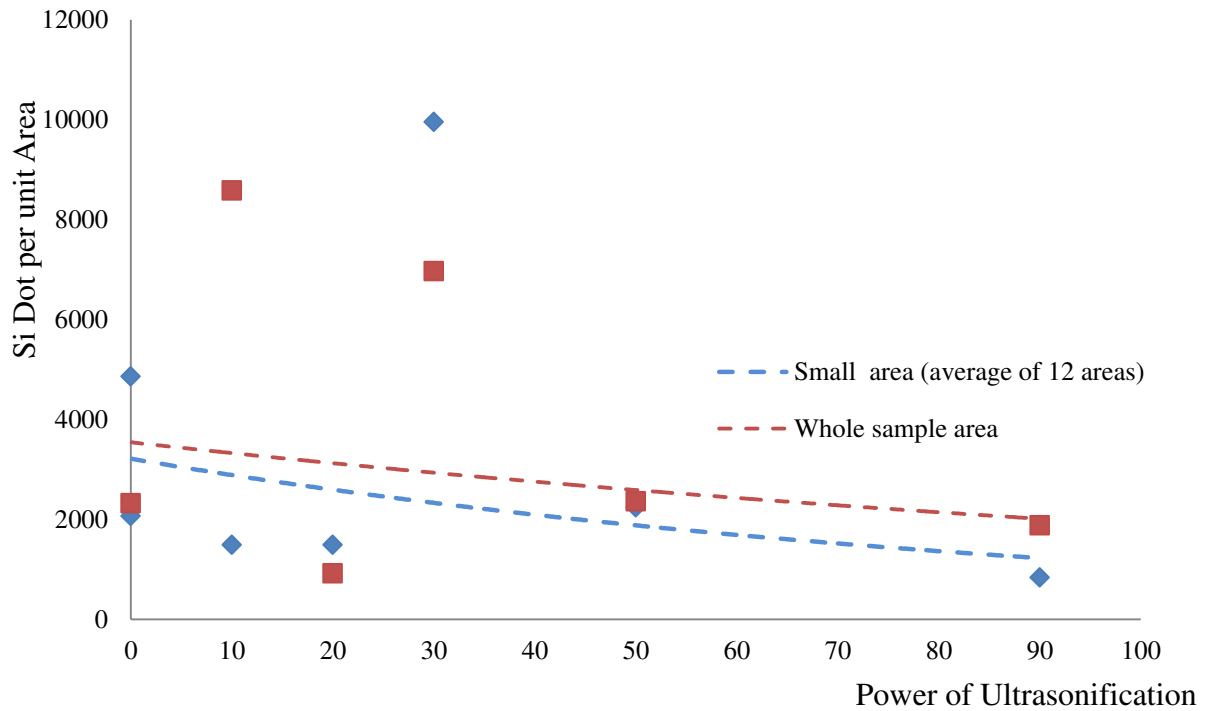


Figure 3.6: Si dots quantification using small area for measurement at one time (averaging the results for 12 samples) and using whole sample area.

3.4.1.3 Transmission electron microscopy

Transmission electron micrographs of PP/1.3T(2 wt%) and PP/1.3T(2 wt%)/90W) are shown in Figure 3.7, which indicates that nanoclayfundamental platelets are more separated, ie, intercalated, in the presence of ultrasonification.

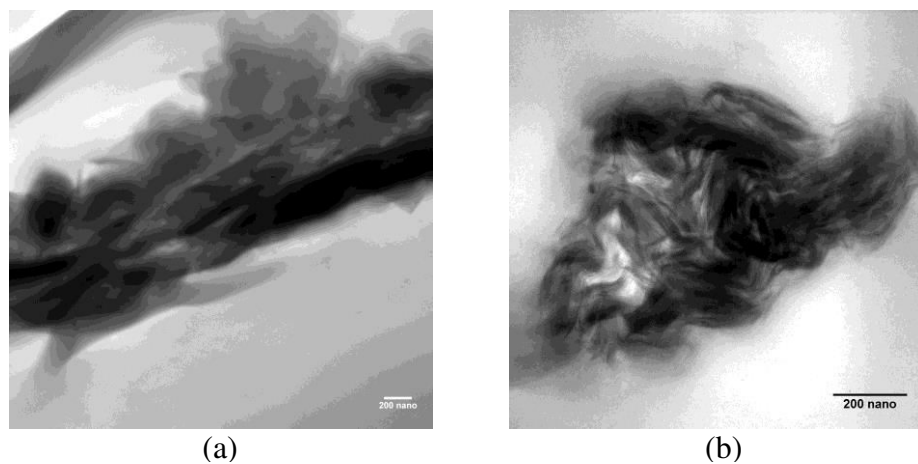


Figure 3.7: Transmission electron micrographs of samples (a) PP/1.3T(2 wt%) and (b) PP/1.3T(2 wt%)/90W.

3.4.2 Thermal stability

Thermal analysis study was performed on compounded polymer chip samples. Selected graphs are shown in Figure 3.8 where it can be seen that PP/1.3T(2 wt%) without /with ultrasonification are very similar in nature. However, PP/1.3T(2 wt%)/APP(5 wt%) after sonification shows changed thermal stability compared to unsonicated samples in terms of shifting the onset of degradation. All of these curves are analysed in Tables 3.4(a) and (b), where it can be seen that additives or ultrasonification have a minimal effect on melting endotherms, implying that the processing of the polymers will not be affected. The initiation of thermal degradation, T_{10} , termed as temperature where 10% mass loss occurs is decreased to 265 °C after sonification (sample PP/1.3T(2 wt%)/90W) compared to 299 °C without sonification in sample PP/1.3T(2 wt%). T_{50} , where 50% mass loss occurs, is also slightly reduced, whereas char yield is increased. However, when APP is also added, T_{10} is increased to 299 °C with sonification (sample PP/1.3T(2 wt%)/APP(5 wt%)/90W) compared to 266 °C without sonification in sample PP/1.3T(2 wt%)/APP(5 wt%). Char yield is also increased. These results show that ultrasonification reduces the thermal stability during the initial stages, but in general, improves it at higher temperatures in terms of increasing residues which comprise both carbonaceous and inorganic contents.

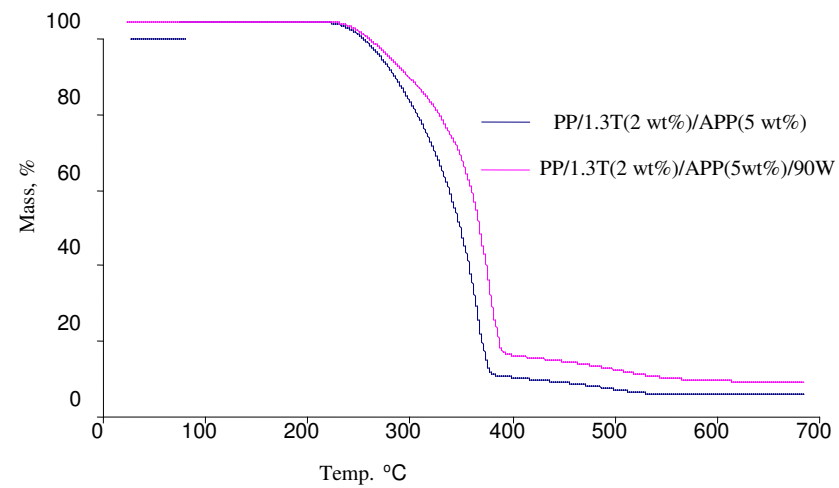
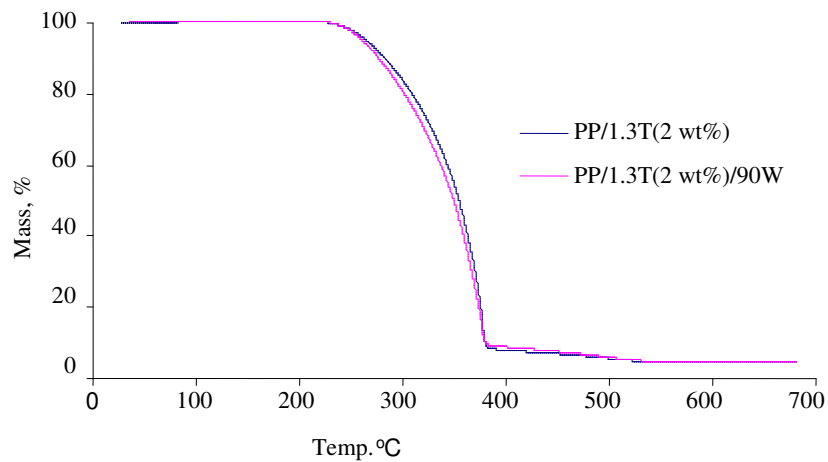
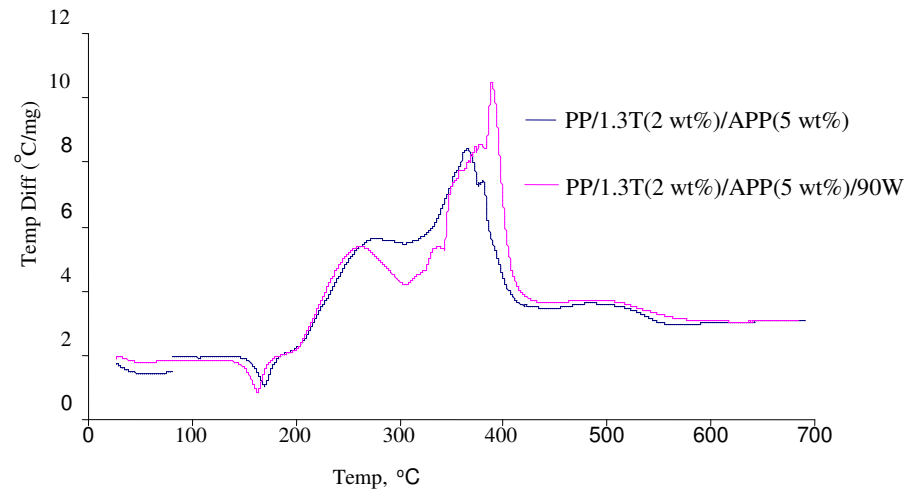
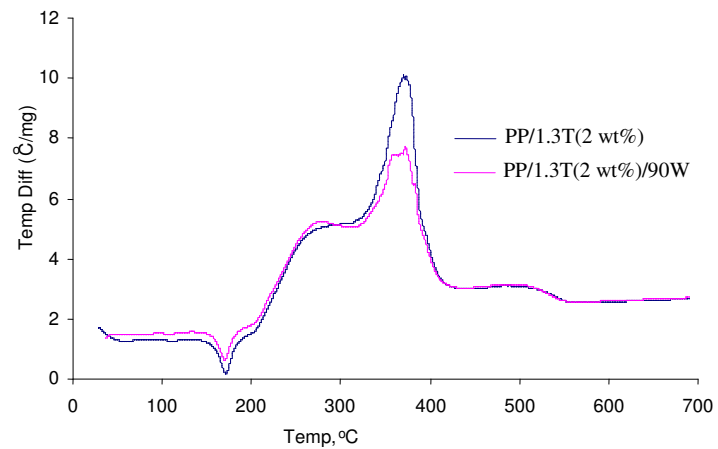


Figure 3.8: DTA and TGA curves of PP/1.3T(2 wt%) and PP/1.3T(2 wt%)/APP(5 wt%) without / with ultrasonification.

Table 3.4 (a): DTA analysis of PP matrix samples.

Samples	Melting peak, Endo		Decomposition, Exo		Char oxidation, Exo	
	Init	Peak Max	Init	Peak Max	Init	Peak Max
	(°C)	(°C)	(°C)	(°C)	(°C)	(°C)
PP	145	171	224	349 (L)	442	490
PP/1.3T(2 wt%)	146	171	205	270 (B), 372 (L)	433	497
PP/1.3T(2 wt%)/90W	150	169	201	276; 357, 369 (d)	428	499
PP/APP(5 wt%)	137	170	224	286, 345, 364, 386, 417	-	-
PP/1.3T(2 wt%)/APP(5 wt%)	144	170	199	274; 365,380 (d)	438	490
PP/1.3T(2 wt%)/APP(5 wt%)/90W	143	170	186	270; 343, 387, 402	451	504

Note: Init = Initial or onset temperature, L = large, s = small, B = broad, d = double peak.

Table 3.4(b): TGA analysis of PP matrix samples.

Samples	T ₁₀ , Temp at 10% mass Loss (°C)	T ₅₀ , Temp at 50% mass Loss (°C)	Char Residue at 600 °C (%)
PP	299	328	0.4
PP/1.3T(2 wt%)	299	358	1.2
PP/1.3T(2 wt%)/90W	265	350	1.4
PP/APP(5 wt%)	291	379	4.3
PP/1.3T(2 wt%)/APP(5 wt%)	273	355	4.5
PP/1.3T(2 wt%)/APP(5 wt%)/90W	299	372	5.2

3.4.3 Effect of ultrasonification on fibre properties

Compounded polypropylene formulations generally were extrudable into filaments and the ease of processing improved if samples had been subjected to ultrasound treatment. This was especially noticeable for the PP/1.3T(2 wt%)/APP(5 wt%) sample containing APP particles. Dependence of the tensile properties of the PP/clay with various amounts of ultrasound power is shown in Table 3.5. Normally the addition of well-dispersed nanoclay would be expected to increase the initial modulus and reduce breaking elongation although little or no effect on tenacity is often seen. Here, all the tensile properties of PP-clay filaments decreased compared to PP, which except for the elongation-at-break values, are unexpected results. It might be due to the poor dispersion and interface adhesion of nanoparticles in the PP matrix at high filler content. When ultrasound was introduced during compounding, it helps to reduce the size of nano particle agglomerates, due to which elongation-at-break improves in most cases. According to the Table 3.5, a mild power (100 W power with 90% amplitude) of ultrasound in our experiment seems more beneficial for enhancing the elongation-at-break. In addition, although the values of the elongation-at-break measured in this work have considerable deviations, the results show a slight decrease in elongation-at-break of PP by adding 1.3T nanoclay in the absence of ultrasound, due to that the fillers cause a reduction in matrix deformation because of the introduction of mechanical restraints. It should be noted once again that the extrusion was undertaken on the Labline extruder which is not designed for fine filaments and there is little or no polymer metering behind the spinneret.

Table 3.5: Tensile properties for PP matrix samples.

Sample	Linear density (tex)	Modulus (cN/tex) and CV(%)	Tenacity (cN/tex) and CV(%)	Elongation- at -break (%) and CV(%)
PP(without compounding)	4.7	358.3 (3.6)	29.2 (13.1)	152.2 (4.9)
PP	4.2	348.4 (15.7)	32.9 (22.7)	151.6 (7.6)
PP/1.3T(2 wt%)	11	311.4 (4.4)	11.5 (13.3)	180.6 (84.1)
PP/1.3T(2 wt%)/90W	12.8	179.6 (16.5)	15.1 (14.8)	238.8 (17.3)
PP/APP(5 wt%)	13.1	251.4 (12.7)	15.4 (15.8)	186.7 (46.9)
PP/1.3T(2 wt%)/APP(5 wt%)	15.4	158.8 (9.6)	6.6 (9.9)	7.9 (15.9)
PP/1.3T(2 wt%)/APP(5 wt%)/90W	10.6	229.6 (23.4)	11.5 (17.4)	8.6 (29.0)

3.4.4 Effect of ultrasonification on flammability of strands and tapes

3.4.4.1 Limiting oxygen index (LOI)

Results of oxygen index for the polymer strands of the PP samples are given in Table 3.6. LOI values of PP and PP/1.3T(2 wt%) remain constant (17.2%), but the burning rate is decreased from 7.1 to 4.4 mm/s. Similar values were obtained in the presence of ultrasound. The LOI value for PP/APP(5 wt%) is slightly increased from 17.2 to 18.2 vol% and rate of burning reduced from 7.1 to 6.2 mm/s. However, the presence of nanoclay with flame retardant has reduced the LOI values slightly to 17.8 vol% as well as the rate of burning which further reduced in the ultrasonicated sample (PP/1.3T(2 wt%)/APP(5 wt%)/90W).

LOI results for the tape samples are given in Table 3.7. In the presence of clay LOI value reduced slightly and these was a little effect of ultrasonic exposure. Presence of flame retardant increased the LOI value which was further increased with the presence of clay and flame retardant, but the presence of ultrasound decreased the LOI values slightly. The rate of burning was unaffected in the presence of clay and use of ultrasonic waves.

From these results it can be seen that the presence of clay while does not increase the LOI, reduces the burning rate, which is further reduced by ultrasonification, which indicates

that ultrasonification enhances dispersion of nanoclays. Similar results are seen with additional APP presence. However, other tests are required to establish the effects of ultrasound; hence UL-94 tests were carried out.

Table 3.6: LOI values of compounded PP strands.

Sample	Diameter of Strands (mm)	LOI vol%	Burning rate (mm/s)
PP	1.8	17.2	7.1
PP/1.3T(2 wt%)	1.9	17.2	4.4
PP/1.3T(2 wt%)/90W	1.6	17.3	3.3
PP/APP(5 wt%)	2.1	18.2	6.2
PP/1.3T(2 wt%)/APP(5 wt%)	2.1	17.8	4.8
PP/1.3T(2 wt%)/APP(5 wt%)/90W	2	17.8	3.2

Table 3.7: LOI values of extruded tapes.

Sample	Thickness of tape (mm)	LOI vol%	Burning rate (mm/s)
PP	0.34	17.9	4.8
PP/1.3T(2 wt%)	0.55	17.7	4.4
PP/1.3T(2 wt%)/90W	0.41	17.8	3.2
PP/APP(5 wt%)	0.38	18.6	4.8
PP/1.3T(2 wt%)/APP(5 wt%)	0.5	19.3	4.6
PP/1.3T(2 wt%)/APP(5 wt%)/90W	0.38	18.9	4.7

3.4.4.2 Flame spread and melt dripping of strands

The flammability properties of all samples in the form of strands have been measured using a modified UL-94 test in both horizontal and vertical orientations at room temperature. The first 10 mm of sample burning was not taken into account and so times of burning were recorded once the flame had reached a line drawn 10 mm from the edge against which flame of 30 mm was applied for 10s as specified in the test [224]. A video film was taken of the burning of each sample from which times to reach 50 mm (T_1) and 100 mm (T_2) marks and / or to achieve flameout were noted. The number of melting / flaming drops was also noted. Three replicates of each sample were burnt and results averaged. Since the diameters of all samples are different, the burning rate and number of drops were normalised with respect to volume of the control PP strand, and these normalised results are presented in Table 3.8.

In the horizontal mode, the PP sample melted and burned with flaming drips. All samples with clay and even with flame retardant APP, burnt completely, which is unexpected, given the low levels (5 wt%) of flame retardants used here. However, the flame spread rates varied as seen from Table 3.8. On the addition of clay to the compounded polymer, a change in burning behaviour was observed in that the total time to burn reduced, which further reduced on sonification. With the addition of clays, the number of drops decreased during the time of burning, which further decreased with sonification. This shows that sonification helps in creating more uniform dispersion, which changes the burning behaviour of samples. Thus the polymer no longer drips, but remains a coherent melting mass which burns. A similar trend is seen for APP-containing samples in that the total time to burn reduced with the clay presence and after sonification the number of melting / flaming drops decreased.

In the vertical mode burning of the control sample was more vigorous with melting drips (see Table 3.8). However, the trend was similar for all samples as seen in horizontal mode. In summary, it is clear that sonification reduces the number of normalised melting drips, expressed with respect to the initial unit volume of each sample, which is due to better dispersion of the clay and possibly flame retardant.

Table 3.8: Details of UL94 result of strands.

Sample	Horizontal flame spread (modified UL-94)						Vertical flame spread (modified UL-94)					
	T ₁	T ₂	BT	BL	Burning rate *	N ^o of drops*	T ₁	T ₂	BT	BL	Burning rate *	N ^o of drops*
	(s)	(s)	(s)	(mm)	(mm/s)		(s)	(s)	(s)	(mm)	(mm/s)	
PP	34	45	79	150	1.9	64	7	15	22	150	8	47
PP/1.3T(2 wt%)	30	28	58	150	2.2	18	9	27	36	150	3.4	23
PP/1.3T(2 wt%)/90W	17	20	37	150	3.9	16	6	10	16	150	9.6	21
PP/APP(5 wt%)	25	44	69	150	1.7	28	7	25	33	150	3.6	34
PP/1.3T(2 wt%)/APP(5 wt%)	27	38	65	150	1.7	15	5	12	17	150	6.8	19
PP/1.3T(2 wt%)/APP(5 wt%)/90W	19	42	61	150	2.2	20	7	18	25	150	5.3	37

Note : T₁ = Time to 50 mm; T₂ = Time to 50 - 100 mm, BT = Total time to burn; BL = Total burnt length; * = Normalised with respect to volume of PP sample; No of drops during total burn time

3.4.5 Effect of ultrasonification on flammability of fabrics

All filaments were knitted into fabrics and the area density of each sample is given in Table 3.9. Flame spread tests were undertaken using the test rig described in BS 5438 [223] used for flammability of textile materials. Due to limited sample sizes, the sample holder, 190 x 70 mm, used in Test 1 for assessing ignition times in this standard has been used. Sample sizes were different for all samples due to the differing availability of extruded filaments / fabrics. The first 10 mm of sample burning was not taken into account and so times of burning were recorded once the flame had reached a line drawn 10 mm from the bottom edge against which the standard flame was applied for 10 s as specified in the test. A video film was taken of the burning of each sample from which total burn time and burnt length were noted. Three replicates of each sample were burnt and results averaged. The melt / flame dripping behaviour of each sample was observed and noted. Since the sample sizes are different, rate of flame spread of different samples and number of flaming drips were normalised to a sample size of 100 x 100 mm in each case and normalised results are presented in Table 3.9.

Addition of clay in PP/1.3T(2 wt%) sample had no effect on the rate of flame spread of PP (1.4 mm/s), which however reduced to 1.1 mm/s after sonification (sample PP/1.3T(2 wt%)/90W). Flaming drop rates also reduced significantly in sonicated samples. In Table 3.9, total mass losses (determined by weighing unburnt fabric or the residual char) of all fabrics are also presented. As can be seen from results, the sonicated samples had recordable residual masses, whereas respective unsonicated samples burnt completely. The charred flaming drops were also collected on an aluminium foil and weighed; the results are presented in last column of Table 3.9 expressed as a percentage of mass of the burning drops. Mass. Mass of the burning drops reduced significantly after sonification. For APP- and clay-containing samples, similar effects were observed, i.e.,sonification reduced the rate of burning from 2.9 (sample PP/1.3T(2 wt%)/APP(5 wt%)) to 1.3 mm/s (sample PP/1.3T(2 wt%)/APP(5 wt%)/90W), with a significant reduction in numbers of melt / flaming drops.

Table 3.9: Flame spread results of PP fabrics.

Sample	Area density of fabric (g/m ²)	Sample Dimension (mm x mm)	Total Burn time (s)	Burnt height (mm)	flame spread* (mm/s)	N ^o of drops*	Mass of the molten / burnt drops (%)
PP	110	130 X 83	83	123	1.4	91	74
PP/1.3T(2 wt%)	100	129 X 80	89	128	1.4	91	77
PP/1.3T(2 wt%)/90W	90	160 X 93	100	160	1.1	30	34
PP/APP(5 wt%)	80	200 X 95	13	75	3.0	10	10
PP/1.3T(2 wt%)/APP(5 wt%)	70	98 X 80	42	98	2.9	55	94
PP/1.3T(2 wt%)/APP(5 wt%)/90W	120	200 X 85	54	121	1.3	25	37

Note : * = Normalised to 100 mm X100 mm sample size

3.5 Conclusions

In general it can be concluded that ultrasonification has helped in improving the dispersion of nanoclays and flame retardants in polypropylene, the effect however is not very significant. There is direct relationship between dispersion and the flame retardant performance of the samples. Well dispersed samples had less burning rates and flaming drips.

Fire performance of PP containing clay and / or flame retardant was studied by using the LOI test and LOI values of samples containing clay and /or flame retardant werenot significantly affected by additive content or the presence of ultrasound. However, the rate of burning is reduced with the presence of clay and / or flame retardant and further reduced by the presence of ultrasound application. A modified UL-94 test was used to further study the fire performance. The presence of nanoclay and / or flame retardant decreased flammability in terms of reducing burning rate, which was further decreased by ultrasonification. A similar trend was seen for knitted fabric samples

Chapter 4: Optimisation and Effects of Ultrasound on Polyamide 6 (PA6) Filament / Fabric Properties

4.1 Introduction

Polyamides are difficult to process with additives and flame retardants because of their melt reactivity. Previous works at Bolton on PA 6 / clay fibres was carried out by melt blending PA6 and nanoclays and then melt spinning, which did not show any signs of degradation of PA6 during processing [145]. Since the processing temperature of PA6 is higher, the flame retardants with decomposition temperature less than 250 °C cannot be used [144, 225].

The effectiveness of nanoclays and flame retardants depends upon their dispersion in a polymer. Fibre forming polymers need good nano-level dispersion in order to be processable. Even using hydrophobic functionalised clays in PP it is difficult to produce good nano dispersion unless a compatibiliser such as graft maleic polypropylene (PPgMA) is present [144, 145], while dispersion in polyamides is generally more easily realisable [153]. Another method of improving nano dispersion is the use of ultrasonic waves by using an ultrasonic probe in the polymer melt [221, 226]. Ultrasound is a tool, generally used to clean the surface or to create homogenous mixtures. Application of ultrasound at the extrusion stage is aimed to improve the physical and chemical properties of a polymer.

In this chapter two nanoclays, Nanomer 1.3T and Cloisite 25A and one flame retardant, aluminiumphosphinate have been used as additives for PA6. All techniques used for compounding, melt spinning and testing are similar to those in Chapter 3.

4.2 Experimental

Small amount of flame retardant is enough to flame retard if applied with a small percentage of nanoclay added to the dispersion. Total additive level was maintained below (< 10 wt%). As explained in Chapter 3, Section 3.2.3, two levels of ultrasonic power were used. 50 and 100W ultrasonic probes were used to ultrasonicate the samples.

4.3 Samples

4.3.1 Materials

In this study the polymer selected was Polyamide 6 (PA6), Technyl C 301 Natural, Rhodia, France, nanoclay as Cloisite 25A, Southern Clay Products, USA; modified with dimethyl, dehydrogenated tallow quaternary ammonium sulphate (2M2HT) and Nanomer 1.3T, Nanomer. The flame retardant was aluminiumphosphinate, Exolit OP 935, Clariant (note that this is fibre grade in that its average particle diameter is $< 10 \mu\text{m}$).

4.3.2 Sample matrix

Sample matrix is shown in the Table 4.1. Polymer pellets were compounded using the twin screw extruder as explained in Chapter 3, Section 3.2.3 and extruded in to filaments as explained in Chapter 3, Section 3.2.4. In each stage of the processing samples were selected as explained in Chapter 3, Section 3.2.2.

In this work the same twin screw extruder has been used to compound samples with and without application of ultrasound under the same conditions as explained in Chapter 3, Section 3.2.3. The temperatures in the six zones of the compounder were 210, 225, 230, 230, 240 and 245 °C.

Table 4.1: Sample matrix for PA6.

Sample	Clay -2 wt%	FR -5 wt%	Without ultrasonic probe	50 W Ultrasonic		100 W Ultrasonic	
				20%, 10 W	100%, 50 W	20%, 20 W	90%, 90 W
PA6	-	-	Ch, St, Tp, Fil, Fab				
PA6/1.3T	1.3T nanomer clay	-	Ch, St, Fil,	Ch, St, Fil, Tp	Ch, St, Fil, Tp	Ch, St, Fil, Tp	Ch, St, Fil, Tp, Fab
PA6/Al-Phos	-	Al- Phos	Ch, St, Fil, Tp, Fab				
PA6/1.3T/Al-Phos	1.3T nanomer clay	Al- Phos	Ch, St,				Ch, St,
PA6/25A	Cloisite 25A	-	Ch, St, Fil, Tp, Fab				Ch, St, Fil, Tp, Fab
PA6/25A/Al-Phos	Cloisite 25A	Al- Phos	Ch, St, Fil, Tp, Fab				Ch, St, Fil, Tp, Fab

Where, Ch = Compounded chips, St = Strands, Tp = Tape, Fil = Filaments, Fab = Fabric

4.3.3 Melt extrusion into filament / tapes and fabric production

Compounded samples were extruded into filament and tape as explained in the Chapter 3, Section 3.2.4 and knitted into fabric as explained in the Chapter 3, Section 3.2.5. All the samples were characterised as explained in the Chapter 3, Section 3.3.

4.4 Results and discussion

All compounded samples could be extruded successfully into filaments. PA6/1.3T(2 wt%) sample could not be extrude into tapes, however with ultrasonification the extrusion into tapes was possible (Table 4.1). It was decided to proceed with 100 W probe and 90% amplitude, because it was found to be excellent for dispersion of clay in PP.

4.4.1 Tensile properties

Compounded PA6 samples were extrudable into filaments and the application of ultrasound treatment ease of processing. Filaments containing 1.3T clay were either impossible to spin into filaments or if spinnable, were too weak to knit into fabrics.

Table 4.2 shows the tensile properties of PA6 filaments. PA6 filaments containing Cloisite 25A showed increased moduli compared to 100% PA6 even when aluminiumphosphinate was present. Tenacity values also increased when this clay was included although in all PA6/25A(2 wt%) combinations the effects of ultrasound at best only maintained these superior properties.

Table 4.2: Tensile properties of PA6.

Sample	Linear density (tex)	Modulus (cN/tex) and CV(%)	Tenacity (cN/tex) and CV(%)	Elongation-at-break (%)and CV(%)
PA6	6.4	86.8 (24.5)	12.8 (26.4)	135.6 (11.9)
PA6/1.3T(2 wt%)	26.2	59.5 (19.3)	4.21 (26.0)	172.7 (26.8)
PA6/1.3T(2 wt%)/90W	13.4	62.3 (6.7)	11.8 (5.5)	287.5 (7.6)
PA6/Al-Phos(5 wt%)	21.9	49.4 (29.6)	9.2 (27.5)	201.5 (22.3)
PA6/25A(2 wt%)	16.2	113.6 (11.9)	21.8 (11.8)	145.2 (5.6)
PA6/25A(2 wt%)/90W	18.2	100.3 (15.4)	21.3 (0.4)	150.1 (13.7)
PA6/25A(2 wt%)/Al-Phos(5 wt%)	25.2	102.6 (9.1)	9.8 (9.7)	352.1 (5.2)
PA6/25A(2 wt%)/Al-Phos(5 wt%)/90W	25.7	134.9 (12.7)	7.5 (9.9)	281.5 (10.7)

4.4.2 Characterisation of tapes

Scanning electron microscopic (SEM) images of the samples are shown in Figure 4.1. From the images it appears that, clay dispersion is better than in formulations of PP. In the absence of ultrasound, no big clusters were obtained. This is due to the polar nature of the polymer and this helps to improve the dispersion of nanoclay particles. Also ultrasound improved the dispersion, as can be seen from Figure 4. EDS images of these samples shown in Figure 4.2. Si, P, Al dots also show better dispersion and the dispersion improves further in the presence of ultrasound. In the PA6/25A(2 wt%)/Al-Phos(5 wt%) sample, nanoparticles are well dispersed. Figure 4.3 shows a TEM image showing improved levels of clay nanodispersion for the Cloisite 25A layers, suggesting much better dispersion as a result of ultrasonication.

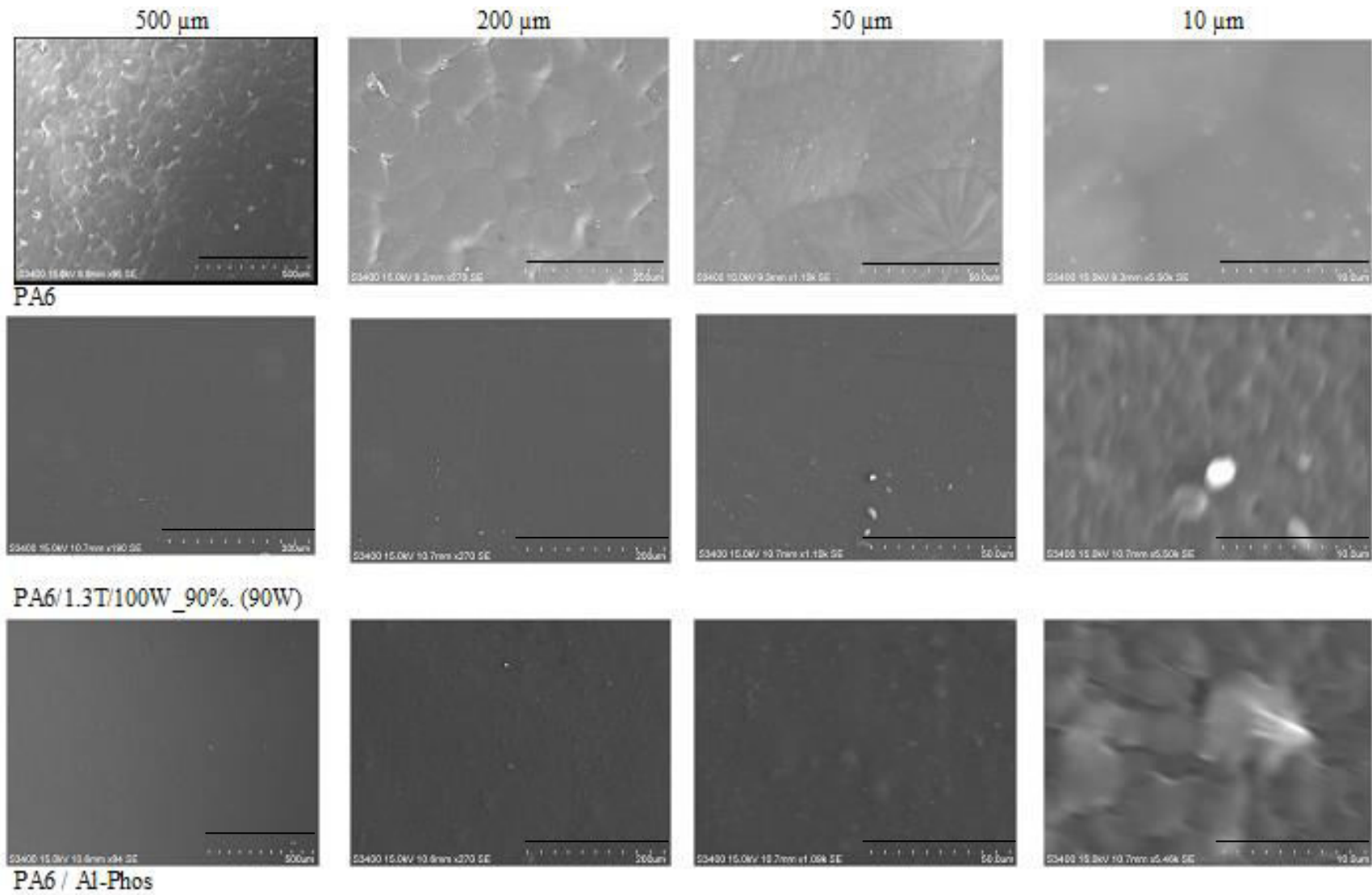
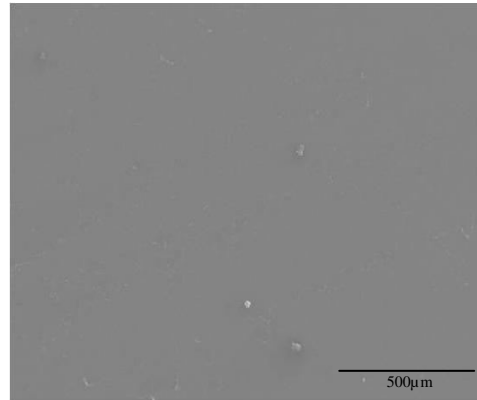


Fig 4.1: SEM images for PA6 tapes with PA6/1.3T(2 wt%)/90W and PA6/Al-Phos(5 wt%).

SEM

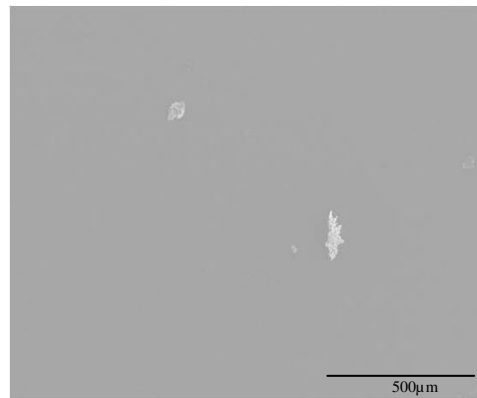


PA6/25A(2 wt%)

Si dots



Si Fa1



PA6/25A(2 wt%)/90W



Si Fa1

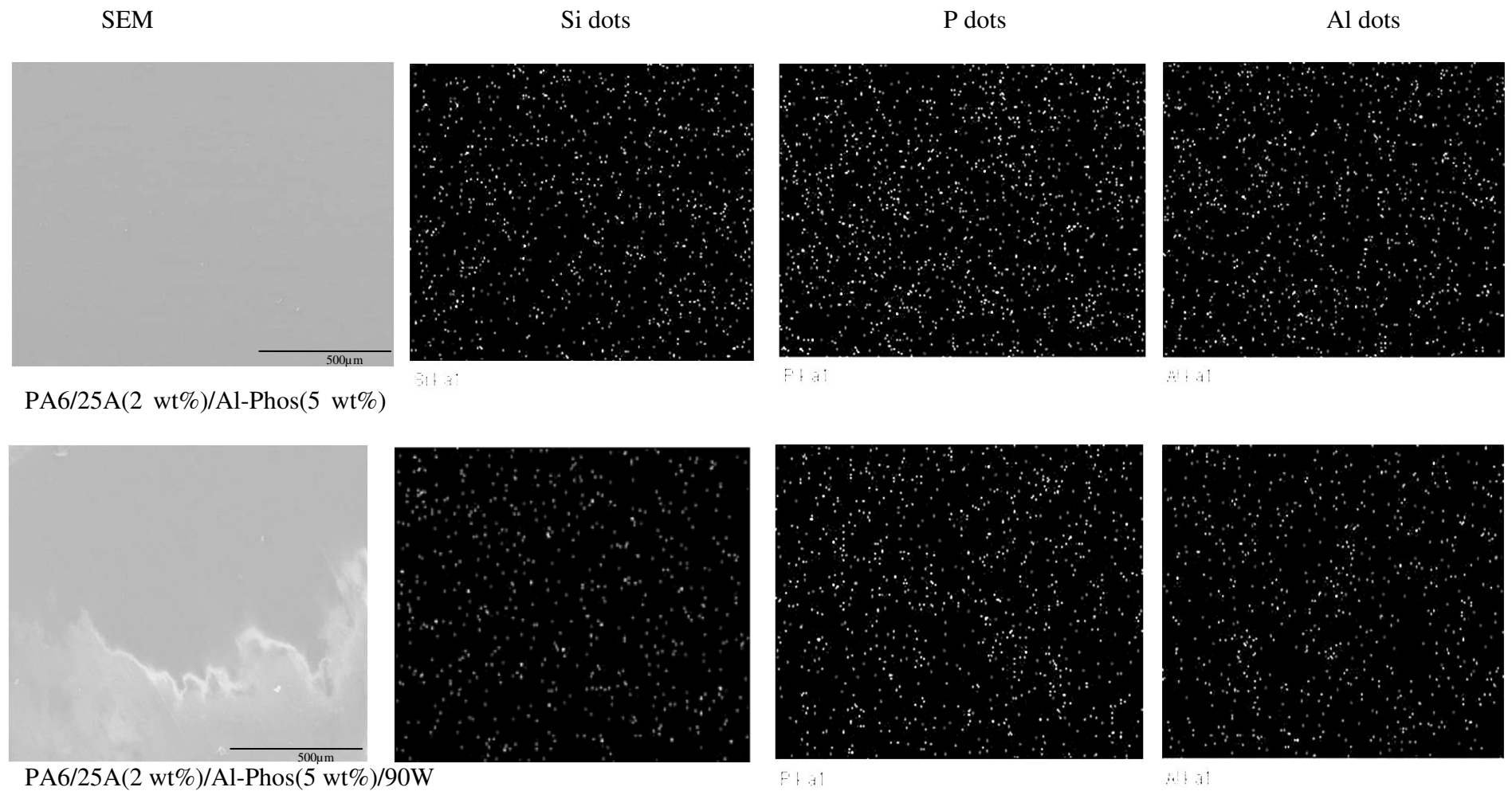


Figure 4.2: EDS images representing Si, P and Al dots.

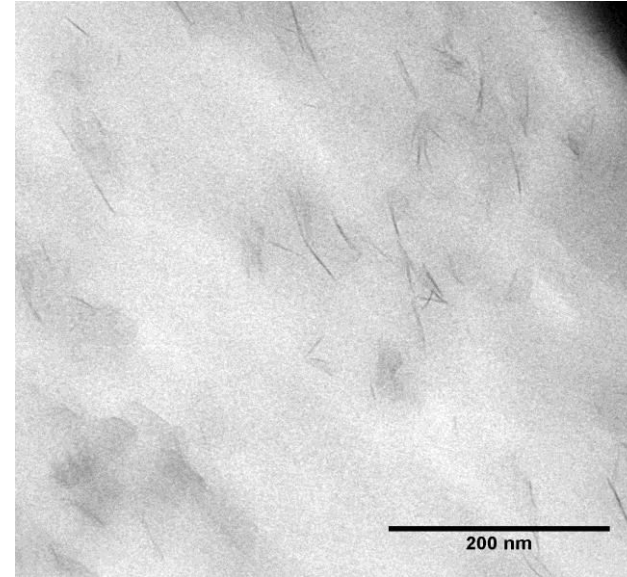
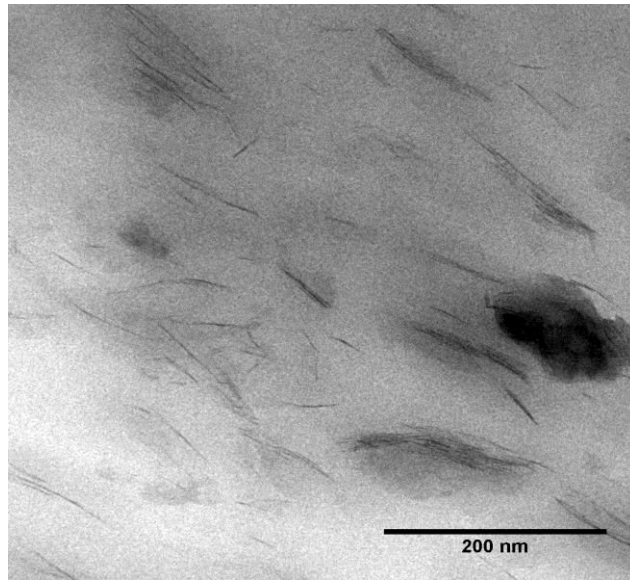


Figure 4.3: TEM micrographs of Cloisite 25A clay particles in polyamide 6 (PA6/25A(2 wt%)) formulations without and with ultrasonification.

4.4.3 Limiting oxygen index

LOI values of strands and tapes are shown in Table 4.3. Addition of both clays reduces LOI value, thus for PA6/1.3T(2 wt%) strand LOI values decreased from 22.5 to 20.3 vol% and it is further reduced for PA6/ 25A (2 wt%) to 18.8 vol%, which is due to the fact that both clays reduce melt dripping (Table 4.3), and hence hold the polymer together, which then burns easily. Presence of ultrasound improves the LOI value for PA6/25A(2 wt%)/90W and it is significantly reduced for PA6/1.3T(2 wt%)/90W. Addition of 5 wt% of aluminiumphosphinate to the PA6/1.3T(2 wt%) is not effective and shows no difference in the presence of ultrasound, but PA6/25A(2 wt%) with 5 wt% of aluminiumphosphinate significantly increased the LOI value and further more increased with the presence of ultrasound. Burning rate was not changed in the first case (PA6/1.3T(2 wt%)) and a significant change occurred in the second case (PA6/25A(2 wt%)). LOI values for the tape samples were not affected by presence of the 1.3T or 25A clays but PA6/25A(2 wt%)/Al-Phos (10 wt%) improved LOI value and decreased the burning rate and ultrasonication further increased LOI, but with no change in burning rate; perhaps because its already highly dispersed. LOI values and burning rates are slightly affected by clay however, in presence of flame retardants significant increase in LOI and reduction in burning rate occurred.

Table 4.3: LOI result for PA6 samples.

Sample	Diameter of strand (mm)	Polymer strands			Tape thickness (mm)	LOI (Vol-%)	Tapes Burn time (s)	Burning rate (mm/s)
		LOI (Vol-%)	Burn time (s)	Burning rate (mm/s)				
PA6	1.2	22.5	45	5.1	0.42	23.1	47	4.4
PA6/1.3T(2 wt%)	1.3	20.3	45	5.3	0.39	-	-	-
PA6/1.3T(2 wt%)/90W	1.2	19.4	47	5.0	0.52	24.2	57	3.8
PA6/Al-Phos(5 wt%)	1.3	19.0	47	4.8	0.48	19.9	47	-
PA6/1.3T(2 wt%)/Al-Phos(5 wt%)	1.5	20.1	52	4.4	0.32	-	-	-
PA6/1.3T(2 wt%)/Al-Phos (5 wt%)/90W	1.4	20.3	45	4.7	.51	-	-	-
PA6/25A(2 wt%)	1.2	18.8	40	5.0	0.36	19.7	47	5.8
PA6/25A(2 wt%)/90W	1.2	19.6	45	5.6	0.39	19.8	55	4.6
PA6/25A(2 wt%)/Al Phos(5 wt%)	1.1	21.1	60	0.8	0.46	20.5	52	0.6
PA6/25A(2 wt%)/Al Phos(5 wt%)/90W	1.3	23.2	40	0.7	0.52	22.9	42	0.6

4.4.4 UL-94

UL-94 equivalent test results for strands are shown in Table 4.4, the samples were mounted both vertically and horizontally in separate experiments. Samples were ignited for 10 seconds on the edge of the samples and started to count the time when flame reached a 10 mm mark on the sample. Time taken after first ignition (T_1) and second (T_2) was noted. Number of burning drips was also counted. Burning rate and number of drops were normalized with respect to the volume of pure PA6, because of the different diameter of the samples which might change burning behaviour of the samples.

For PA6/1.3T (2 wt%), burning rate increased in comparison with pure PA6 and further increased upon the application of ultrasound. Similar trend was observed for the PA6/25A(2 wt%) and PA6/Al-Phos(5 wt%). PA6/25A(2 wt%)/Al-Phos(5 wt%) shows decreased burning rate, which further decreased on the application of ultrasound, in both horizontal and vertical tests. There was no dripping in horizontal test and number of drops was decreased in the vertical test.

Table 4.4: Flame spread UL94 result for compounded PA6 strands.

Sample	Horizontal flame spread (modified UL-94)						Vertical flame spread (modified UL-94)					
	T ₁	BL ₁	T ₂	BL ₂	Burning rate*	N ^o of drops with*	T ₁	BL ₁	T ₂	BL ₂	Burning rate*	N ^o of drops*
	(s)	(mm)	(s)	(mm)	(mm/s)		(s)	(mm)	(s)	(mm)	(mm/s)	
PA6	30	18	60	122	1.6	13	38	150			3.9	18
PA6/1.3T(2 wt%)	63	150			1.9	4	36	150			3.6	10
PA6/1.3T(2 wt%)/90W	32	68	20	72	2.6	8	34	150			4.3	12
PA6/Al-Phos(5 wt%)	16	25	18	115	3.5	6	23	150			5.5	5
PA6/1.3T(2 wt%)/Al-Phos(5 wt%)	11	12	18	128	3.2	3	16	28	4	112	5.1	4
PA6/1.3T(2 wt%)/Al-Phos(5 wt%)/90W	13	25	63	115	1.5	13	14	150			8.7	3
PA6 / 25A(2 wt%)	15	25	19	115	4.4	8	18	150			8.8	5
PA6 / 25A(2 wt%)/90W	19	18	92	122	1.4	17	16	150			10.5	4
PA6 / 25A(2 wt%)/Al-Phos(5 wt%)	96	150			1.8	0	25	29	15	111	4.4	10
PA6 / 25A(2 wt%)/Al-Phos(5 wt%)/90W	103	150			1.1	0	25	28	16	112	3.1	8

Note : * = Normalized with respect to the volume of pure PA6.

4.4.5 Fabric flame spread

Only with PA6 samples containing cloisite 25A clay was it possible to produce sufficient fabrics for the vertical flame spread test. The results are given in Table 4.5. As can be seen area densities of samples are not similar. The difficulties in spinning compounded polymers into filaments explains not only the variations in yarn linear densities between samples (see Table 4.5), but also those in resulting fabric area densities. Due to the limited amount of fabric samples, sample sizes were different. Since the sample sizes are different, rate of flame spread of different samples and number of flaming drips were normalised to a sample size of 100 x 100 mm in each case and normalised results are presented in Table 4.5.

Normalised burning rate of PA6/25A(2 wt%) is decreased with respect to the value of PA6, which is partly due to the clay presence and partly due to the higher area density (100 g/m^2) of the PA6/25A(2 wt%) fabric (fabric area density of PA6 = 60 g/m^2). Normalised number of drops of PA6/25A(2 wt%) is increased with respect to the value of PA6, melt dripping increased due to the presence of Cloisite 25A but it reduced by the addition of Al-Phos. Sonification reduced these values. With the presence of both Al-Phos and Cloisite 25A the number of drops decreased and this was further more decreased by ultrasonification. Burning behaviour of fabric is shown in Figure 4.4 with captured photographs of burning behaviours at 0, 10 and 20 second after the ignition had been place. Melt and shrinkage back of PA6/25A(2 wt%) or PA6/Al-Phos(5 wt%) is less than PA6 fabric, but sonicated PA6/25A(2 wt%) sample appears to restore the thermoplastic / shrinking behavior. The PA6/25A(2 wt%)/Al-Phos(5 wt%) sample melts and shrinkage was most similar to the PA6/25A(2 wt%) or PA6/Al-Phos(5 wt%). The sonicated PA6/25A(2 wt%)/Al-Phos(5 wt%)/90W fabric is more flammable immediately after igniting with the applied flame but recovered afterwards. Clearly this is a confusing picture and these results do not correlate well with LOI burn rates in Table 4.3.

Table 4.5: Fabric flame spread.

Sample	Area density of fabric (g/m ²)	Sample Dimension (mm×mm)	Total Burn time (s)	Burnt height (mm)	Rate of flame spread* (mm/s)	N ^o of drops*	Total mass loss (%)	Mass of the molten /burnt drops (%)
PA6	60	157 X 93	45	103	1.6	19	42	19
PA6/Al- Phos(5 wt%)	50	200 X 85	18	70	2.3	4	14	11
PA6/25A(2 wt%)	100	185 X 90	89	113	0.8	53	33	17
PA6/25A(2 wt%)/90W	90	165 X 75	44	99	1.8	31	34	21
PA6/25A(2 wt%)/Al-Phos(5 wt%)	90	191 X 87	101	156	0.9	4	65	41
PA6/25A(2 wt%)/Al-Phos(5 wt%)/90W	70	195 X 80	47	158	2.2	4	45	26

Note : * = Normalised to 100 mm X100 mm sample size

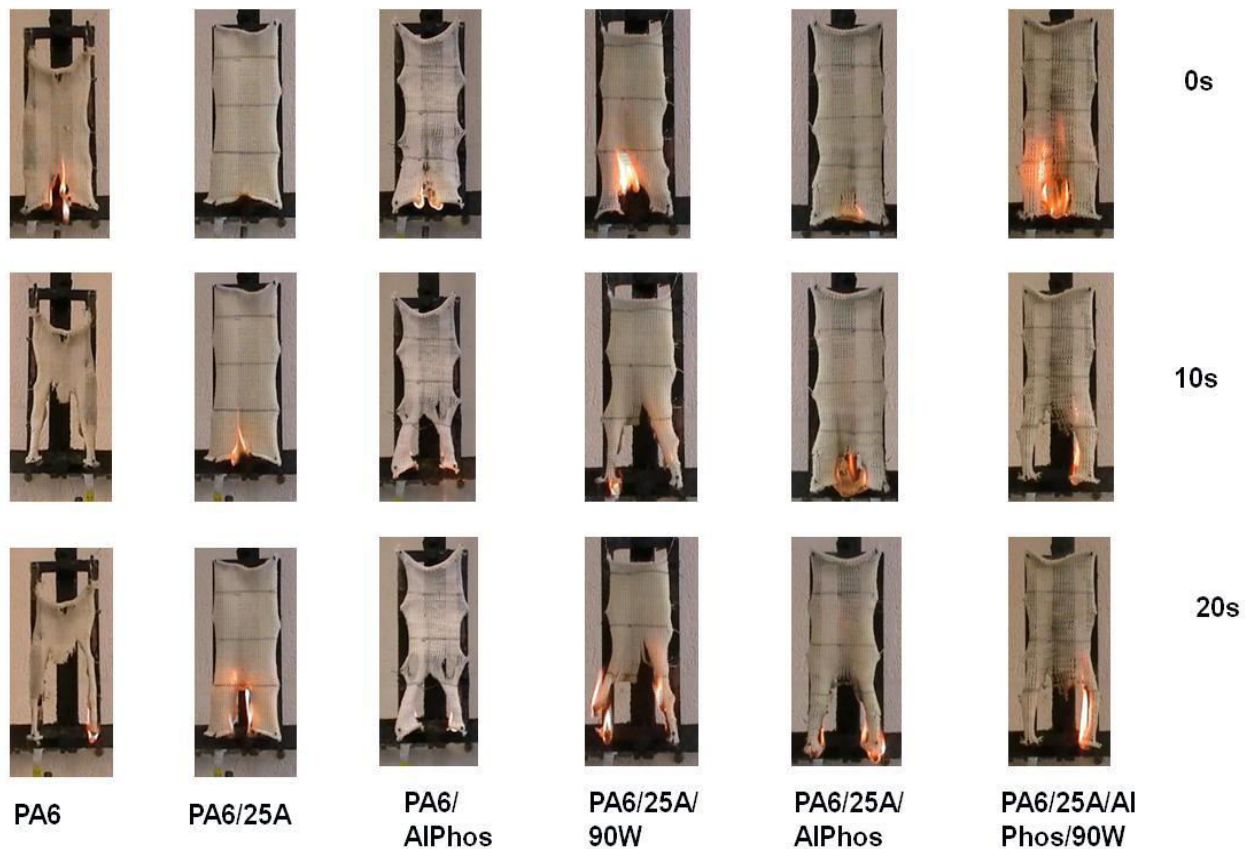


Figure 4.4: Vertical flame test result for fabric at 0, 10 and 20 seconds after ignition.

4.5 Conclusions

Results reported above give a number of mixed results with regard to the possible advantages that ultrasonification of polymer melts during compounding may have on final flammability properties. It is clearly evident that ultrasonification has improved dispersion of additives at micro- and nanolevels. In polyamide 6 where clay and additive dispersion is much more facile because of its polar nature, ultrasonification has been shown to increase exfoliation by TEM.

It is also clear that ultrasonification improves nanocomposite polymer processibility and the ease of extruding filaments from compounded formulations is definitely improved.

In terms of improving flame retardance or fire performance, the effects of ultrasound are more mixed. Here any positive effects of ultrasound treatment are only really notable for the PA6/25A(2 wt%)/AI-Phos(5 wt%) formulations where an increase in LOI is noted (see

Table 4.3). Actual vertical strip burning behaviour is both interesting and puzzling in that the tendency of a PA6 fabric to melt and shrink back is reduced significantly when either Cloisite 25A or aluminiumphosphate are present alone only to reappear after sonification of the PA6/25A(2 wt%) sample. Furthermore, ultrasonification of the PA6/25A(2 wt%)/Al-Phos(5 wt%) fabric appears to cause an apparent increase in flammability immediately after ignition coupled with increased thermoplastic / shrinking property after longer burning times.

It is possible that in PA6, increasing aluminium phosphinate concentration from 5 to 10 wt% should create filaments with acceptable levels of flame retardancy and that the application of ultrasound will enable such larger levels to be dispersed within the polymer matrix thereby maintaining acceptable fibre tensile properties. Chapter 5 explores these proposals with the added advantage of being able to use the more sophisticated filament extruder.

Chapter 5: Effects of Ultrasound on Polyamide 6 (PA6) Filament / Fabric Properties

5.1 Introduction

In our previous work (Chapter 4) we used 2 wt% of nanoclay with different levels of ultrasonic power and concluded that the 100 W ultrasonic power unit with 90% amplitude (90 W) was the most effective in terms of maximising dispersion. In this study using the same ultrasonic power, compounded samples of PA6 containing various flame retardants present at 10 wt% in the absence and presence of selected clays at 1 and 2 wt% are produced and filaments were extruded using the more recently purchased Fibre Extrusion Technology (FET) extruder designed to produce finer and more regular filaments than the Lab-line extruder used in the previous chapter. In using this newer extruder, which extruded filaments vertically and replicated more accurately a commercial extrusion system, it was expected that higher quality and finer filaments will be produced which will facilitate their more accurate characterisation and also conversion into knitted fabrics for subsequent testing. The effect of ultrasound on potential polymer degradation has been studied by measuring relative viscosity and crystallinity of the samples without / with application of ultrasound.

5.2 The flame retardant potential of nanoclays dispersed with aluminium diethyl phosphinate in PA6

In this work, the flame retardant aluminium diethyl phosphinate as Exolit OP 935 was introduced at the increased concentration of 10 wt% compared with the 5 wt% level used in the previous chapter. The clay selected was Cloisite 25A which was shown to be unreactive with the molten polyamide 6.

5.2.1 Materials

The grade of polyamide 6 selected was the same as in the previous chapter, namely, Technyl C 301 Natural, Rhodia, France and the nanoclay was Cloisite 25A, Southern Clay Products, USA, modified with dimethyl, dehydrogenated tallow quaternary ammonium sulphate (2M2HT). The flame retardant again was aluminium diethyl phosphinate, Exolit OP 935, Clariant (note that this is fibre grade in that its average particle diameter is < 10 μm).

5.2.2 Sample matrix

The sample matrix is shown in Table 5.1 and was designed based on previous experience. In each stage of the processing samples were selected as explained in the Chapter 3, Section 3.2.2.

In this work the same twin screw extruder has been used to compound samples with and without application of ultrasound at 90 W as explained in the Chapter 3, Section 3.2.3. The temperatures in the six zones of the compounder were 210, 225, 230, 230, 240 and 245 °C.

Table 5.1: Sample matrix for PA6.

Sample	Without ultrasonic probe	100W Ultrasonic probe with 90% amplitude (90W)
PA6	Ch, St, Tp, Fil, Fab	Ch, St, Tp, Fil, Fab
PA6/25A(1 wt%)	Ch, St, Tp, Fil, Fab	Ch, St, Tp, Fil, Fab
PA6/25A(2 wt%)	Ch, St, Tp, Fil, Fab	Ch, St, Tp, Fil, Fab
PA6/Al-Phos(10 wt%)	Ch, St, Tp, Fil, Fab	Ch, St, Tp, Fil, Fab
PA6/25A(2 wt%)/Al-Phos(10 wt%)	Ch, St, Tp, Fil, Fab	Ch, St, Tp, Fil, Fab

Notes: Ch = Compounded chips, St = Strands, Tp = Tape, Fil = Filaments, Fab = Fabric.

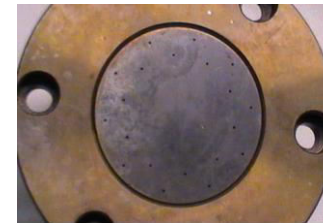
5.2.3 Melt extrusion in to filaments / tapes

The above compounded samples were extruded into filaments by using 20 holes spinneret (\varnothing 0.8 mm) and tapes by using 20 mm tape spinneret as shown in Figures 5.1(b and c) using the recently installed Fiber Extrusion Technology (FET) extruder (Figure 5.1(a)). Samples were introduced into the extruder through the hopper with diameter of 51 mm

and it was passed through the extruder screw (ϕ 21 mm with L/D = 30:1 with four different temperature zones and finally via a metering pump which accurately feeds molten polymer to the spinneret die head where it was extruded by using either a spinneret die into 0.8 mm filaments or a tape die with a 20 mm wide slit. Extruded filaments were air-quenched then had applied a spin finish and passed through three sets of godets to draw the filaments. Finally drawn filaments were wound by using Leesona winder (Figure 5.1(d)).

In greater detail, the pellet samples were dried in a laboratory oven at 80 °C for 24 hours to avoid the effect of moisture in the extrusion process. The FET extruder barrels has four zone barrels and die head zone maintained at temperatures of 235, 245, 245, 245 and 245 °C respectively. During the extrusion process for all PA6 samples as shown in Table 5.1, the pre-pump pressure was 50 bar, the metering pump and screw speed as 10 rpm. To avoid the blockage of the capillary of spinneret die due to the particles (by the so-called “bridging effect”) in the extrusion process of the additives with PA6, the 0.80 mm capillary dimension spinneret die was used because the 0.50 mm capillary diameter one failed to extrude continuous filaments due to the bridging of particles in the spinneret die capillaries causing their blockage. The 0.80 mm capillary die gave good linear density uniformity and enabled adequate molten filament draw down to yield good spinning performance. Molten filaments were quenched with air at a controlled temperature of 15 °C and 20 m³/s flow rate to ensure good linear density and orientation uniformity. When either temperature or flow rate was lower than this value, filaments were breaking, whereas and higher values made them brittle. Spin finish was applied to the extruded filaments through a 30 rpm pump, which passed through a dual type nozzle application system using low friction ceramic nozzles. When the speed increased above 30 rpm, filaments started to stick on the godet rollers and if it reduced filaments were broken. These oil-dispersion jets are claimed to distribute the spin-finish evenly around and within the filament yarn cross-section. For preparing spin finish solution, we used water with 5 vol% of spin finish. Spin finish selected for PA6 is JKI-N815 (combination of triglyceride, non-ionic emulsifiers and antistats). The filaments were then collected over the cooling rollers or godets. The collecting godet pair below the spin-finish application zone had a surface speed of 100 m/min at 25 °C temperature. The filament bundle then passed to a further two godet pairs which form the stretching zone for drawing the filaments in stages. This set of godets was adjusted to a surface speed of 105 m/min and 50 °C temperature.

The third pair was maintained on 130 m/min and 50 °C temperature. These temperatures and relative speed differences help to keep tension to ease the winding process. At the end of the process filament yarn bundle was wound by a Leeson winder (see Figure 5.1(d)) maintained on 135 m/min. All the processing conditions were controlled and monitored by a Human Machine Interface (HMI) PC system with draw ratio of 1.3:1. Tapes were collected instantly after the extrusion of tape without drawing.



(b) Single filament spinnerette (20 holes Ø 0.8)



(c) Tape spinnerette



(d) Leesona winder

Figure 5.1: Photographic, labelled diagrams of the FET extruder.

5.2.4 Fabric production

For each filament yarn sample, sufficient lengths were extruded to test them as filament yarns and to knit into fabrics using a hand-powered V-bed rib flat machine. The area density of each fabric was controlled by the gauge of the machine. The flat knitting machine used employs straight needle beds carrying independently operated needles and their gauge selected was 11.

5.2.5 Characterisation of filaments / tapes / fabric samples

All the above filament samples were characterised as described previously in the Chapter 3, Section 3.3 and the same equipment and procedures were used under the same conditions as explained in the section.

5.3 Results and discussion

5.3.1 Tensile properties

Tensile testing of filament yarns was carried out by using a Textechnic Statimat M test. Results together with yarn linear densities are shown in Table 5.2. Generally well-dispersed nanoclay increases the initial modulus, reduces breaking elongation and has a small effect on tenacity. According to the results in the Table 5.2, the initial modulus is slightly changed but not significantly in the presence of nanoclay or flame retardant with respect to the value of PA6 of 110 ± 21 cN/tex, but its increased to 149 cN/tex ($\pm 9\%$) with the presence of both nanoclay and flame retardant and little changed after exposure to ultrasound. Generally, however, exposure to ultrasound has slightly increased the modulus for all of the samples except PA6/Al-Phos(10 wt%)/90W, although these increases are within the error of results and so may not be real. Coefficients of variation (CV) of modulus have decreased with the presence of nanoclay and / or flame retardant and are little affected by ultrasound.

According to Table 5.2, elongation-at-break for the samples containing nanoclay with and without ultrasound fluctuate with respect to the value of $292 \pm 23\%$ for 100% PA6, but in the presence of Al-Phos(10 wt%) shows a reduction of nearly 50% although this has increased following exposure to ultrasound. Samples containing nanoclay and flame retardant (PA6/Al-Phos(10 wt%)/25A(2 wt%)) also show a considerably decreased value

for elongation-at-break and this is significantly decreased further after exposure to ultrasound.

Table 5.2: Tensile properties for PA6 filament yarns

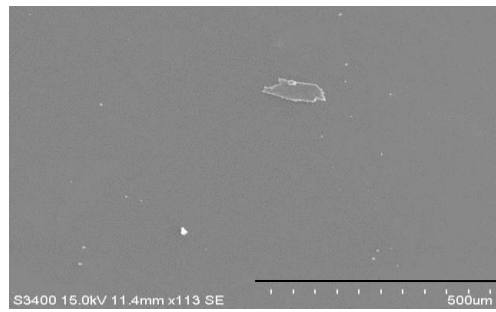
Sample	Linear density (tex)	Modulus (cN/tex) and CV(%)	Tenacity (cN/tex) and CV(%)	Elongation-at -break (%) and CV(%)
PA6	86	110 (21)	18 (24)	292 (23)
PA6/25A(1 wt%)	79	110 (12)	17 (15)	320 (3)
PA6/25A(1 wt%)/90W	50	113 (12)	16 (10)	288 (9)
PA6/25A(2 wt%)	86	96 (8)	18 (8)	242 (7)
PA6/25A(2 wt%)/90W	79	106 (11)	16 (6)	312 (8)
PA6/Al-Phos(10 wt%)	82	107 (15)	8 (7)	166 (5)
PA6/Al-Phos(10 wt%)/90W	76	96 (14)	14 (6)	215 (10)
PA6/25A(2 wt%)/Al-Phos(10 wt%)	87	149 (9)	14 (0)	242 (3)
PA6/25A(2 wt%)/Al-Phos(10 wt%)/90W	79	150 (4)	14 (24)	217 (30)

5.3.2 Characterisation of tapes by SEM and EDS

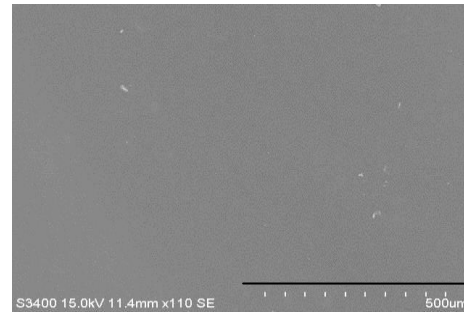
Extruded tapes were examined by scanning electron microscopy (SEM). The SEM images are shown in Figure 5.2, from which it may be seen that the PA6/25A(1 wt%)/90W sample shows no white clay aggregates and so the clay is more dispersed than in PA6/25A(1 wt%) where a small number of aggregates is evident. PA6/25A(2 wt%)/Al-Phos(10 wt%)/90W shows significant improvement in dispersion after ultrasonic application. This is the evidence that shows that ultrasonication helps to improve the clay and flame retardant dispersion as observed previously in Chapter 4 (Section 4.4.1).

EDS images were shown to be better indicators of particle dispersion in the previous work on PP and PA6 (see Chapters 3 and 4) and so again this technique was used to map silicon aggregates as well as for the elements P and Al for the samples containing Al-Phos flame retardant. EDS images are given in Figure 5.3, from which it is evident that the number of Si dots in the PA6/25A clay-only samples appears to be decreased after ultrasound

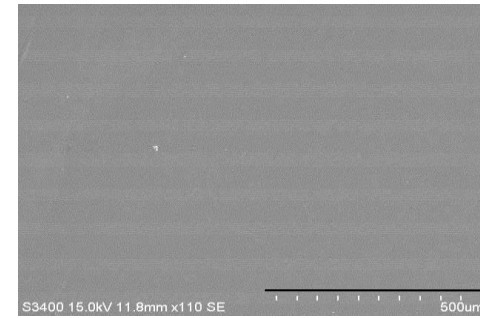
exposure and same is observed for P and Al elemental aggregations in the flame retarded samples in Figures 5.4 and 5.5 respectively. It must be remembered that the resolution of the SEM/EDS equipment is sufficient only to resolve details of 1 micron or greater and so a reduction in dot frequency may be assumed to be matched by an increase in nanoparticle density. Thus Figures 5.4 and 5.5 suggest that application of ultrasound reduces P and Al dot intensity as the Al-Phos aggregates are reduced in size. To confirm these results the Data Cell software was used for the quantitative analysis of Si, P and Al mappings and Tables 5.3, 5.4 and 5.5 summarize these results and included in Table 5.3 are the Si results for the PA6 granules prior to extrusion into tapes. Surprisingly the PA6/Al-Phos samples, while showing low concentrations of Si dots, also show the highest Si dot area densities and this may be a consequence of contamination of the sample because of the difficulty of purging - both compounder and extruder after each experiment, PA6 samples also show some P and Al concentrations due to the contamination. P dots per unit area of the samples slightly decreased only for the PA6/25A(2 wt%)/Al-Phos(10 wt%) sample with the presence of ultrasound but Al dot numbers decreased for both Al-Phos-containing samples.



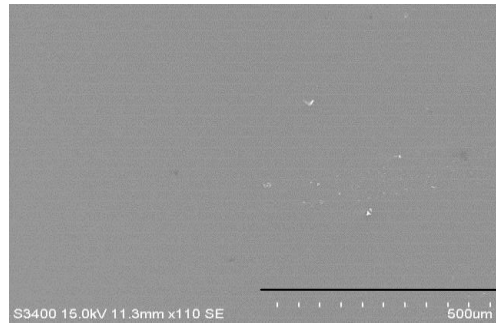
PA 6



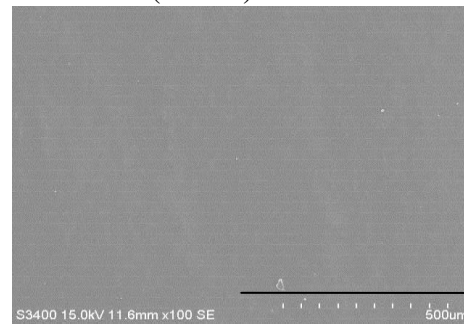
PA6/25A(1 wt%)



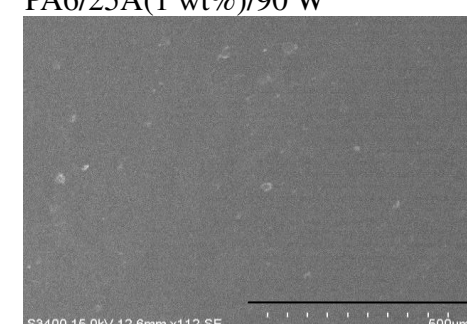
PA6/25A(1 wt%)/90 W



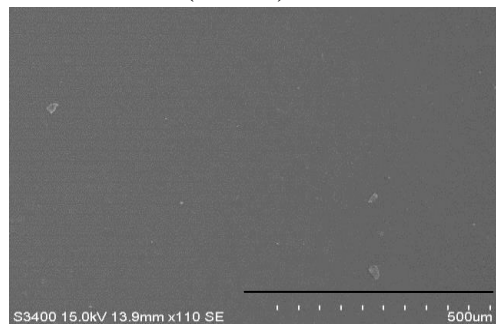
PA 6/25A(2 wt%)



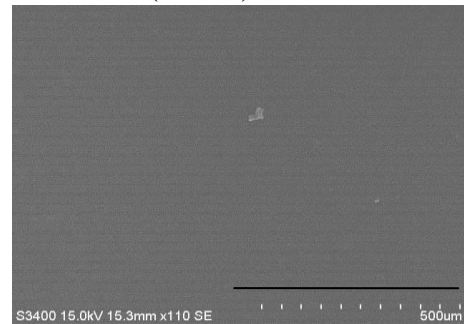
PA 6/25A(2 wt%)/90W



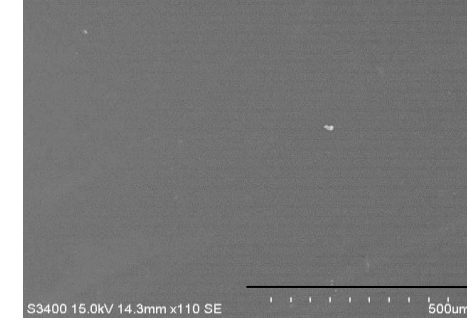
PA6/Al-Phos(10 wt%)



PA6/Al-Phos(10 wt%)/90W



PA 6/25A(2 wt%)/Al-Phos(10 wt%)



PA 6/25A(2 wt%)/Al-Phos(10 wt%)/90W

Figure.5.2: SEM images for compounded PA6 samples.

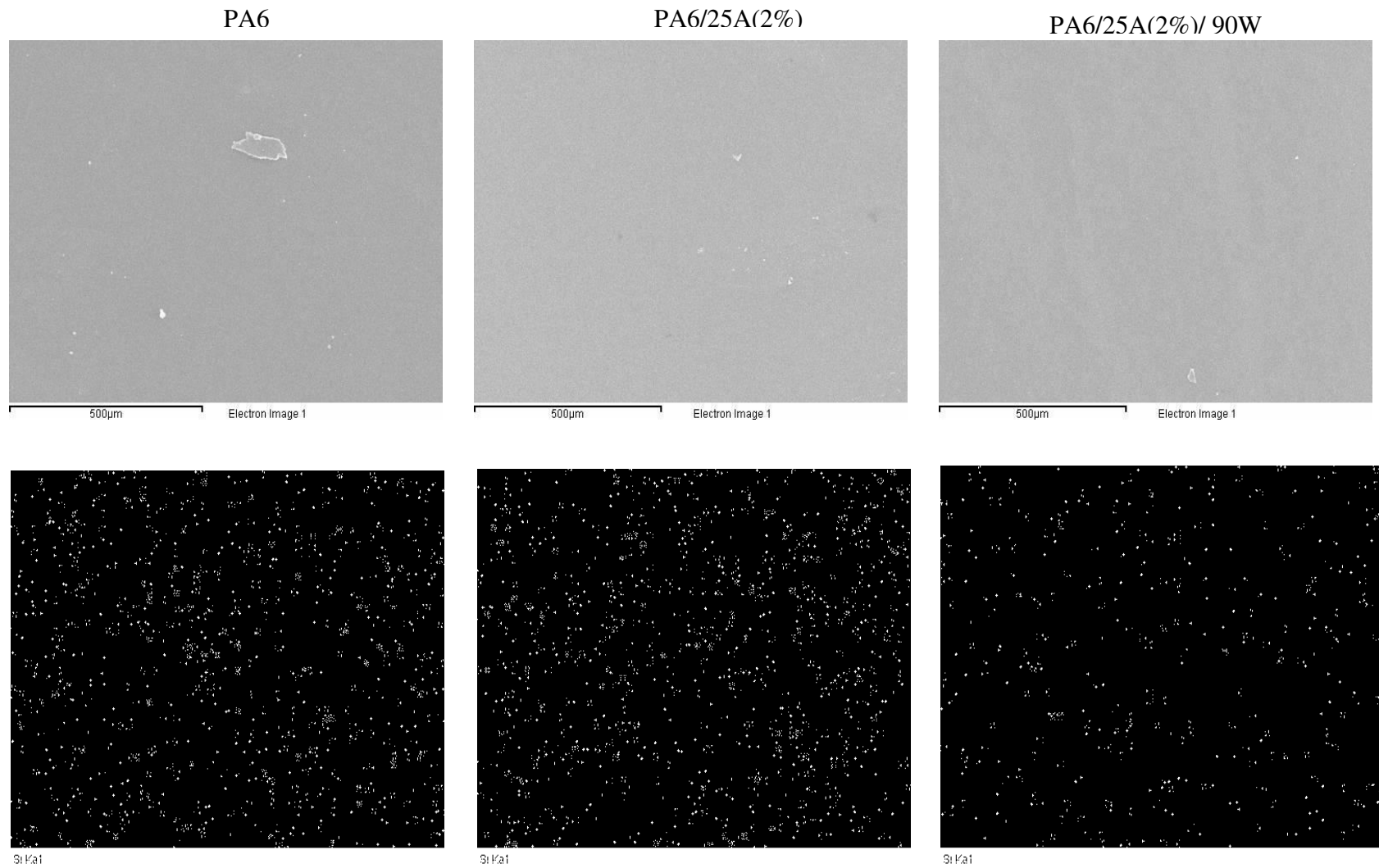
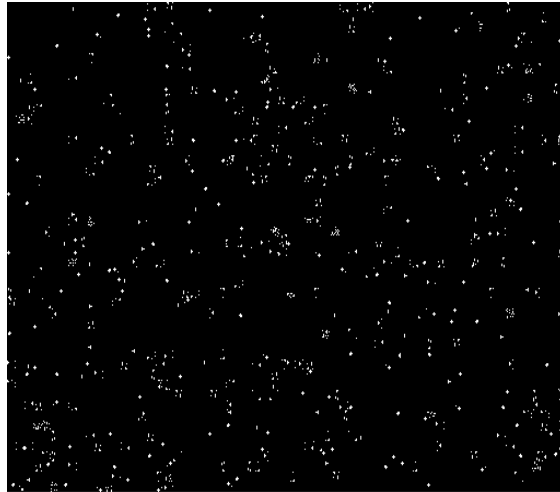


Figure 5.3: EDS silicon dot images alongside their respective SEM images for PA6 containing 2 wt% clay only (Si dots).

PA6/ Al-Phos(10%)



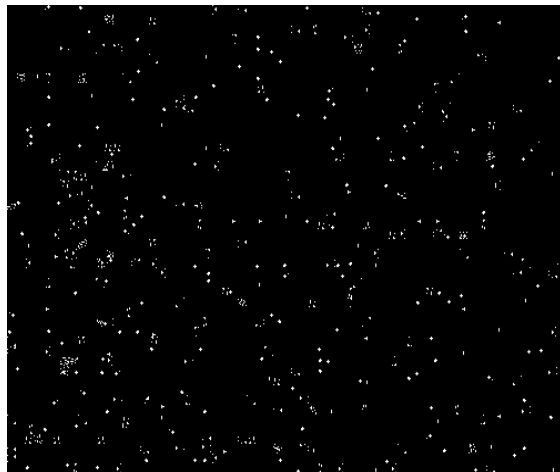
P Kα1

PA6/ Al-Phos(10%)/90W



P Kα1

PA6/25A(2%)/ Al-Phos(10%)



P Kα1

PA6/25A(2%)/Al-Phos(10%)/90W



P Kα1

Figure 5.4: EDS images phosphorus dots for PA6 samples containing Al-Phos (P dots).

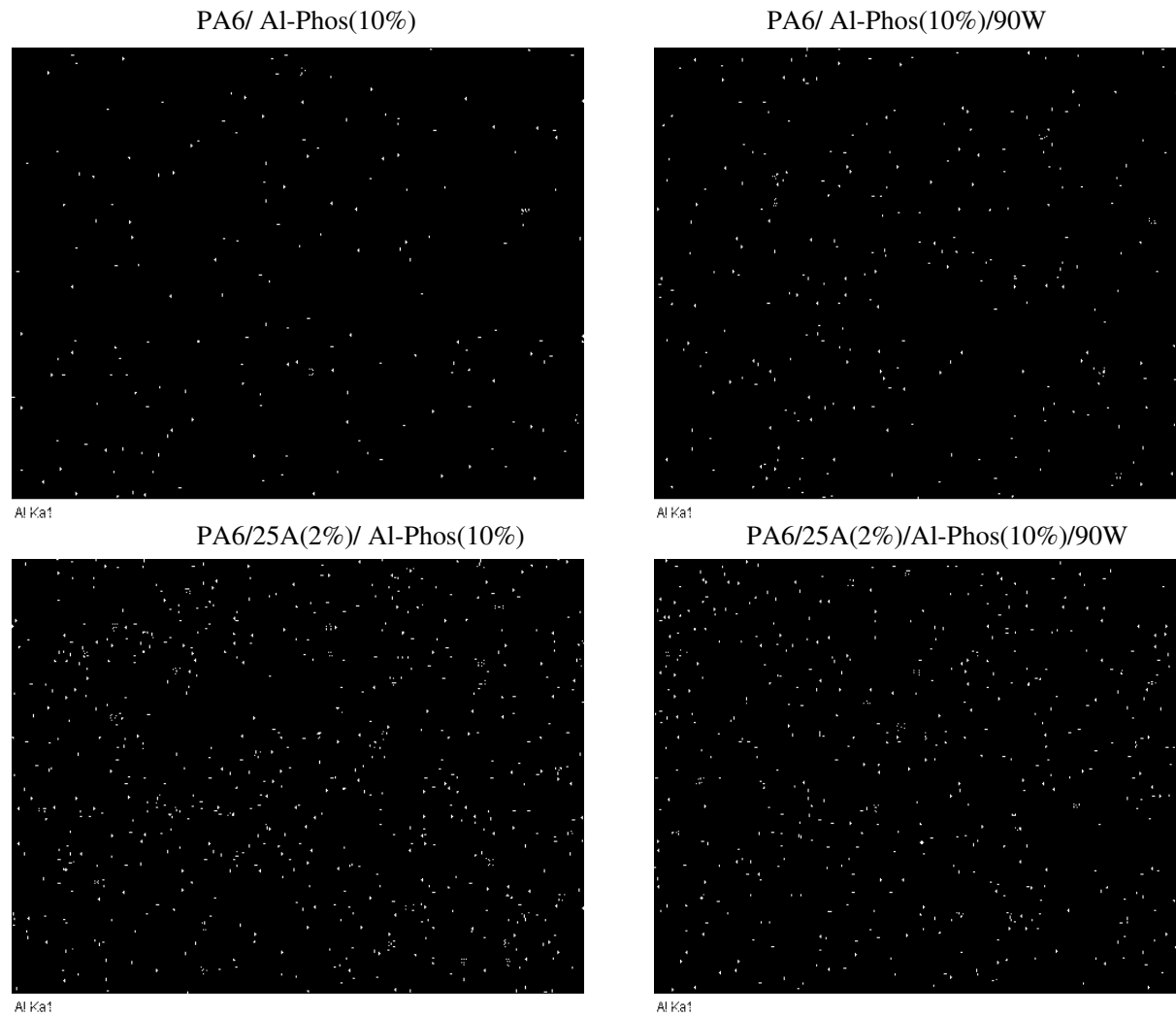


Figure 5.5: EDS images for aluminium dots for PA6 samples containing Al-Phos (Al dots).

Table 5.3: Si dot quantitative analysis.

Sample	Number of Si Dots and CV(%)	Si Dot Ratio	Si Dot per unit area and CV(%) (Dots/mm ²)
PA6(granule)	7 (17)	0.987	135923 (18)
PA 6(tapes)	25 (18)	0.987	494257 (14)
PA6/25A(1 wt%)	24 (15)	0.987	448341 (8)
PA6/25A(1 wt%)/90W	28 (9)	0.986	490564 (7)
PA6/25A(2 wt%)	44 (7)	0.979	526721 (8)
PA6/25A(2 wt%)/90W	29 (24)	0.983	420665 (7)
PA6/Al-Phos(10 wt%)	13 (9)	0.996	538413 (20)
PA6/Al-Phos(10 wt%)/90W	6 (13)	0.997	498984 (16)
PA6/25A(2 wt%)/Al-Phos(10 wt%)	25 (10)	0.989	504083 (15)
PA6/25A(2 wt%)/Al-Phos(10 wt%)/90W	21 (9)	0.987	486548 (9)

Table 5.4: P dot quantitative analysis.

Sample	Number of P Dots and CV(%)	P Dot Ratio	P Dot per unit area and CV(%) (Dots/mm ²)
PA6	8 (10)	0.085	12525 (9)
PA6/Al-Phos(10 wt%)	23 (10)	0.987	446315 (7)
PA6/Al-Phos(10 wt%)/90W	30 (24)	0.983	429026 (6)
PA6/25A(2 wt %)/Al-Phos(10 wt%)	36 (14)	0.983	508043 (8)
PA6/25A(2 wt %)/Al-Phos(10 wt%)/90W	16 (49)	0.992	493352 (8)

Table 5.5: Al dot quantitative analysis.

Sample	Number of Al Dots and CV(%)	Al Dot Ratio	Al Dot per unit area and CV(%) (Dots/mm ²)
PA6	4 (2)	0.0521	9425 (6)
PA6/Al-Phos(10 wt%)	12 (30)	0.994	459720 (8)
PA6/Al-Phos(10 wt%)/90W	8 (45)	0.996	482446 (10)
PA6/25A(2 wt %)/Al-Phos(10 wt%)	22 (30)	0.989	468183 (2)
PA6/25A(2 wt %)/Al-Phos(10 wt%)/90W	10 (37)	0.995	444319 (9)

5.3.3 Limiting oxygen index

Limiting oxygen index tests were carried out by using the standard ASTM- 2863 test method on tapes and results are given in Table 5.6. According to these results, LOI values are unchanged with and without exposure to ultrasound in the presence of nanoclay and similar to the PA6 value of 20.6 vol%. Addition of the flame retardant Al-Phos has increased the LOI value to 23.9 vol% without and further increased to 24.6 vol% after ultrasound exposure of the sample. Addition of both clay and flame retardant showed a further significant increase to 24.3 vol% and ultrasound exposure gave the highest value of 25.2 vol%. Burning rates of the samples decreased in the presence of clay only and further decreased following the addition of flame retardant. Exposure to ultrasound appears to reduce the respective burning rates of PA6/25A(2 wt%) and PA6/Al-Phos(10 wt%) samples with little effect on the values for PA6/25A(2 wt%)/Al-Phos(5 wt%) samples.

The above results show the expected effects of clay on burning rate and of Al-Phos on both LOI and burning rate. The effect of ultrasound also appears to have a generally beneficial effect in improving the flame retardancy of the PA6 compounded samples containing either or both of these additives.

Table 5.6: Limiting oxygen index values of PA6 tapes.

Sample	LOI (Vol-%)	Burn time (s)	Burn Length (mm)	Burning rate (mm/s)
PA 6	20.6	50	80	1.60
PA 6/25A(1 wt%)	20.8	85	60	0.71
PA 6/25A(1 wt%)/90W	20.2	65	30	0.46
PA 6/25A(2 wt%)	20.3	50	20	0.40
PA 6/25A(2 wt%)/ 90W	20.5	80	30	0.38
PA6/Al-Phos(10 wt%)	23.9	15	10	0.67
PA6/Al-Phos(10 wt%)/90W	24.6	20	10	0.50
PA6/Al-Phos(10 wt%)/25A(2 wt%)	24.3	30	10	0.33
PA6/Al-Phos(10 wt%)/25A(2 wt%)/90W	25.2	30	10	0.33

5.3.4 UL-94 testing

Cast plaques were tested to the UL-94 procedure both in horizontal and vertical orientations according to the separate standard test methods. Times for the flame to extinguish after 1st (T₁) and after 2nd (T₂) ignitions were recorded. The melt drips were counted by used the video clips for the corresponding experiments. Table 5.7 illustrates the vertical and Table 5.8 the horizontal modified UL-94 results. Each sample was tested three times to give the individual and averaged results in these tables.

According to the vertical UL-94 test result from the point of view of the pass / fail criteria, all samples failed. However, the presence of nanoclay and flame retardant together helped to reduce burning rate, as illustrated by the PA6/Al-Phos(10 wt%) sample having a reduced burning rate of 0.8 mm/s compared with 0.9 mm/s for the 100% PA6 sample. The effect of ultrasonification was mixed with the PA6/25A(2 wt%) and PA6/Al-Phos(5 wt%) samples showing an increase and the PA6/25A(2 wt%)/Al-Phos(5 wt%) sample a decrease compared with the respective unsonicated samples. The number of drops per second reduced in presence of clay and / or flame retardant with and without ultrasound and with the latter having the greatest effect.

When burning rates and dripping rates are considered together, in the case of PA6/25A(2 wt%)/Al-Phos(10 wt%), the burning rate has decreased from 0.9 of 100% PA6 to 0.7-mm/s and number of drops per second has reduced from 1.3 of 100 % PA6 to 0.04 s⁻¹. Both these values further decreased in the sample exposed to ultrasonic power. Furthermore, while presence of nanoclay alone at 1 and 2 wt% levels reduced the rate of dripping of PA6 and these respective values reduced further in the sonicated samples. However, presence of the flame retardant changed the dripping behaviour to one of burning aggregates or lumps and ultrasound now appeared to have little effect on dripping rate for both the PA6/Al-Phos(10 wt%) and PA6/25A(2 wt%)/Al-Phos(10 wt%) samples.

According to the horizontal UL94 test results in Table 5.8, samples again fail. In fact, while the addition of nanoclay alone increases the burning rate at 2 wt % level and ultrasonification increases it for both 1 and 2 wt% clay levels, in the PA6/Al-Phos(10 wt%) samples, no burning after ignition flame removal is observed. When both clay and flame reatardant are present, still some burning does occur and ultrasonification appears to increase the burning rate of the PA6/25A(2 wt%)/Al-Phos(10 wt%) sample.

Table 5.7: Flame spread results after UL-94 testing in the vertical orientation.

Sample	Sample 1				Sample 2				Sample 3				Average		Pass / Fail
	T1 (s)	T2 (s)	Number of drops	Burnt length (mm)	T1 (s)	T2 (s)	Number of drops	Burnt length (mm)	T1 (s)	T2 (s)	Number of drops	Burnt length (mm)	Burning Rate (mm/ s)	Number of drops per second (s ⁻¹)	
PA6	10	42	72	50	46	18	75	75	112	0	136	75	0.9	1.3	Fail
PA6/25A(1 wt%)	25	11	28	25	33	38	80	75	26	13	41	40	0.9	1	Fail
PA6/25A(1 wt%)/90W	10	65	68	50	5	7	12	30	38	16	40	50	1.4	0.9	Fail
PA6/25A(2 wt%)	145	0	127	100	146	0	109	100	147	0	147	100	0.7	0.9	Fail
PA6/25A(2 wt%)/90W	28	7	22	50	139	0	112	100	65	20	47	65	1	0.7	Fail
PA6/Al-Phos(10 wt%)	0	2	No	No	0	75	1 Lump	50	0	55	No	50	0.8	0.01	Fail
PA6/Al-Phos(10 wt%)/90W	6	12	No	No	0	151	No	No	97	0	2 Lumps	100	1	0.02	Fail
PA6/25A(2 wt%)/Al-Phos(10 wt%)	24	9	2 Lumps	50	105	3	3 Lumps	90	19	37	No	0	0.7	0.04	Fail
PA6/25A(2 wt%)/Al-Phos(10 wt%)/90W	36	4	2 Lumps	35	83	43	1 Lump	50	42	13	3 Lumps	25	0.6	0.04	Fail

Table 5.8: Flame spread results after UL-94 testing in the horizontal orientation.

Sample	Sample 1				Sample 2				Sample 3				Average	
	T1 (s)	T2 (s)	Number of drops	Burnt length (mm)	T1 (s)	T2 (s)	Number of drops	Burnt length (mm)	T1 (s)	T2 (s)	Number of drops	Burnt Length (mm)	Burning Rate (mm/ s)	Number of drops per second (s ⁻¹)
PA6	25	385	360	100	334	0	344	100	371	0	360	100	0.3	1
PA6/25A(1 wt%)	361	0	344	100	459	0	344	100	348	0	295	100	0.3	0.8
PA6/25A(1 wt%)/90W	300	0	287	100	218	215	355	100	108	131	206	75	0.3	1.2
PA6/25A(2 wt%)	270	0	212	100	279	0	193	100	348	0	212	100	0.4	0.7
PA6/25A(2 wt%)/90W	248	0	212	100	294	0	201	100	260	0	205	100	0.4	0.8
PA6/Al-Phos(10 wt%)	Not Burnt													
PA6/Al-Phos(10 wt%)/90W	Not Burnt													
PA6/25A(2 wt%)/Al-Phos(10 wt%)	2	26	No	5	4	58	No	5	0	28	No	No	0.13	No
PA6/25A(2 wt%)/Al-Phos(10 wt%)/90W	0	97	1 Lump	50	2	2	No	No	0	5	No	No	0.51	0.01

5.3.5 Vertical fabric strip testing and flame spread





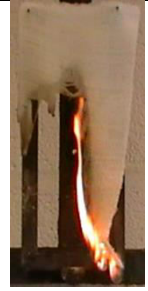


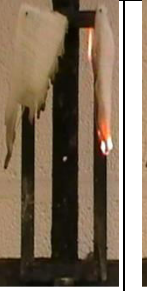
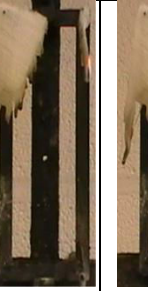



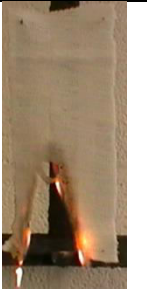



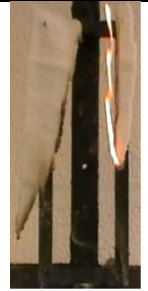






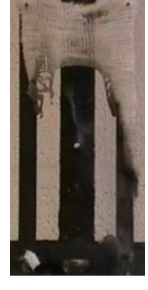
All knitted fabrics were used for flame spread test using the rig described in BS 5438 and their summarized test results are given in Table 5.9. Area densities of fabrics have increased with the presence of nanoclay and / or flame retardants and then appeared to have decreased with the presence of ultrasonic application. Generally ultrasonic cavitation generates high shear that breaks up single dispersed particles; due to this reason area density might be decreased with the application of ultrasound. However, these trends could also result from effects of introducing clay and flame retardant of higher densities to the polymer they replace coupled with the effects that additive and ultrasound have on the spinning characteristics of respective polymer formulations.

With regard to burn time and length effects, in the case of PA6/25A(2 wt%) with and without ultrasound no significant differences are seen, but presence of flame retardants with and without ultrasonic significantly effect the burnt time and burnt length. Presence of flame retardant significantly decreased the burning time from 61 s for 100 % PA6 to 22 s, also its reduced number of drops per second from 1.8 for 100 % PA6 to 0.3 drops per second. Addition of nanoclay and flame retardant slightly increased the rate of burning, but significantly decreased the number of drops per second from 1.8 of 100 % PA6 to 0.1s^{-1} and this further reduced after exposure of ultrasound. Percentages of mass of the molten / burnt drop of PA6/Al-Phos(10 wt%)/25A(2 wt%)/90W reduced by half of the 100 % PA6 value. Figure 5.6 shows the burning behaviour in 10 s of time interval, when the addition of flame retardant reducing shrinkage and number of lumps; also ultrasound decreased number of lumps. Hence, the application of ultrasound helped to reduce flame spread.

Table 5.9: Flame spread results of PA6 fabrics.

Sample	Area density of fabric (g/m ²)	Total Burn time and CV% (s)	Burnt height and CV% (mm)	flame spread (mm/s)	Number of drops	Number of drops per second and CV% (s ⁻¹)	Total mass loss (%)	Mass of the molten /burnt drops (g)	Mass of the molten /burnt drops (%)
PA 6	400	61 (27)	173(14)	3.0(26)	107	1.8(16)	15	3.7	55
PA 6/25A(1 wt%)	499	75(23)	168(24)	2.2(11)	161	2.2(8)	19	4.4	50
PA 6/25A(1 wt%)/90W	429	65(48)	159(35)	3.2(83)	122	2.0(22)	17	3.5	46
PA 6/25A(2 wt%)	505	61(14)	187(11)	3.0(8)	119	1.9(12)	20	3.5	38
PA 6/25A(2 wt%)/ 90W	459	86(47)	196(14)	2.6(35)	155	1.9(29)	18	3.9	47
PA6/Al-Phos(10 wt%)	412	22(34)	173(5)	9.4(60)	17	0.3(86)	32	1.0	19
PA6/Al-Phos(10 wt%)/90W	452	55(50)	200(2)	4.1(31)	14	0.3(36)	21	2.6	33
PA6/Al-Phos(10 wt%)/25A(2 wt%)	453	52(28)	198(4)	4.0(21)	3	0.1(49)	26	3.7	48
PA6/Al-Phos(10 wt%)/25A(2 wt%)/90W	508	93(36)	196(4)	2.4(37)	3	0.0(53)	41	2.1	24

Time (s)	0	10	20	30	40	50	60	70	80	90	100
PA6											
PA6 / 25A(1%)											
PA6 / 25A(1%) / 90W											

Time (s)	0	10	20	30	40	50	60	70	80	90	100
PA6 / 25A(2%)											
PA6 / 25A(2%)/90W											
PA6 / Al-Phos(10%)											









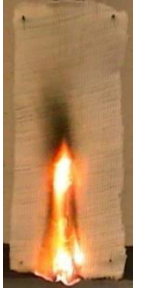

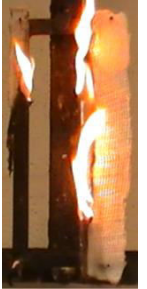




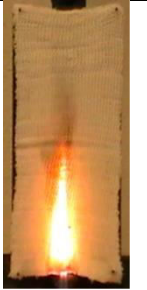


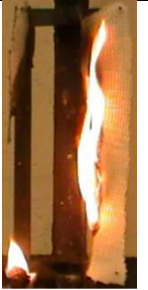


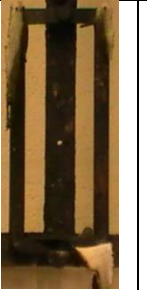
Time (s)	0	10	20	30	40	50	60	70	80	90	100
PAG / Al-Phos(10%)/90W											
PA 6 / Al-Phos (10%) / 25A (2 %)											
PA 6 / Al-Phos (10%) / 25A (2 %) / 90W											

Figure 5.6: Snap shots of the flame spread experiment in 10s time interval.

5.3.6 Effect of ultrasound on PA6 degradation

5.3.6.1 Relative viscosity measurements

High intensity ultrasound can cause chemical changes in the PA6 by changing the structures of the original molecules, resulting in changes in molecular weight and molecular weight distribution. This could also affect its viscosity and hence melt dripping behaviours as well as subsequent filament physical properties.

Relative viscosity of polymer solutions enables a simple semi-quantitative measure of changes in molecular weight to be determined. This technique was undertaken using an ASTM D 445 Ubbelohde viscometer. The viscometer is size 1 with an inside diameter of $0.58 \text{ mm} \pm 2\%$. To 5.5 g of nylon polymer 50 ml of 94 % formic acid was added at $25 \text{ }^\circ\text{C}$ in a 100 ml glass beaker. The mixture was stirred using a magnetic stirrer until all polymer was dissolved. 10-18 ml of above solution was added to the viscometer with a volumetric pipette. The viscometer was immersed in a constant temperature bath at $25 \text{ }^\circ\text{C}$ and kept there for 20 minutes. The air arm (see Figure 5.7) was blocked and air pressure was applied to the capillary arm tube by using pipette filler rubber bulb. Solution then passed into the capillary until solution meniscus reached above the upper timing mark. The air arm was un-blocked and solution was allowed to flow down. The time (t) was recorded for the solution to fall from the upper timing mark to the lower timing mark as show in the Figure 5.6.

The kinematic viscosity (ν) = kt , where k is the viscometer constant and the relative viscosity (RV) is defined as the kinematic viscosity of the polymer solution divided by that of the pure solvent. Thus $RV = t_{ps} / t_s$ where t_{ps} is the time of flow of the polymer solution and t_s that of the pure solvent.

The relative viscosity values are as shown in Table 5.10. Addition of nanoclay and / or flame retardant slightly increased the density, which was not much affected by ultrasonication. Viscosity values are slightly increased with the presence of nanoclay and / or flame rertardant, but presence of ultrasound slightly decreased these values except for the PA6/Al-Phos(10 wt%)/90W condition.

Generally RV values increase as clay and flame retardant are added and the effect of ultrasound appears to have a marginal effect suggesting that any accompanying chemical degradation is negligible or absent.

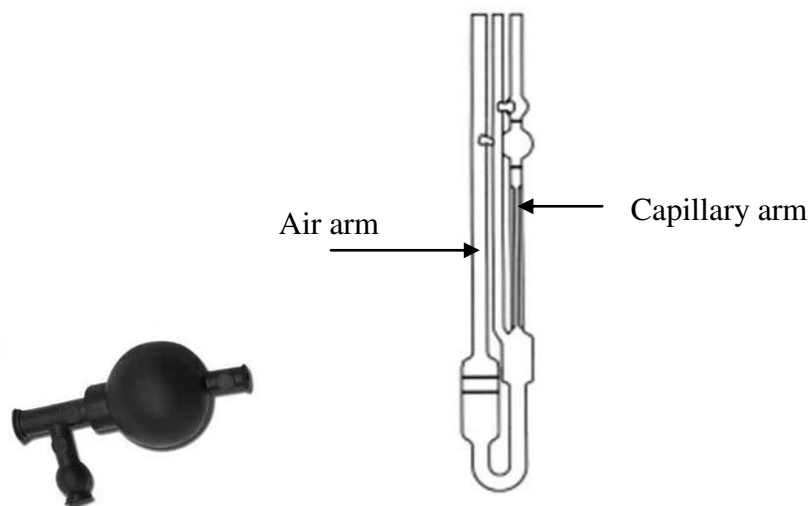


Figure 5.7: Volumetric pipette and Ubbelohde viscometer.

Table 5.10: Relative viscosity of PA 6.

Sample	Density (d_p) (g/ml)	Time (t) (s)	Viscosity $R_v \propto t_p \times d_p$	RV Relative Viscosity
Formic Acid	1.00	341	343	-
PA 6	1.01	3229	3261	9
PA 6/25A(1 wt%)	1.03	5660	5830	17
PA 6/25A(1 wt%)/90W	1.02	5213	5317	15
PA 6/25A(2 wt%)	1.04	6142	6388	19
PA 6/25A(2 wt%)/ 90W	1.04	5949	6187	18
PA6/Al-Phos(10 wt%)	1.17	8240	9641	28
PA6/Al-Phos(10 wt%)/90W	1.17	8649	10162	30
PA6/Al-Phos(10 wt%)/25A(2 wt%)	1.21	9600	11615	34
PA6/Al-Phos(10 wt%)/25A(2 wt%)/90W	1.21	9435	11464	33

5.3.7 Crystallinity

Differential scanning calorimetric (DSC) is a technique that measures heat flow into or out of a material as a function of time or temperature. Polymer crystallinity can be determined with DSC by quantifying the heat associated with melting of the polymer. This heat is reported as percent crystallinity by normalizing the observed heat of fusion to that of a 100 % crystalline sample of the same polymer. 100% polymers are rare, literature values are often used for this value.

Differential scanning calorimetric (DSC) experiments were conducted using a TA –DSC instrument, under flowing nitrogen atmosphere (50 ml/min) and a heating rate of 10 °C/min from room temperature to 300 °C. About 10 mg of sample was taken in each case against an empty pan as reference. As heat was transferred through the sensor, the differential heat flow to the sample and reference was monitored by thermocouples. The melting endotherm was recorded and Universal Analysis Software was used to calculate percent crystallinity based upon 230.1 J/g for the 100% crystalline material and the results displayed in Table 5.11.

Results showed that the degree of crystallinity of the PA6/25A(1 wt%) slightly increased and remains unaffected by the presence of ultrasound. It tends to decrease slightly with increasing clay content as 2 wt% and decreased considerably with the presence of ultrasound.

The degree of crystallinity decreased with the presence of flame retardant only (Al-Phos (10 wt%)) and remained unchanged after exposure to ultrasonic power. However, a significant reduction occurred in the presence of both clay and flame retardant (from 26.1 to 22.5%) and further decreased when the presence of ultrasound (from 22.5 to 19.5%).

This is due to the creation of higher interfacial area between the polymer matrix and the clay, which acts to reduce the mobility of polymer chains. Apparently, the interaction of polymer matrix and clay may be increased by ultrasonic treatment, thus decreasing crystallinity.

Table 5.11: Relative crystallinities of PA6 formulations.

Sample	Melt on Temperature (°C)	Melt peak Temperature (°C)	Enthalpy (J/g)	Crystallinity (%)
PA6	211.69	223.10	60.17	26.15
PA6/25A(1 wt%)	211.06	222.17	64.39	27.98
PA6/25A(1 wt%)/90W	212.07	222.46	66.51	28.90
PA 6/25A(2 wt%)	209.63	222.21	60.51	26.30
PA 6/25A(2 wt%)/90W	210.87	222.30	58.75	25.53
PA 6/Al-Phos (10 wt%)	210.66	222.79	58.48	25.42
PA 6/Al-Phos (10 wt%)/90W	210.24	222.17	59.22	25.74
PA 6/25A(2 wt%)/Al-Phos (10 wt%)	208.82	221.89	51.73	22.48
PA 6/25A(2 wt%)/Al-Phos (10 wt%)/90W	207.97	221.05	44.06	19.15

5.4 Conclusions

Nanoclay dispersion of both clay and flame retardant in PA6 in the presence of ultrasound of 100 W with 90 % amplitude (90 W) has generally improved compared to that observed in previous work in Chapters 3 and 4, SEM and EDS image analyses have indicated that ultrasonic application improves the nanoclay dispersion.

To test flammability properties, BS5438, LOI and UL-94 tests were undertaken. LOI values slightly increased in sample containing the nanoclay and / or flame retardant and further increased with the presence of ultrasound. Modified vertical and horizontal UL-94 test demonstrated that nanoclay and / or flame retardant reduced rates of burning and number of molten drops formed, which further decreased with the presence of ultrasound. For example, in PA6/25A(2 wt%)/AlPhos(10 wt%) the burning rate and number of drops have significantly decreased, which further decreased following exposure to ultrasonic. According to the above work and analysis of the results, the PA6/25A(2 wt%)/AlPhos(10 wt%) sample shows superior performance than the others studied and its performance was enhanced by ultrasonification during compounding. The relative viscosity values increase as clay and flame retardant are added and the effect of ultrasound appears to have a marginal effect suggesting that any accompanying chemical degradation is negligible or absent.

Chapter 6: Effects of Nanoparticles on the Flame Retardancy of Ammoniumsulphamate (AS) and Dipentaerythritol (DP) Flame-Retardant System in Polyamide 6 (PA6)

6.1 Introduction

As previously stated, it has been observed that quite small additions of nanoclays can significantly improve effectiveness of conventional flame retardant treatments and nanoparticles added in the production of flame retardant products. Of particular interest is that Lewin et al confirm that small concentrations (< 2 w%) of ammoniumsulphamate (AS) and dipentaerythritol (DP) yield positive improvements in the flame retardancy of PA6 and that the further additions of nanoclays show interesting effects [88]. The background to this work has been discussed in the Literature Study, Chapter 2, Section 2.5.2. To investigate whether this effect has the potential for application to PA6 fibres, the work in Chapter 5 was extended to include ammoniumsulphamate (AS) and dipentaerythritol (DP) as combined flame retardants together with selected nanoclays in PA6. This chapter is based on our publication, which reported the flammability behaviour of polyamide 6 (PA6) nanocomposites comprising AS and DP in the presence and absence of various nanoclays and fumed silica as hot-pressed plaque samples [92]. This work was essentially that of a visiting research fellow, Dr Jai Dahyia, who compounded the samples in Table 6.1 below with assistance from myself. I also assisted other parts of this work including the thermal analysis and determination of the flammable properties. These compounded samples were examined for their thermal (TGA, DTA) and flammability properties (UL-94, LOI), and from the encouraging nature of the results, a set of samples (Table 6.2) was proposed for extrusion into filaments which would be characterised for their tensile behaviour and flammability properties after knitting into

fabric. This extension to the published work [92] is wholly my own work as a part of my PhD research.

6.2 Experimental

6.2.1 Materials

Polyamide 6, Rhodia, (Technyl C 301 Natural, Rhodia, France) was selected as polymer, ammonium sulphamate (Sigma-Aldrich) and dipentaerythritol (Fisher Scientific) were selected as flame retardants. Various nanoclays were selected namely, Nanofil 116 (pristine clay: Bentonite, particle size < 20 μm), Cloisite 25A (functionalised with dimethyl, n-hexyl, hydrogenated tallowquaternary ammonium sulphate), Cloisite 30B (functionalized with methyl, tallow, bis-2-hydroxyethyl, quaternary ammonium chloride) (Rockwood additives Ltd, Southern Clay Products Inc.) and the nano-additive, fumed silica, particle size = 0.014 μm (Sigma-Aldrich).

6.2.2 Sample preparation

Polyamide 6 (PA6) samples containing ammonium sulphamate (AS), dipentaerythritol (DP) with or without nanoclays and silica were pre-dried for 24h at 80 °C before the compounding and hand-mixed in a plastic container to distribute the components. Compounding was performed as in Chapters 3-5 using the Eurolab 16 twin screw extruder with screw speed of 350 rpm and temperature range 210 – 245 °C from the feed zone to die zone.

The samples prepared as shown in Table 6.1 were those included within the above published study. Here AS and DP were set at 2.5 wt% and 1.0 wt% respectively with or without nanoclays or fumed silica at 1 wt% or 2 wt%.

Extruded strands from the twin screw compounder before pelletising and pellets after pelletising were collected. Hot-pressed plaques were moulded from pellets with a thickness of 2.5 mm by compression moulding with spacer plates between aluminium foil-coated steel plates at a set plate temperature of 190 °C for 2.5 minutes followed by rapid cooling.

Table 6.1: Composition of PA6 samples with AS, DP, nanoclays and silica.

Sample	Formulation	PA6 %	AS %	DP %	25A %	30B %	116 %	Silica %
1	PA6	100	-	-	-	-	-	-
2	PA6/AS/DP	96.5	2.5	1.0	-	-	-	-
3	PA6/AS/DP/25A(1 wt%)	95.5	2.5	1.0	1.0	-	-	-
4	PA6/AS/DP/25A(2 wt%)	94.5	2.5	1.0	2.0	-	-	-
5	PA6/AS/DP/30B(1 wt%)	95.5	2.5	1.0	-	1.0	-	-
6	PA6/AS/DP/30B(2 wt%)	94.5	2.5	1.0	-	2.0	-	-
7	PA6/AS/DP/116(1 wt%)	95.5	2.5	1.0	-	-	1.0	-
8	PA6/AS/DP/116(2 wt%)	94.5	2.5	1.0	-	-	2.0	-
9	PA6/AS/DP/Silica(1wt%)	95.5	2.5	1.0	-	-	-	1.0
10	PA6/AS/DP/Silica(2 wt%)	94.5	2.5	1.0	-	-	-	2.0

6.2.3 Melt extrusion in to filaments

From the flammability properties of the polymer formulations compounded (Table 6.1) and analysed by Dahyia in the jointly published work [92], a set of samples was selected for extrusion into fibres for processing and analysis within this thesis. These samples are listed in Table 6.2. The compounded samples were extruded into filaments using a 20 holespinneret (diameter, $\phi = 0.8$ mm), using the recently installed Fibre Extrusion Technology (FET) extruder as explained in Chapter 5, Section 5.2.3. The pellet samples were dried in a laboratory oven at 80 °C for 24 h to avoid the effect of moisture on the extrusion process. The FET extruder barrel four zone bands and the die head zone were maintained at temperatures of 190, 200, 210, 220 and 235 °C respectively for all the selected samples in the Table 6.2. During the extrusion process for all PA6 samples, the pre-pump pressure was maintained at 50 bar and the metering pump and screw speed were maintained at 10 rpm. The filaments were then collected over the cooling rollers or godets. The collecting godet pair below the spin-finish application zone had a surface speed of 100 m/min at 25 °C temperature. The filament bundle then passed to a further two godet pairs which form the stretching zone for

drawing the filaments in stages. This set of godets was adjusted to a surface speed of 105 m/min and 50 °C temperature. The third pair was maintained at 130 m/min and 50 °C temperature. These temperatures and relative speed differences help to keep tension in the thread line to ease the winding process. At the end of the process the filament yarn bundle was wound by a Leeson (see Figure 1(d) in the Chapter 5) winder maintained on 135 m/min. All the processing conditions were controlled and monitored by a Human Machine Interface (HMI) PC system with draw ratio of 1.3:1.

Table.6.2: Selected samples for the extrusion into filaments and knitting.

100% PA6
PA6/AS(2.5 wt%)/DP(1 wt%)
PA6/AS(2.5 wt%)/DP(1 wt%)/25A(2 wt%)
PA6/AS(2.5 wt%)/DP(1 wt%)/30B(2 wt%)
PA6/AS(2.5 wt%)/DP(1 wt%)/116(2 wt%)

6.2.4 Fabric production

For each sample, a sufficient length of undrawn fibre was extruded in order to test tensile properties and to allow knitting into fabric using a hand-powered V-bed rib flat machine. Attempts to draw the filaments at the extrusion stage failed due to the nature of the filaments which were difficult to control without breakage. However, samples were cool drawn with 1:2 draw ratio by used the Instron for the tensile test only. The area density of each fabric was controlled by the gauge of the machine. The flat knitting machine used employs straight needle beds carrying independently operated needles and the gauge selected was 11.

6.2.5 Characterisation of samples

All the above samples were characterised as described in the Chapter 3, Section 3.3 and the same equipment and procedures were used under the same conditions as explained in the Chapter 3, Section 3.3 except for the tensile properties and thermal analysis. Tensile testing of the filaments was conducted using an Instron with a gauge length of 100 mm, load cell 10 N and test speed 100 mm/min. The reported values of linear density, modulus, tenacity and elongation-at-break are the average values taken from ten tests. The filaments were cold drawn with a draw ratio of 1:2 by used the Instron and the same tensile testing was carried out on those drawn samples and their results averaged.

Thermal analysis (TG & DTA) of samples was carried out from ambient temperature to 700 °C at a heating rate of 10 °C/min in an air atmosphere using a TA Instruments, SDT 2960 simultaneous TGA-DTA.

6.3 Results and discussion

6.3.1 Thermal stability of compounded samples

Thermal analysis was under taken on compounded polymer chips samples listed in Table 6.1 by using the TGA-DTA analyser in air and their results are given in the Table 6.3. The temperature ranges, mass losses, endothermic peak temperatures, 5% ($T_{5\%}$), 10% ($T_{10\%}$) and 50% ($T_{50\%}$) mass loss temperatures are presented in the Table 6.3. The major weight loss of the PA6 is in the temperature range of 375-485 °C (86% weight loss), because most of the material volatilises at this temperature range following random chain scission at the alkylamide bonds. The rate of weight loss slows down at about 485 °C which is probably the consequence of the formation of a more thermally stable cross-linked structure, the precursor to char formation. The cross-linked structure is oxidized by air present on further heating and leaves negligible char at 600 °C.

PA6 treated with AS and DP show different mass loss behaviours in the initial stages of degradation, where an additional DTG maximum peak is observed at 314 °C. The onset temperature of degradation ($T_{5\%} = 272$ °C) of PA6/AS(2.5 wt%)/DP(1 wt%) is reduced by about 110 °C compared to pure PA6. These occur in the temperature range 200–270 °C where

according to Lewin et al [88, 89] sulphation of primary amino groups of PA6 as well as the hydroxyl group of DP coupled with dimerization of AS to diammoniumimidobisulfonate take place, both reactions releasing ammonia. Above 275 °C, attack by AS promotes scission of the alkylamide bond thereby starting the second stage of degradation in the temperature range 300–385 °C where a further 6.5 % wt loss occurs. However, in air, as with pure PA6, Table 6.3 shows that most of the weight loss (82.5%) for PA6/AS(2.5 wt%)/DP(1 wt%) formulations takes place in temperature range 385–470 °C in a third stage of degradation. On addition of 1wt% organoclay (25A and 30B), the onset temperature ($T_{5\%}$) is reduced with respect to the PA6/AS(2.5 wt%)/DP(1 wt%) sample, particularly in case of 30B, and on increasing the addition to 2 wt%, respective values recover slightly. The 30B clay shows a greater catalytic effect on degradation of AS- and DP-containing formulations than the 25A clay.

At the nanodispersed level, it could be that 30B containing samples (which have pendant –OH groups within the functionalising ammonium complex) are more exfoliated and hence exhibit higher specific surface areas with respect to influencing the sulphation rates and catalytic effects. Furthermore, these same primary –OH groups through their tendency to dehydrate and promote char may also contribute to the greater catalytic effect of the 30B clay.

1 wt% of pristine clay and silica added separately to PA6/AS(2.5 wt%)/DP(1 wt%), yield $T_{5\%}$ values which are higher than those of organoclay containing formulations, although they are still lower than the parent PA6/AS(2.5 wt%)/DP(1 wt%) sample value. This demonstrates the effect that the absence of functionalising species present in the organoclays may have on the overall degradation mechanism although some degree of catalytic effect is still evident at reduced levels of dispersion. However, addition of 2 wt% of pristine clay and silica appears to negate these effects by raising respective $T_{5\%}$ values above that for the PA6/AS(2.5 wt%)/DP(1 wt %) sample.

Table 6.3: TGA-DTA data of PA6 blended with 2.5 wt% AS, 1 wt% DP and with nanoparticles (1 and 2 wt%).

Sample	Stage	Temp range, °C	Mass loss, %	DTG maxima, °C	DTA Maxima, °C	T _{5%} , °C	T _{10%} , °C	T _{50%} , °C	Char at 500°C, %
PA6	1 st	0-375	3.7	--	Endo 224	384	398	443	8.9
	2 nd	375-485	86.4	457	Endo 440				
	3 rd	485-595		524	Exo 507				
PA6/AS(2.5%)/DP(1%)	1 st	0-300	5.5	--	Endo 225	272	367	438	0.0
	2 nd	300-385	6.5	314	Endo 425				
	3 rd	385-470	82.5	453	Exo 439				
	4 th	470-548		504	Exo 461,500				
PA6/AS(2.5%)/DP(1%)/25A(1%)	1 st	0-255	5.3	--	Endo 220	217	354	431	0.2
	2 nd	255-395	10.0	308	Endo 420				
	3 rd	395-470	79.6	439	Exo 432				
	4 th	470-550		498	Exo 453,495				
PA6/AS(2.5%)/DP(1%)/25A(2%)	1 st	0-265	5.27	--	Endo 222	250	337	437	4.4
	2 nd	265-400	13.5	305	Endo 411				
	3 rd	400-470	71.2	446	Exo 461,503				
	4 th	470-550		507					
PA6/AS(2.5%)/DP(1%)/30B(1%)	1 st	0-290	7.3	--	Endo 224	131	311	435	2.5
	2 nd	290-375	6.1	306	Endo 445				
	3 rd	375-480	81.3	447	Exo 510				
	4 th	480-555		517					
PA6/AS(2.5%)/DP(1%)/30B(2%)	1 st	0-295	7.8	--	Endo 223	141	331	439	2.8
	2 nd	295-375	5.4	314	Endo 431				
	3 rd	375-485	82.3	454	Exo 490,518				
	4 th	485-550		525					
PA6/AS(2.5%)/DP(1%)/116(1%)	1 st	0-290	5.6	--	Endo 223	252	370	441	1.6
	2 nd	290-395	7.6	315	Endo 438				
	3 rd	395-470	79.5	452	Exo 465,499				
	4 th	470-535		501					
PA6/AS(2.5%)/DP(1%)/116(2%)	1 st	0-280	4.6	--	Endo 223	301	383	444	2.5
	2 nd	280-390	6.8	340	Endo 408				
	3 rd	390-475	82.2	456	Exo 459,493				
	4 th	475-535		496					
PA6/AS(2.5%)/DP(1%)/Silica(1%)	1 st	0-285	5.7	--	Endo 223	225	365	443	2.3
	2 nd	285-400	10.3	307	Endo 420,				
	3 rd	400-470	77.4	460	Exo 459				
	4 th	470-535		516	Exo 495,512				
PA6/AS(2.5%)/DP(1%)/Silica(2%)	1 st	0-375	6.6	307	Endo 223	337	395	443	11.6
	2 nd	375-475	80.0	455	Endo 452				
	3 rd	475-576		527	Exo 513				

6.3.2. Limiting oxygen index of plaques and strands

LOI values of cast plaques and strands reproduced from the joint project [92] are shown in the Table 6.4. Introduction of AS(2.5 wt%)/DP(1 wt %) to PA6 increases the LOI values of both cast plaques and strands. The LOI values of the plaques are increased from 20.5 to 25.0 vol% and for strands from 21.9 to 29.8 vol%. Addition of clays to the above combination of samples causes reductions to the LOI values of the plaques with respect to the PA6/AS(2.5

wt%)/DP(1 wt %) value but this reduction is minimal for the 116 and silica-containing yarns. Higher LOI values are obtained for strand samples (24.9 and 30.4 vol%) but this may be due to shrinkage of the strands during ignition and melt dripping.

The addition of PA6/AS(2.5 wt%)/DP(1 wt%) compounded with PA6 gives an average increase of the LOI of 4.5% for plaques and 8% for strands when compared with PA6 alone. However, the increases for these same formulations with the addition of nanoclays are only 3.3% (average plaques) and 7.8% (average strands) for 25A and 1.4% (average plaques) and 5.6% (average strands) for 30B. The addition of unmodified clay and fumed silica promote little reductions in LOI from those of PA6/AS(2.5 wt%)/DP(1 wt%) plaque and strand samples. Generally, it has been shown that addition of a nanoclay, which generates a nanocomposite structure in either PA6 or PA6.6, reduces the LOI value as a consequence of increased melt viscosity and a reduced melt drip rate [153]. This effect is seen here only for the 25A and 30B-containing polymer samples. The negligible effect of silica on LOI with respect to the PA6/AS(2.5 wt%)/DP(1 wt%) samples caused the PA6/AS/DP/silica samples to be omitted from the fibre extrusion part of this work.

Table 6.4: Limiting oxygen index values of PA6 plaques and strands.

Sample	LOI, vol%	
	Plaques	Strand
PA6	20.5	21.9
PA6/AS(2.5 wt%)/DP(1 wt%)	25.0	29.8
PA6/AS(2.5 wt%)/DP(1 wt%)/25A(1 wt%)	23.7	29.4
PA6/AS(2.5 wt%)/DP(1 wt%)/25A(2 wt%)	23.8	28.0
PA6/AS(2.5 wt%)/DP(1 wt%)/30B(1 wt%)	22.0	30.0
PA6/AS(2.5 wt%)/DP(1 wt%)/30B(2 wt%)	21.8	24.9
PA6/AS(2.5 wt%)/DP(1 wt%)/116(1 wt%)	22.9	26.3
PA6/AS(2.5 wt%)/DP(1 wt%)/116(2 wt%)	24.4	30.0
PA6/AS(2.5 wt%)/DP(1 wt%)/Silica(1 wt%)	24.5	27.2
PA6/AS(2.5 wt%)/DP(1 wt%)/Silica(2 wt%)	24.6	30.4

6.3.3. UL 94 results for plaques

UL-94 test results in both horizontal and vertical modes are given in Table 6.5 where the average burning time, average dripping rate after first and second application of flame and UL 94 ratings are summarised. In both test geometries, pure PA6 burned completely and could not be rated, but on the addition of PA6/AS(2.5 wt%)/DP(1 wt%) with and without clay tests HB rating for the horizontal test and V-2 ratings in the vertical test were obtained. The percentage of the clay in the PA6 with flame retardant did not change the UL-94 result.

Table 6.5: Flame spread UL94 result for PA6 plaque samples.

Sample	UL-94 Horizontal			UL-94-Vertical		
	t ₁ /t ₂ s	R ₁ /R ₂	Rating	t ₁ /t ₂ s	R ₁ /R ₂	Rating
PA6	BC	0.95/1.09	NR	BC	0.94/1.12	NR
PA6/AS(2.5 wt%)/DP(1 wt%)	5.0/2.0	0.50/0.12	HB	1.6/3.4	0.88/0.57	V-2
PA6/AS(2.5 wt%)/DP(1 wt%)/25A(1 wt%)	3.0/1.5	0.75/0.75	HB	3.4/11.4	1.63/0.32	V-2
PA6/AS(2.5 wt%)/DP(1 wt%)/25A(2 wt%)	4.0/1.5	0.50/0.75	HB	3.0/9.6	3.13/0.31	V-2
PA6/AS(2.5 wt%)/DP(1 wt%)/30B(1 wt%)	12.5/3.0	0.76/0.87	HB	7.8/11.0	4.48/0.42	V-2
PA6/AS(2.5 wt%)/DP(1 wt%)/30B(2 wt%)	12.0/3.0	0.58/0.62	HB	9.0/8.0	4.22/0.35	V-2
PA6/AS(2.5 wt%)/DP(1 wt%)/116(1 wt%)	11.0/2.5	0.40/0.16	HB	5.2/9.0	5.80/0.20	V-2
PA6/AS(2.5 wt%)/DP(1 wt%)/116(2 wt%)	5.0/3.5	0.20/0.35	HB	3.8/8.8	3.00/0.24	V-2
PA6/AS(2.5 wt%)/DP(1 wt%)/Silica(1 wt%)	4.5/10.0	0.22/0.02	HB	1.6/9.8	1.50/0.35	V-2
PA6/AS(2.5 wt%)/DP(1 wt%)/Silica(2 wt%)	4.5/5.0	0.32/0.40	HB	1.6/7.8	2.50/0.35	V-2

t₁ = average burning time after the first application of flame

t₂ = average burning time after the second application of flame

R₁ = average dripping rate after the first application of flame

R₂ = average dripping rate after the second application of flame

NR = not rated; BC = burns to clamp

6.3.4. Tensile properties of filament yarns

The results of physical testing of the undrawn filament yarns samples are shown in Table 6.6. These reveal that there is considerable variation in the filament yarn properties within samples. Acceptable levels of increase in linear density are recorded for the addition of PA6/AS(2.5 wt%)/DP(1 wt%) and the linear density level is unchanged with the addition of 25A (2 wt%) or 30B (2 wt%) nanoclays, but it has decreased with the addition of 116 (2 wt%). These variations in linear density might be due to the modification of the clay particles and their effect on the extrusion variables such as melt viscosity and hence need to change conditions slightly to obtain stable thread lines during melt extrusion.

The addition of AS(2.5 wt%)/DP(1 wt%) show an increase in modulus of $66 \pm 9\%$ relative to the 100% PA6 yarn modulus value of $47 \pm 11\%$ cN/tex. Addition of 25A (2 wt%) or 30B (2 wt%) show further increases in the modulus, but it is reduced with the addition of 116 (2 wt%) to below that of the PA6/AS(2.5 wt%)/DP(1 wt%) sample.

The tenacity value of 100% PA6 decreases following addition of AS(2.5 wt%)/DP(1 wt%) but then remains largely unchanged with the addition of clay. This suggests that the addition of AS and DP have promoted degradation of the polymer as noted by Lewin et al [89]. Breaking elongations show a significant increase upon the addition of AS(2.5 wt%)/DP(1 wt%) and are further increased when clay is added, which might suggest that any thermal degradation is minimal although able to reduce the tenacity.

Table 6.7 summarizes test data for the samples after cold drawing using the Instron with a draw ratio of 1:2. The drawn filament yarns show linear density values reduced by 50% as expected, modulus values which have nearly doubled and tenacity values nearly three times respective undrawn values although breaking elongation values have reduced to approximately 10% as might be expected.

After cold drawing it is observed that the modulus is nearly double for 30B (2 wt%) and 116 (2 wt%) samples in comparison with the 100% PA6 drawn filament yarn value. The tenacity value has again reduced with the addition of AS(2.5 wt%)/DP(1 wt%) but it is almost unchanged with the addition of nanoclays as noted for the undrawn analogous filament yarns.

Breaking elongation has hardly changed with the addition of AS(2.5 wt%)/DP(1 wt%) and it is slightly increased with the addition of 25A (2 wt%) and 116 (2 wt%), but slightly decreased with the addition of 30B.

Table 6.6: Physical properties of undrawn filament yarn samples.

Sample	Linear density tex	Modulus cN/tex	Tenacity CN/tex	Elongation- at -break %
PA 6	77	47 ± 5	7 ± 2.0	221 ± 63
PA6/AS(2.5 wt%)/DP(1 wt%)	101	66 ± 6	4 ± 0.5	240 ± 29
PA6/AS(2.5 wt%)/DP(1 wt%)/25A(2 wt%)	101	83 ± 17	5 ± 0.5	300 ± 42
PA6/AS(2.5 wt%)/DP(1 wt%)/30B(2 wt%)	101	91 ± 21	5 ± 1.0	298 ± 58
PA6/AS(2.5 wt%)/DP(1 wt%)/116(2 wt%)	79	58 ± 13	5 ± 0.4	273 ± 33

Table 6.7: Physical properties of filament yarn after drawing with cool draw ratio of 1:2.

Sample	Linear density tex	Modulus cN/tex	Tenacity CN/tex	Elongation- at -break %
PA 6	38	102 ± 14	22 ± 2.0	26 ± 4
PA6/AS(2.5 wt%)/DP(1 wt%)	56	153 ± 23	12 ± 1.0	27 ± 6
PA6/AS(2.5 wt%)/DP(1 wt%)/25A(2 wt%)	49	176 ± 9	13 ± 1.0	33 ± 5
PA6/AS(2.5 wt%)/DP(1 wt%)/30B(2 wt%)	47	202 ± 17	13 ± 1.0	23 ± 4
PA6/AS(2.5 wt%)/DP(1 wt%)/116(2 wt%)	39	193 ± 41	14 ± 2.0	35 ± 9

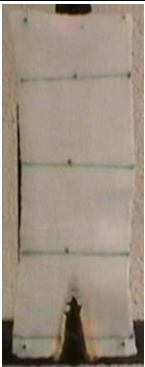
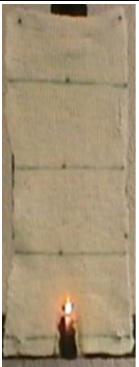


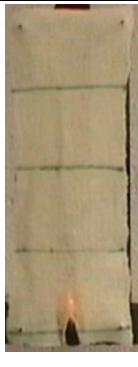
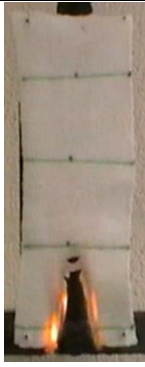



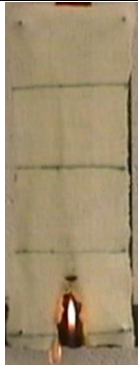
6.3.5 Fabric flame spread



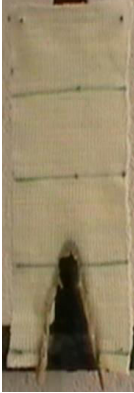

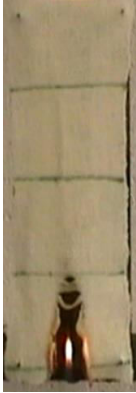





All filaments were knitted into fabrics and flame spread tests were undertaken using conditions described in BS 5438 and their test results interpreted in Table 6.8 and Figure 6.1. Addition of AS(2.5 wt%)/DP(1 wt%) has the effect of reducing the area density of fabric with respect to pure PA6 and this effect is reversed slightly with the addition of organoclay, but it is reduced slightly further with addition of pristine clay. However, it is considered that overall the area density is within an acceptable range between 527 and 638 gm⁻² in that such a range should have minimal effects on overall flammability properties. Presence of the AS and DP flame retardants help to decrease the burning time by about 40% and number of drops by about 61% with respect to pure PA6, and these are further reduced with the addition of 25A (2 wt%) organoclay; presence of 30B (2 wt%) and 116 (2 wt%) clays, however, show a reversal of this trend. According to the test results of mass loss of the sample, burning time, number of drops and drops rate, PA6/AS(2.5 wt%)/DP(1 wt%)/25A (2 wt%) is superior to the others.





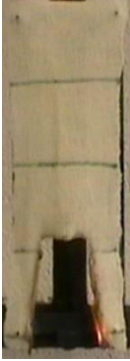



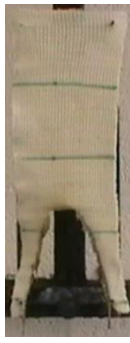
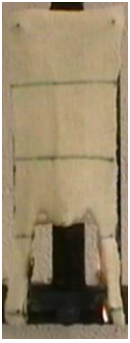
The number of drops measured indicates the effect of formulation components upon flaming melt viscosity and thermo plasticity of the burning fabric region and thus potential burning rate. Figure 6.1 illustrates how the flame spread behaves during a flame spread test for a 5 seconds time interval after the ignition source has been removed. Captured photographs clearly show that addition of AS(2.5 wt%)/DP(1 wt%) significantly reduces melt and shrink back when compared to pure PA6, this is further reduced on the addition of 25A(2 wt%) clay, but the effect is slightly reversed with the addition of 30B and 116 clays.



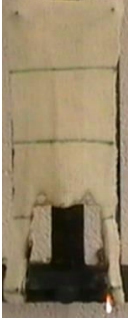


Table 6.8: Fabric flame spread.

Sample	Dimension of fabric sample		Initial mass of fabric sample g	Area density of fabric gm^{-2}	Total time to burnt s	Burnt length mm	Flame spread mms^{-1}	Sample catch on tin foil g	Mass on frame g	Mass loss of the sample g	Number of drops
	Length mm	Width mm									
PA 6	203	81	10.5 ± 1.5	638 ± 69	51 ± 5	131 ± 12	2.6	2.6	6.3	4.2	111 ± 13
PA6/AS(2.5 wt%)/DP(1 wt%)	202	81	8.9 ± 1.8	542 ± 56	31 ± 6	51 ± 9	1.6	0.7	7.8	1.1	43 ± 7
PA6/AS(2.5 wt%)/DP(1 wt%)/25A(2 wt%)	203	79	9.3 ± 2.1	578 ± 75	23 ± 4	40 ± 10	1.7	0.9	8.2	1.1	24 ± 4
PA6/AS(2.5 wt%)/DP(1 wt%)/30B(2 wt%)	203	78	8.9 ± 1.8	560 ± 45	39 ± 3	53 ± 15	1.4	1.8	6.3	2.6	45 ± 4
PA6/AS(2.5 wt%)/DP(1 wt%)/116(2 wt%)	204	80	8.6 ± 2.2	527 ± 52	35 ± 6	52 ± 16	1.5	1.2	5.6	3	30 ± 6

Time	PA6	PA6/AS(2.5 wt %)/ DP(1 wt %)	PA6/AS(2.5 wt %)/ DP(1 wt %)/25A(2 wt %)	PA6/AS(2.5 wt %)/ DP(1 wt %)/30B(2 wt %)	PA6/AS(2.5 wt %)/ DP(1 wt %)/116(2 wt %)
0s					
5s					

10s					
15s					

20s					
25s					

30s					
35s					


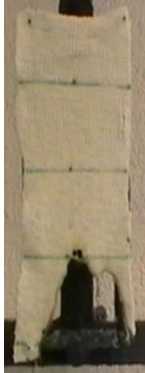


40s					
45s					
50s					

Figure 6.1: Vertical flame test result for fabric in 5 seconds time interval after ignition.

6.4 Conclusions

The work in this chapter is built on the Lewin et al's work, as explained in the Chapter 2, Section 2.5.2, in which Dr Jai Dahyia compounded the PA6/AS/DP samples with addition of different clays and silica in Table 6.1 and examined them for their thermal analytical and flammable properties with assistance from myself. Based on the conclusions of the burning behaviour of plaques of PA6 samples comprising additions of the flame retardants ammonium sulphamate and dipentaerythritol and a number of functionalised and pristine nanoparticles [92], a sub-set (see Table 6.2) was extruded into filaments whose properties were analysed before and after drawing. Extruded filaments of all except silica-containing formulations were tested for their tensile properties under two conditions using an Instron tensile tester. The initial tests were on the undrawn yarn and then repeated on the cold drawn yarns. Modulus and breaking elongations are significantly increased but tenacity values are slightly decreased upon the addition of flame retardant with and without nanoclay. This is due to some degree to the competing effects of thermal degradation caused by the AS/DP flame retardant as well as the reinforcing effects of the nanoparticles when a nanocomposite structure is present. Undrawn filaments were used to knit samples into fabrics and examined for their flame spread behaviour from which it is deduced that addition of flame retardant alone reduced burning time and both the number of burning drops with respect to pure PA6. The PA6/AS(2.5 wt%)/DP(1 wt%)/25A(2 wt%) combination, however, was found to have superior (ie reduced) flame spread test and tensile properties among all other formulations.

Chapter 7: Bicomponent Filament / Fabric Properties

7.1 Introduction

Bicomponent fibre technology combines two polymers by co-extruding them to form a single filament with a designed cross-sectional arrangement [227]. Various cross sections can be produced, which include side-by-side, sheath and core and other more complex geometries. In this way, bicomponent fibres can be created that combine the properties of two individual polymers [228]. Bicomponent extrusion allows the simultaneous extrusion of two different polymers through the same orifice by melt extrusion and can be thought of as two extruders working one inside the other [229]. In this work polymer with nanoclay and/or flame retardant is introduced into the core or sheath of the bicomponent fibre.

7.2 Experimental

Based on the previous work described in Chapters 3-6, total additive level was maintained below (< 10 wt%) and, as explained in Section 3.2.3, the 100 W ultrasonic probe with 90 % amplitude was used to ultrasonicate the samples during compounding and prior to melt extrusion.

7.3 Samples

7.3.1 Materials

In this study the polymer selected was polyamide 6 (PA6), Technyl C 301 Natural, Rhodia, France, nanoclay as Cloisite 25A, Southern Clay Products, USA; modified with dimethyl, dehydrogenated tallow quaternary ammonium sulphate (2M2HT). The flame retardant was aluminium phosphinate, Exolit OP 935, Clariant (note that this is fibre grade in that its average particle diameter is < 10 µm).

7.3.2 Sample matrix

Sample matrices are shown in the Tables 7.1 and 7.2. Polymer pellets were compounded using the twin screw extruder as explained in Section 3.2.3 and extruded into core-sheath bicomponent filaments using a Fibre Extrusion Technology (FET) extruder.

In this work the same twin screw compounder has been used to compound samples with and without application of ultrasound under the same conditions as explained in the Section 3.2.3. The temperatures in the six zones of the compounder were 210, 225, 230, 230, 240 and 245 °C.

Table 7.1: Sample matrix for PA6 bicomponent samples without application of ultrasonic energy

	Core	Sheath
1	PA6	PA6
2	PA6	PA6 / 25A (2 wt%)
3	PA6 / 25A (2 wt%)	PA6
4	PA6	PA6 / Al-Phos (10 wt%)
5	PA6 / Al-Phos (10 wt%)	PA6

Table 7.2: Sample matrix for PA6 bicomponent samples with 100W, 90% amplitude application of ultrasonic energy (90 W).

Ref No	Core	Sheath
1	PA6	PA6/25A(2 wt%)/90W
2	PA6/25A(2 wt%)/90W	PA6
3	PA6	PA6/Al-Phos(10 wt%)/90W
4	PA6/Al-Phos(10 wt%)/90W	PA6
5	PA6/25A(2 wt%)/90W	PA6/Al-Phos(10 wt%)/90W
6	PA6/Al-Phos(10 wt%)/90W	PA6/25A(2 wt%)/90W
7	PA6	PA6/25A(2 wt%)/Al-Phos(10 wt %)/ 90W
8	PA6/25A(2 wt %)/Al-Phos(10 wt %)/90W	PA6

7.3.3 Melt extrusion into filaments

The path from polymer pellets to wound up fibre is shown in the Chapter 5, Figure 5.1(a). The compounded polymer pellets are fed separately into extruders for sheath and core respectively. The extruder temperatures are selected as shown in the Table 7.3. The extruder has two separate screws; extruder 1 consists of \varnothing 20 mm and extruder 2, \varnothing 25 mm, both with L/D ratio of 30. Each melt is transported through heated barrels to the spinning pumps, the pumps' sizes are $0.6 \text{ cm}^3/\text{revolution}$ for the first pump and $1.2 \text{ cm}^3/\text{revolution}$ for the second pump, respectively. The first pump set to the speed of 10 rpm and second to 5 rpm. The molten polymers are pumped into the bicomponent breaker plate through the pre distribution plate, where metal screen filters are attached to filter out impurities. The filter comprises multiple screens in the order of 200, 100, 80 and 40 meshes from top to bottom. After passing through the filtration stage the melts flow into the capillary of the bicomponent breaker plate. The capillary diameter of core is 0.2mm and 0.6 mm for sheath. At the end of the capillary, the melt exits and passes through the top, bottom distribution plates and then spinneret to produce 24 core and sheath filaments (Figure 7.1). Improper spin pack set-up can lead to high pressure and pack leaks. Upon exiting the 24-hole spinneret, the filaments were subjected to an air quench with air flow rate of $20 \text{ m}^3/\text{s}$ and $15 \text{ }^\circ\text{C}$ controlled temperature to ensure good linear density and orientation uniformity. Prior to the first godet, spin finish was applied. Spin finish helps to avoid static electricity, and provide lubrication and cohesion of filaments. The filaments were then collected over the cooling rollers or godets.

Table 7.3: Extruder conditions.

Spinning conditions					Extruder 1	Extruder 2
Pre pump pressure / bar					50	50
Metering pump speed / rpm					10	5
Screw barrel and head temperatures, $^\circ\text{C}$	Zone 1				235	235
	Zone 2				245	245
	Zone 3				245	245
	Zone 4				245	245
	Metering pump				245	245
Die block					245	245

The collecting godet pair below the spin-finish application zone had a surface speed of 100 m/min at 25 °C temperature. The filament bundle was then passed to a further two godet pairs which form the stretching zone for drawing the filaments in stages. This set of godets was adjusted to a surface speed of 105 m/min and 50 °C temperature. The third pair was maintained on 130 m/min and 50 °C temperature. These temperatures and relative speed differences help to keep tension to ease the winding process. The first set of godet served to tension the fibres descending from the stack, while the next two godets draw the fibres with a draw ratio of 1.3:1. At the end of the process the yarn bundle was wound by a Leesona (Refer to Figure 5.1(d) in Chapter 5) winder maintained on 135 m/min and bicomponent fibres were wound on a winding tube of 142 mm diameter and 189 mm length. All the processing conditions were controlled and monitored by a Human Machine Interface (HMI) PC system.

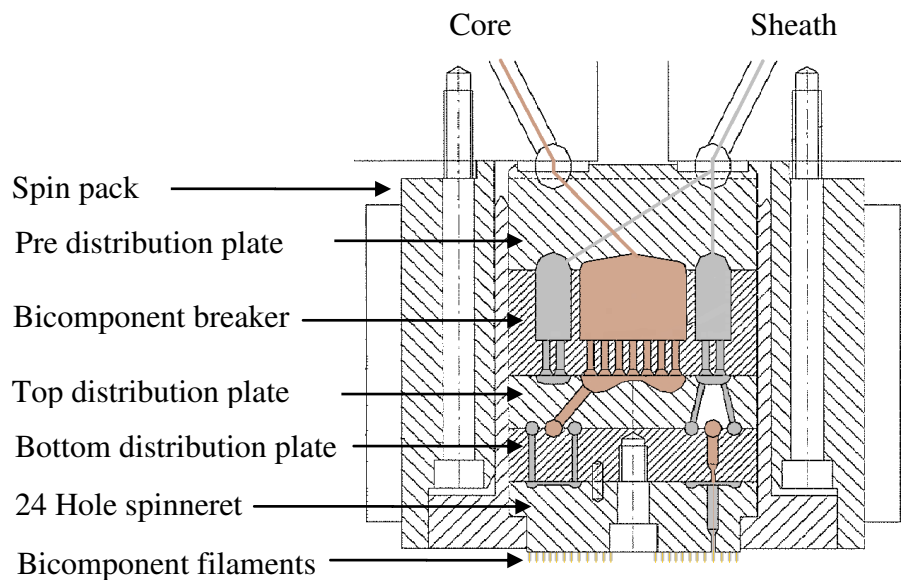


Figure 7.1: Symmetric diagram of bicomponent spinneret (Core/Sheath).

7.4 Results and discussion

7.4.1 Morphology of bicomponent filaments

The images of fibres were taken on an optical Aigo LCD digital microscope DMS012, with 1600 x 1200 pixel arrays. The images were captured using an LED light panel and a 2 megapixel camera. In Figure 7.2, optical microscope images of the bicomponent fibres of PA6 as the sheath and the PA6/Al-Phos(10 wt%) formulation as the core are shown. The images show that uniform core/sheath geometric distribution with a defined boundary layer were achieved, matching the expected filament bicomponent structure for a typical core / sheath formulation.

Scanning electron microscopy (SEM) and EDS analysis was conducted on the region of core and sheath, images as shown in Figure.7.3. SEM images typified by that in Figure 7.3 clearly show the core and sheath structure of the bicomponent filament. EDS was performed on several spatial positions within the cross-section of the filament and the core-sheath geometry is particularly noticeable in the P-dots EDS image. Examination of the cross-section at greater magnification of each of the two regions marked as sheath (edge of the sample – Figure 7.4) and core (centre of the sample – Figure 7.5) indicates that the number and densities of P and Al dots are greater in the latter. These results indicate that there was little evidence of mixing across the cross-section of the fibre.

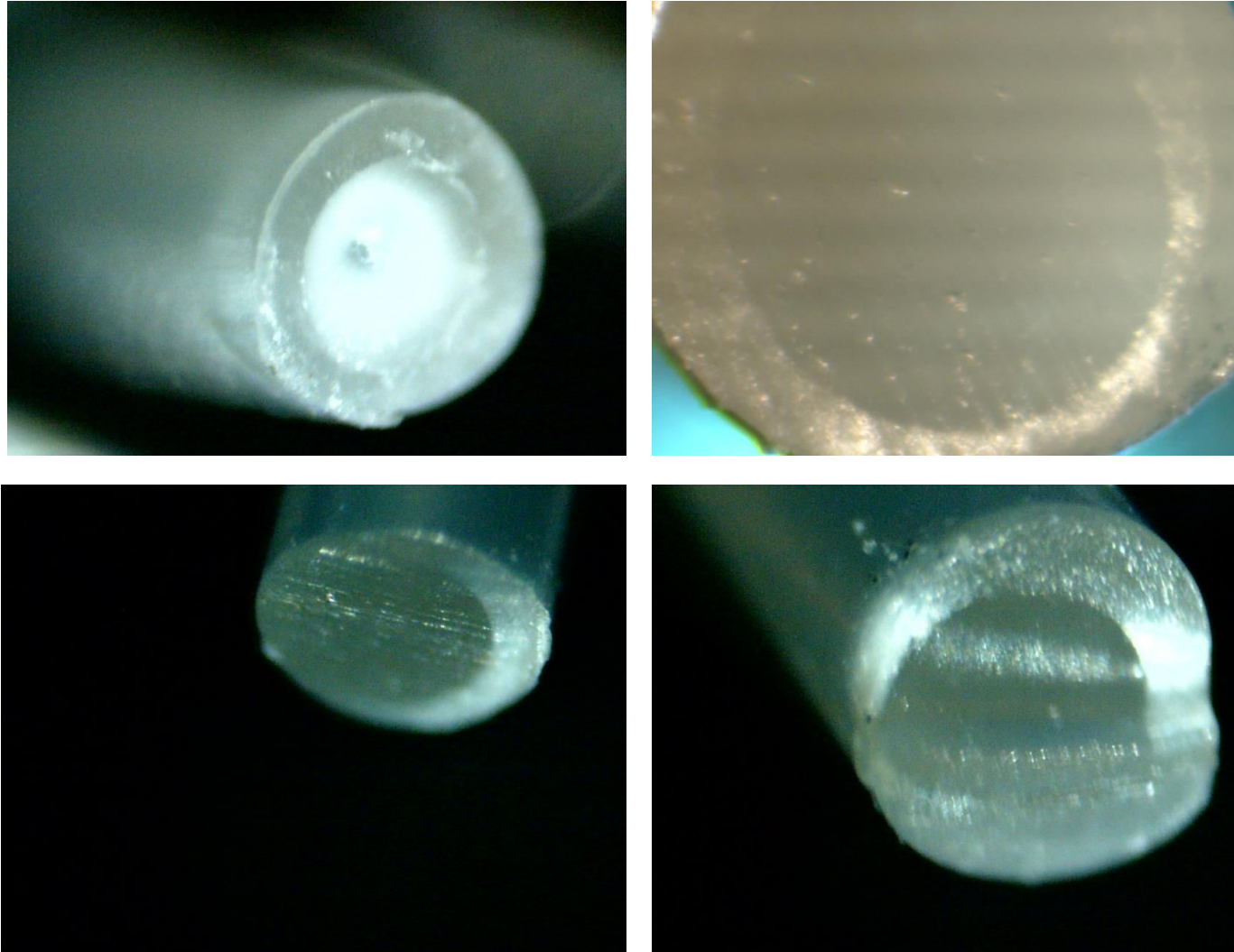


Figure 7.2: Optical images (40 X) of PA6 in sheath and PA6/Al-Phos(10 wt%) core bicomponent fibre.

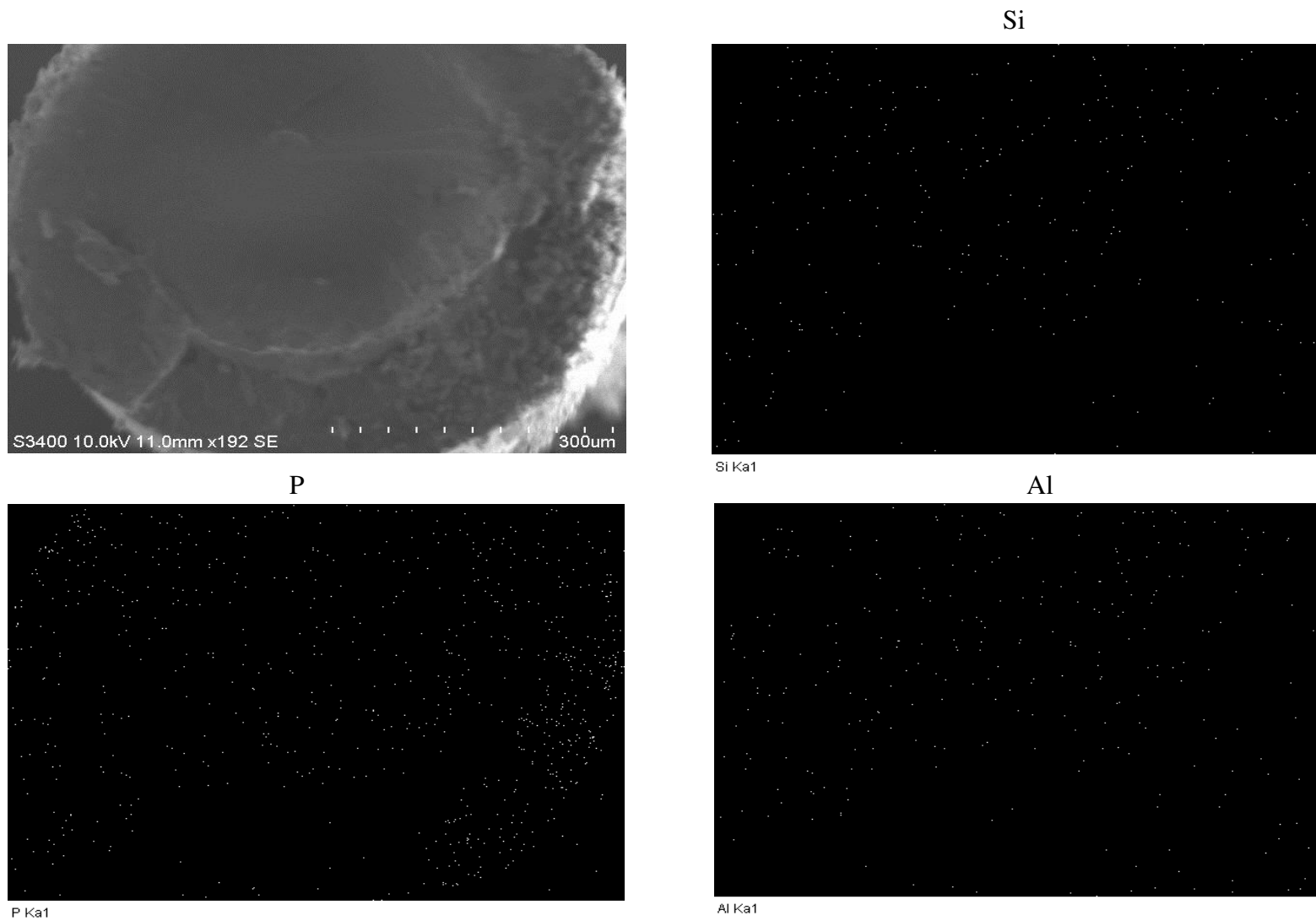


Figure 7.3: SEM and EDS images of PA6 in sheath and PA6/Al-Phos(10 wt%) core bicomponent fibre.

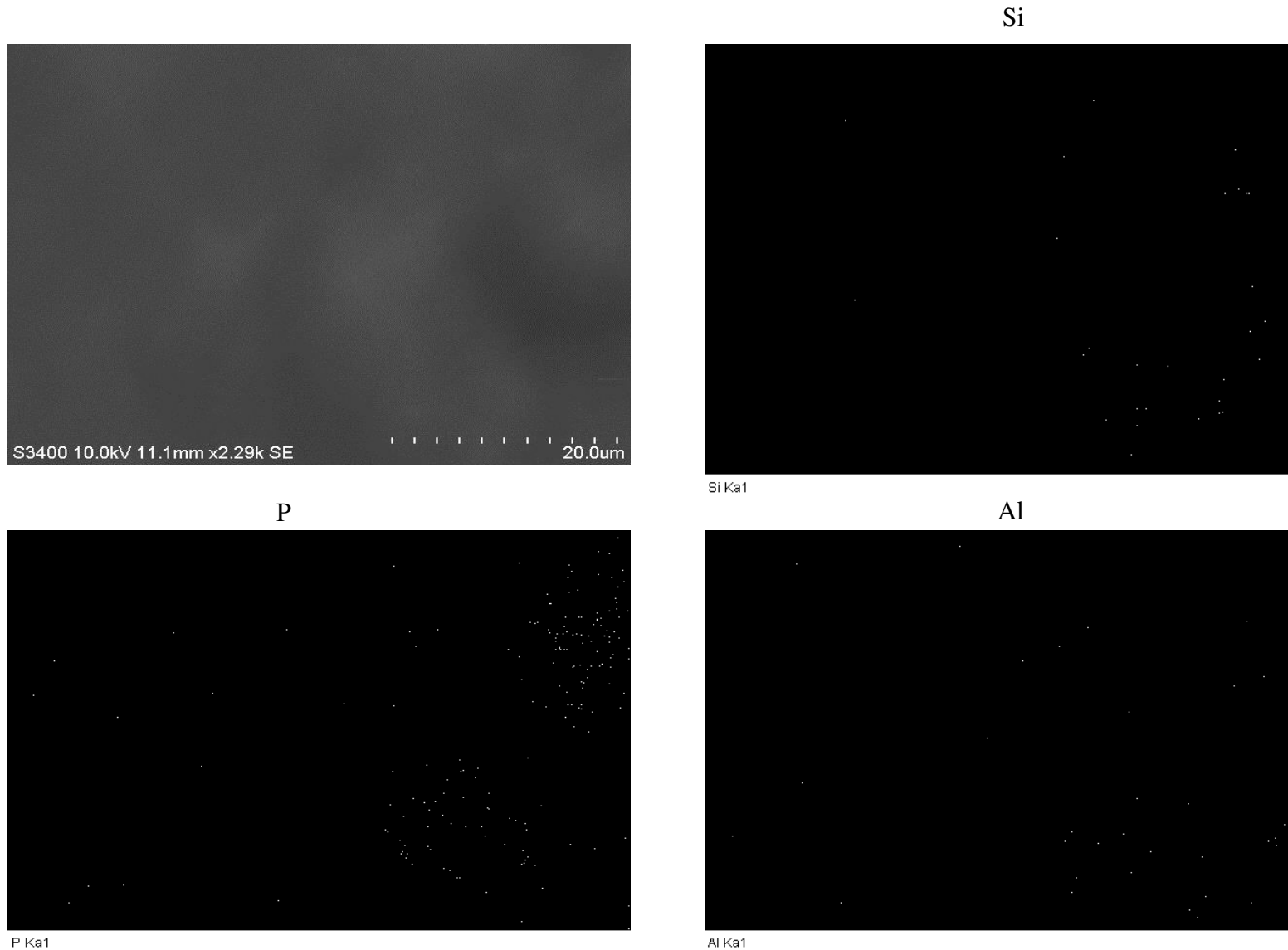


Figure 7.4: SEM and EDS images of 20 μm sheath (edge) of PA6 in sheath and PA6/Al-Phos(10 wt%) core bicomponent fibre.

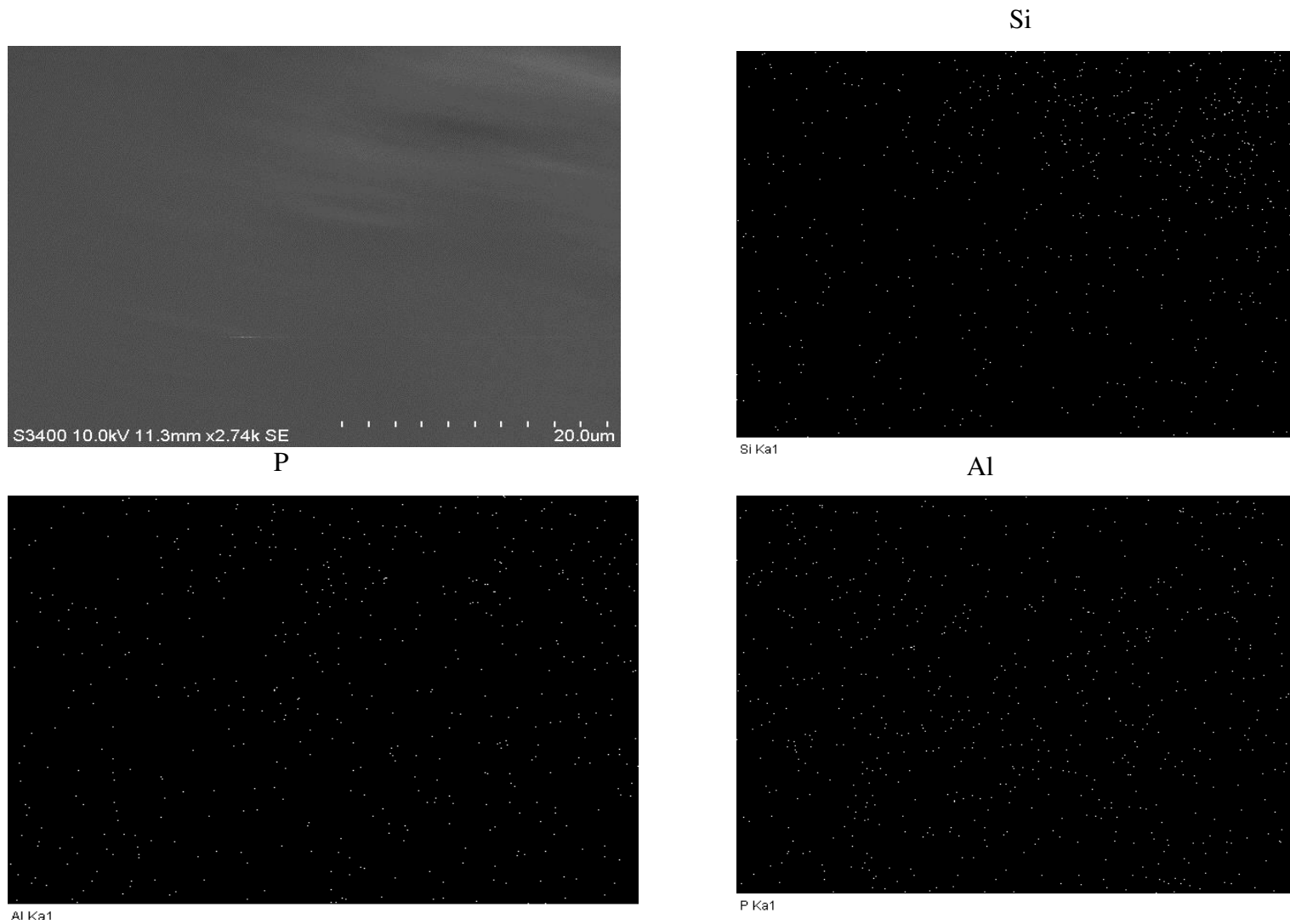


Figure 7.5: SEM and EDS images of 20 μm centre (core) of PA6 in sheath and PA6/Al-Phos(10 wt%) core bicomponent fibre.

7.4.2 Tensile properties

Table 7.4 shows the linear density, modulus, tenacity and elongation-at-break of the various PA6 bicomponent filament yarns produced from compounded components extruded without the application of ultrasound prior to formation of the initial starting pellets.

The linear densities of the filament yarns are in the range 113 to 122 tex, so the filaments are closely similar and the addition of nanoclay or flame retardant has not affected the linear density of the samples. The addition of nanoclay to the core or sheath brings about a small reduction in the modulus; there is a more marked reduction with the fire retardant system, which is most marked when the Al-Phos (10 wt%) is present in the core.

The introduction of the clay or flame retardant reduces tenacity with respect to the control and introduction of flame retardant reduces tenacity more than clay and especially when it is in the core. Elongation-at-break values are reduced on the addition of flame retardant in the core or sheath; for example, the control PA6-C/PA6-S sample value reduced from $217 \pm 20\%$ to $165 \pm 11\%$ when flame retardant was introduced into the core (PA6/Al-Phos (10 wt%) – C/PA6-S). Nanoclay presence in the core promotes a reduction in the elongation-at-break but this is increased when it is in the sheath. Addition of nanoparticles in a polymer usually decreases elongation-at-break and so the increase when in the sheath is not easy to explain without further study.

To improve the nanoclay dispersion, ultrasound was applied at the compounding stage at 90W as described in the Section 3.2.3 and these pellets were then used to extrude bicomponent filament set in Table 7.2. The dependence of tensile properties of the bicomponent fibres with nanoclay and / or flame retardant compounded in the presence of ultrasound is summarised in Table 7.5. The linear density, modulus and tenacity of yarns incorporating nanoclay in core or sheath when compounded under ultrasound are not significantly different from those of corresponding samples produced without ultrasound. The elongation-at-break values while being generally higher, show the same between-sample trends as seen in Table 7.4 for unsonicated samples. Thus the combination of PA6 core or sheath with PA6/25A(2 wt%) core or sheath without ultrasound shows significantly lower elongation-at-break than samples produced with ultrasound (90 W). It should be noted that all but one of the combinations of additives when compounded without ultrasound showed lower elongation-at-break values than neat PA6-C/PA6-S,

while all but two after ultrasonification (samples 3 and 5 in Table 7.5) show higher values. The modulus values of the samples containing flame retardant in core or sheath compounded under ultrasound are reduced when compared with those produced without ultrasound (see also Table 7.5, reference samples 3 and 4). The PA6/25A(2 wt%)/Al-Phos (10 wt%) formulation when sonicated gives an improvement in filament elongation-at-break values when incorporated in either core or sheath, the results for this formulation (see Table 7.5, reference samples 7 & 8).

Table 7.4: Tensile properties of bicomponent fibres without application of ultrasound.

Sample (Core-C / Sheath-S)	linear density (tex)	Modulus (cN/tex)	Tenacity (CN/tex)	Elongation -at -break (%)
PA6- C PA6- S	118	76 ± 23	10 ± 1.0	217 ± 20
PA6- C PA6/ 25A(2 wt%)- S	113	66 ± 10	6 ± 1.0	263 ± 22
PA6/ 25A(2 wt%)- C PA6- S	122	64 ± 9	7 ± 2.0	185 ± 40
PA6- C PA6/ Al-Phos (10 wt%)- S	115	53 ± 5	4 ± 1.0	179 ± 17
PA6/ Al-Phos (10 wt%)- C PA6- S	115	35 ± 6	2 ± 1.0	165 ± 11

Table 7.5: Tensile properties of bicomponent fibres with application of ultrasound.

Ref No	Sample	Linear density (tex)	Modulus (cN/tex)	Tenacity (CN/tex)	Elongation at -break (%)
1	PA6- C PA6/25A(2 wt%)/90W- S	113	61 ± 7	7 ± 1.0	258 ± 25
2	PA6/25A(2 wt%)/90W- C PA6- S	118	64 ± 17	7 ± 1.0	322 ± 62
3	PA6- C PA6/Al-Phos (10 wt%)/90W- S	120	40 ± 7	1 ± 0.3	127 ± 21
4	PA6/Al-Phos (10 wt%)/90W- C PA6- S	144	22 ± 2	7 ± 1.0	269 ± 51
5	PA6/25A(2 wt%)/90W- C PA6/Al-Phos (10 wt%)/90W- S	122	43 ± 7	2 ± 0.4	226 ± 13
6	PA6/Al-Phos (10 wt%)/90W- C PA6/25A(2 wt%)/90W- S	118	58 ± 11	3 ± 0.2	179 ± 27
7	PA6- C PA6/25A(2 wt%)/Al-Phos (10 wt%)/90W- S	120	43 ± 4	7 ± 1.0	288 ± 20
8	PA6/25A(2 wt%)/Al-Phos (10 wt%)/90W- C PA6- S	123	46 ± 3	6 ± 1.0	288 ± 19

7.4.3 Vertical fabric strip testing and flame spread.

The knitted fabrics derived from the bicomponent filament yarns were placed in 3000 ml of a solution, containing 1.0 w/v tribasic sodium phosphate and 0.2% v/v polyethylene glycol-200 grade (Laboratory reagent grade, fisher scientific) at 40 °C for one hour with continuous stirring. Samples were then removed, rinsed with distilled water and allowed to dry overnight at room temperature.

Washed, dried fabrics were used for the vertical flame spread test and their results are given in Tables 7.6 and 7.7 for samples both without and with ultrasound compounding respectively. When the igniting flame is introduced to each fabric, it starts to shrink and then ignite with the vertical flame starting to spread out to the edges of the fabric which then releases burning drips. This phenomenon is clearly seen in the Figures 7.6 and 7.7, where captured photographs of the burning behaviours in 10 seconds of time interval after extinction of the igniting flame has taken place until the flame has extinguished. Here it is generally evident that the fabrics tendency to melting and shrinking back is reduced when nanoclay and / or flame retardant are present as was seen in Chapter 4 for the single component filament fabric samples (see Figure 4.4)

Behaviour of unsonicated samples: The addition of clay alone to the PA6 in core or sheath increases area density, mass loss, total burning time and number of drops. The incorporation of fire retardant alone into the PA6 sheath or core appears to give fabrics reduced area density, but this is determined largely by the respective filament linear density and ease of knittability and hence loop density. In Table 7.4, filament yarn linear densities are little affected by the addition of flame retardant and so the reason for the lower area density must be its ease of knittability and related fabric geometric effects. Addition of Al-Phos does not have a large effect on burn time but it does, however, increase burn length and speed of flame spread. There is also an increase in sample mass loss during burning, although the drop formation has decreased suggesting the effect of the FR is to increase melt viscosity. An increase in melt viscosity, will of course, impede melt dripping and so produce the increase in burn time and burning length observed. These effects are independent of whether the Al-Phos is in the core or the sheath.

It is illuminating to compare the combustion properties observed for the various FR systems as illustrated in both the single component filament and bicomponent filament fabrics in the Tables 5.9 and 7.6 respectively. In the Table 5.9, addition of 2 wt% of

nanoclay into the PA6 increased the area density, burn length, number of drops and total mass loss but had no effect on the speed of flame spread. In the Table 7.6, samples with addition of 2 wt% of nanoclay into the sheath show significantly lower values in all burning parameters than the nanoclay in the core. This effect might be due to the char forming character of the clay. Overall, most of the characteristic are similar in the both cases (Tables 5.9 and 7.6) upon nanoclay addition. However, in the Table 5.9, addition of flame retardant shows slightly increased area density values but for bicomponent flame retardant system decreased values. Addition of flame retardant in both cases (Tables 5.9 and 7.6), increased speed of flame spread, mass loss and decreased the number of drops. This latter effect is most likely due to a slight char forming effect of the flame retardant.

Behaviour of sonicated samples: Addition of clay to either the sheath or core give fabrics having very similar burning behaviour irrespective of the location of the clay (compare sample reference numbers 1 and 2). Samples containing flame retardant in the core or sheath (reference numbers 3 and 4 respectively) exposed to ultrasound have significantly reduced times to burn and numbers of drops relative to the clay-containing samples, although the total times to burning, burning length and mass loss are similar to these latter. When the clay and flame retardant are present individually, either in the sheath or the core (reference numbers 5 and 6 respectively), their burning properties are little changed from those of the Al-Phos-containing-only samples, although the number of drops formed has significantly reduced further. The effect of clay on melt viscosity of one component plus that of the flame retardant on the other are significant factors here. Finally, the presence of both nanoclay and flame retardant together in either the sheath or core (reference numbers 7 and 8 respectively) gives fabrics having reduced area densities, show further reduced total times to burn although burning lengths and flame spread lengths are greater than these might suggest. While mass losses of samples are the lowest of all samples tested, the numbers of drops formed have started to increase relative to the previous samples.

Addition of clay or flame retardant followed by application of ultrasound in either the core or sheath (Table 7.7) show minimally different effects on burning behaviour when compared with similar samples not exposed to ultrasound (Table 7.6). Addition of flame retardant and ultrasound exposure decreased the number of drops, however, compared to the same set of samples without exposed to ultrasound. Thus in summary, according to these two sets of results, the PA6-C / PA6/25A(2 wt %)/Al-Phos (10 wt %)/90W-S sample

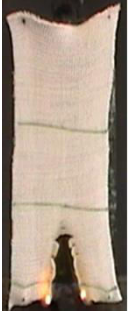
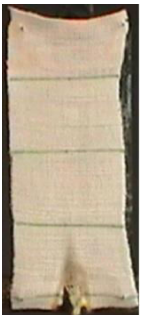



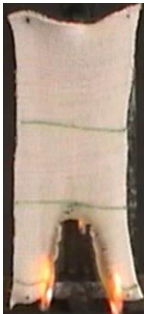
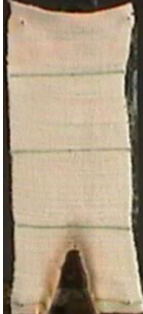





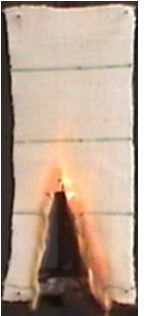



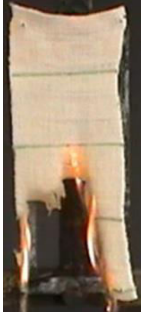



(reference 7) is superior to all others in terms of their reduced flammable properties, defined as minimal burn time, although its values of burn length, flame spread rate and number of drops are not the lowest values. In conclusion, it might be stated that the increased level of nanoclay and flame retardant dispersion achieved by used ultrasound appears to have a minimal effect on the overall fabric burning behavior with a tendency towards reducing times to burn and number of drops when clay only is present and reducing the number of drops when flame retardant only is present.



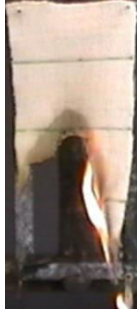











Table 7.6: Flame spread results of bicomponent fabrics without exposure to ultrasound.

Sample (Core / Sheath)	Dimension		Initial mass of sample G	Area density gm ⁻²	Total time to burn s	Burning length mm	Flame spread mms ⁻¹	Mass loss of the sample G	Sample catch on tin foil G	Mass on frame g	Number of drops
	mm	mm									
PA6- C PA6- S	193	82	10	657 ± 26	44 ± 0	109±33	2 ± 1	2.0 ± 1	1.7 ± 1	7.9 ± 3	76 ± 11
PA6- C PA6/ 25A(2%)- S	201	80	11	682 ±22	76 ± 29	141±43	2 ± 0	5.8 ± 1	4.4 ± 1	5.2 ± 1	137 ± 33
PA6/ 25A(2%)- C PA6- S	201	80	11	700 ± 36	88 ± 28	167 ± 58	2 ± 1	7 ± 2	5.0 ± 2	4.0 ± 3	185 ± 52
PA6- C PA6/ Al-Phos (10%)- S	201	79	9	541 ± 4	45 ± 3	165±13	4 ± 1	5 ± 0.2	3.2 ±0.5	4.0 ± 0.6	63 ± 8
PA6/ Al-Phos (10%)- C PA6- S	205	77	9	580 ± 14	51 ± 20	144±24	3 ± 1	2.8 ± 1.2	1.9 ± 1	6.2 ± 1	42 ± 11

Table 7.7: Flame spread results of bicomponent fabricsexposed to ultrasound during compounding.

Ref No	Sample (Core / Sheath)	Dimension		Initial mass of sample	Area density	Total time to burn	Burning length	Flame spread	Mass loss of the sample	Sample catch on tin foil	Mass on frame	Number of drops
		mm	mm	G	gm ⁻²	s	Mm	mms ⁻¹	g	g	g	
1	PA6- C PA6/25A(2%)/90W- S	198	80	11	700 ± 17	68 ± 13	105 ± 21	2 ± 0.2	4 ± 0.9	2 ± 1	7 ± 1	131 ± 34
2	PA6/25A(2%)/90W- C PA6- S	202	77	10	638 ± 25	80 ± 21	161 ± 32	2 ± 0.2	6 ± 1	4 ± 0.4	4 ± 1	127 ± 43
3	PA6- C PA6/Al-Phos (10%)/90W- S	204	78	9	557 ± 9	44 ± 10	140 ± 7	3 ± 1.2	4 ± 0.6	2 ± 0.4	5 ± 0.3	49 ± 8
4	PA6/Al-Phos (10%)/90W- C PA6- S	204	79	11	706 ± 12	55 ± 11	172 ± 26	3 ± 0.4	6 ± 1	3 ± 1	5 ± 1	31 ± 9
5	PA6/25A(2%)/90W- C PA6/Al-Phos (10%)/90W- S	201	79	11	671 ± 41	47 ± 12	166 ± 34	4 ± 0.2	6 ± 2	3 ± 1	5 ± 2	16 ± 4
6	PA6/Al-Phos (10%)/90W- C PA6/25A(2%)/90W- S	202	79	11	704 ± 37	39 ± 6	153 ± 20	4 ± 1	5 ± 1	3 ± 1	6 ± 1	16 ± 2
7	PA6- C PA6/25A(2%)/Al-Phos (10%)/90W- S	197	79	8	524 ± 12	28 ± 6	129 ± 20	5 ± 1	4 ± 1	3 ± 0.3	4 ± 1	22 ± 6
8	PA6/25A(2%)/Al-Phos (10%)/90W- C PA6 – S	198	74	9	650 ± 12	42 ± 8	120 ± 6	3 ± 0.3	3 ± 1	2 ± 1	6 ± 1	67 ± 11

Sample	PA6- C PA6-S	PA6-C PA6/25A(2%)- S	PA6/25A(2%)- C PA6- S	PA6- C PA6/Al-Phos (10%)- S	PA6/Al- Phos(10%)-C PA6-S
0					
10					
20					
30					

40					
50					
60					
70					















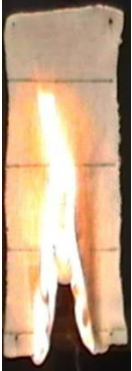
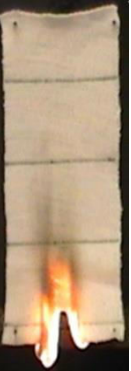


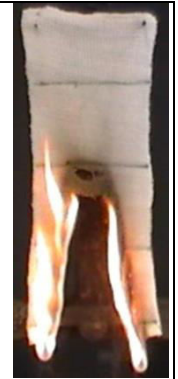
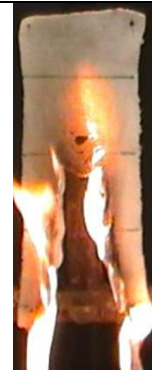
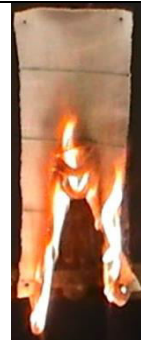
80					
90					

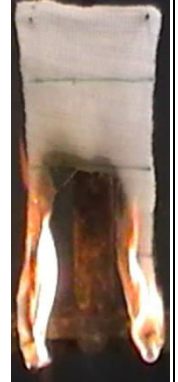
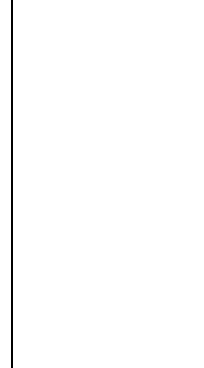
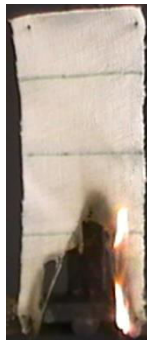
Figure 7.6 : Snap shots of the flame spread experiment to the samples not exposed to ultrasound during compounding.

Sample (Core / Sheath)	PA6-C PA6/25A(2%)/9 0W-S	PA6/25A(2%)/ 90W-C PA6-S	PA6-C PA6/Al- Phos(10%)/90W- S	PA6/Al- Phos(10%)/90 W-C PA6-S	PA6/25A(2%)/9 0W-C PA6/Al- Phos(10%)/90 W-S	PA6/Al- Phos(10%)/90 W-C PA6/25A(2%)/9 0W-S	PA6-C PA6/25A(2%)/A I- Phos(10%)/90 W-S	PA6/25A(2%) /Al- Phos(10%)/9 0W-C PA6-S
0								
10								

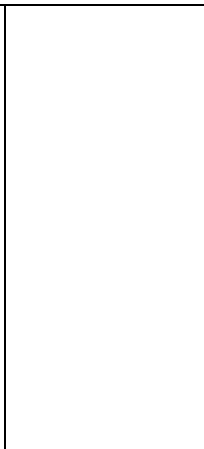
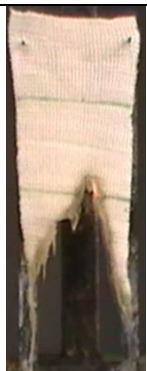
20



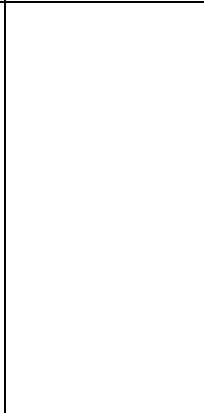
30



40



50



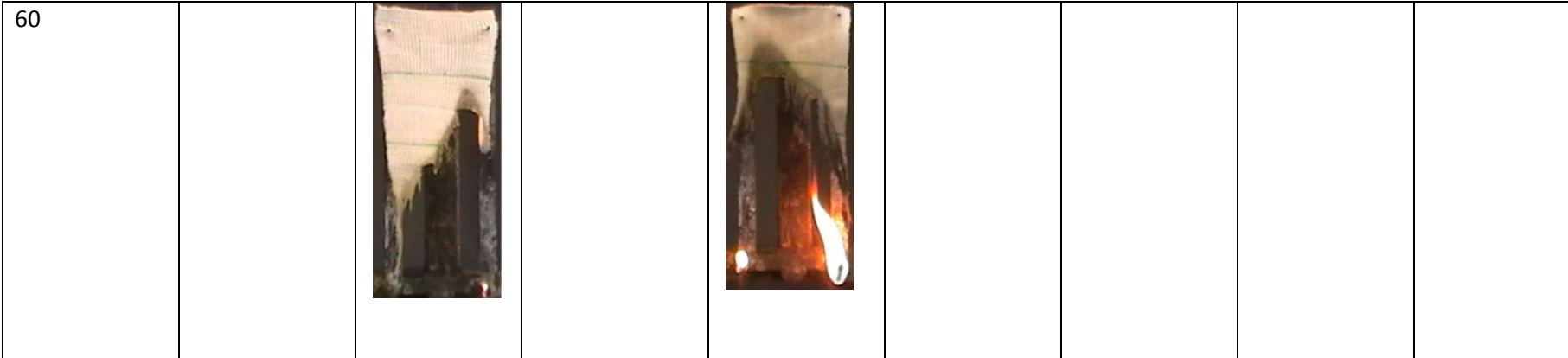


Figure 7.7: Snap shots of the flame spread experiment to the samples after exposure to ultrasound during compounding.

7.5 Conclusions

PA6 bicomponent fibres spun on a Fibre Extrusion Technology (FET) melt spinning extruder unit were produced, knitted into fabrics and their properties investigated. Clear phase separation between core and sheath in the bicomponent fibres supported by optical, SEM and EDS images was observed in the bicomponent filaments produced. The filaments were tensile tested and the presence of a low level of nanoclay or flame retardant in the core or sheath of the fibres slightly reduced the tensile modulus and elongation-at-break values and has not affected the linear density values with respect to a control filament PA6-C/PA6-S yarn. For a second set of samples to improve nanoclay dispersion, ultrasound was applied at the compounding stage at 90W power. The linear density, modulus and tenacity of filament yarns incorporating nanoclay or flame retardant in core or sheath when compounded under ultrasound are not significantly different from those of corresponding samples without ultrasound. However, relative to a C-PA6/PA6-S control filament yarn, elongation-at-break values slightly improved when nanoclay or flame retardant were present in the core and again its increased exposed to ultrasound. When Al-Phos is present in either sheath or core, the modulus, already less than for the control C-PA6/PA6-S filament yarn is further reduced when compounded with ultrasound exposure. When clay is added to the non-flame retardant-containing component, the respective moduli (samples 5 and 6, Table 7.5) are partly restored. However, no further increase is observed when both clay and flame retardant components are together in either sheath or core.

Knitted, washed and dried fabrics were assessed for vertical flame spread, and melting behaviour. It was generally evident that melting and shrinking were reduced when nanoclay and / or flame retardant were introduced, but little effect on the flammable properties was observed. However samples containing flame retardant in the core or sheath exposed to ultrasound showed improved levels of flame retardant properties in terms of reduced burn time, flame spread and number of melt drips. A simplified version of Table 7.7 is presented in Table 7.8 in which the changes in the more significant burning parameters are defined in terms of an increase (↑), decrease (↓) or no change (-) within experimental error for each sample compared with PA6-C/PA6-S behaviour (see Table 7.6).

Table 7.8: Changes in the more important burning parameters of samples in Table 7.7 compared with those of the PA6-C/PA6-S sample in Table 7.6

Ref No	Sample (Core / Sheath)	Total time to burn s	Flame spread mms ⁻¹	Mass loss of the sample g	Number of drops
1	PA6- C PA6/25A(2 wt%)/90W- S	↑	-	↑	↑
2	PA6/25A(2 wt %)/90W- C PA6- S	↑	-	↑	↑
3	PA6- C PA6/Al-Phos (10 wt%)/90W- S	-	↑	↑	↓
4	PA6/Al-Phos (10 wt%)/90W- C PA6- S	↑	↑	↑	↓
5	PA6/25A(2 wt%)/90W- C PA6/Al-Phos (10 wt%)/90W- S	-	↑	↑	↓
6	PA6/Al-Phos (10 wt%)/90W- C PA6/25A(2 wt%)/90W- S	↓	↑	↑	↓
7	PA6- C PA6/25A(2 wt%)/Al-Phos (10 wt%)/ 90W- S	↓	↑	↑	↓
8	PA6/25A(2 wt%)/Al-Phos (10 wt%)/90W- C PA6 – S	-	↑	↑	-

In both cases of the bicomponent samples, when flame retardant is in the sheath, fabrics show reduced flammable properties and the PA6-C/PA6/25A(2 wt%)/Al-Phos (10 wt%)/90W-S sample (reference 7, Table 7.7) is superior to all others in terms of their reduced flammable properties defined as minimal burn time, although its values of burn length, flame spread rate and number of drops are not the lowest values.

Chapter 8: Overall Conclusions

8.1 Ultrasonic exposure of fibre-forming polymers

In this study polypropylene and polyamide 6 were selected with nanoclay and / or flame retardant to test their morphological, mechanical and flammable properties with and without exposure to ultrasound during the compounding stage.

8.1.1 Effects of ultrasound on clay dispersion and properties of polypropylene (Chapter 3)

Initially different levels of ultrasonic power were applied at the compounding stage of the polypropylene to optimise the ultrasonification conditions (see Chapter 3). The PP plus Nanomer 1.3T (PP/1.3T) formulation was used with 100 W and 50 W ultrasonic probes at different intensities between 20 and 100 %. The ultrasonic exposed samples were extruded into filaments and tapes. The tapes were used for morphological studies to optimise ultrasonification conditions. With regard to investigating the influence of ultrasound on clay dispersion, optical and SEM images did not show any specific result apart from spherulitic structures separated by inter-spherulite voids, but EDS images of samples were used to examine silicon elemental and hence clay intensity maps in defined specimen areas. For the PP/1.3T sample, clusters of Si dots were more uniformly distributed when ultrasound was used and decreased in number with increasing amplitude. It was concluded that with increase in ultrasonic power, the larger clay aggregates were being broken down and dispersed into particle sizes having dimensions less than the resolving power of the SEM (~100nm). No clusters were observed when the 100 W ultrasonic probe was used at close to 100% intensity. To quantify the observed results, Datacell software was used to calculate the number of Si dots in the specimens both for separate, defined areas within and for the whole area of the sample. The number of particles within a defined area (average of 12 results) and whole area as a function of ultrasonic power has been plotted as shown in Figure 3.6, but graphs were not conclusive. However, based on the qualitative observations, the 100 W probe at 90% amplitude was selected for the further studies.

Polypropylene with addition of 2 wt% of 1.3T clay and / or 5 wt% of APP was selected for compounding with and without exposure to ultrasound. Polymer pellets were tested for their thermal stability and according to the results (Chapter 3, Section 3.4.2) ultrasonification reduces the thermal stability during the initial stages, but in general, improves it at higher temperatures in terms of increasing residues which comprise both carbonaceous and inorganic contents. The compounded samples were extruded into filaments and tapes and increased ease of extrusion of the ultrasonicated samples suggests that ultrasound helped to improve nanodispersion. The extruded filaments were tested for their tensile properties, but all the tensile properties of PP-clay filaments decreased compared to 100% PP filaments, which except for the elongation-at-break values, are unexpected results. This might be due to the poor dispersion and interface adhesion of nanoparticles in the PP matrix at high filler content. When ultrasound was introduced during compounding, it helps to reduce the size of nanoparticle agglomerates, due to which elongation-at-break improves in most cases. The unexpected results with regard to tenacity and modulus values suggested that the Lab-line extruder was not suitable for the fine filament production. LOI values of compounded strands and tapes were not changed with and without application of ultrasound, but burning rates reduced with the presence of clay and / or flame retardant and reduced further more with the application of ultrasound, which indicates that ultrasonification has enhanced dispersion of nanoclay and also the APP particles. However, these results are not enough to indicate real reductions in the flammability of these samples, since industrial tests like the modified UL-94 test, applied in horizontal and vertical orientations produced no improvements in ratings. In the horizontal mode of PP samples burnt completely even samples with clay and / or flame retardant, although the number of drops formed reduced with addition of clay and / or flame retardant and further reduced after samples being exposed to ultrasound. The same trend was obtained for the vertical mode test. In summary it is clear that sonification reduces the number of normalised melting drips, expressed with respect to the initial unit volume of each sample and that this is probably due to better dispersion of the clay and possibly flame retardant. The extruded samples were knitted and tested to a non-standard the vertical flame spread test and according to the results, sonification reduced the rate of burning although with no reduction in number of molten drips and a slight reduction in drip rate.

8.1.2 Effects of ultrasound on the properties of polyamide 6 tapes and filaments (Chapter 4)

Polyamide 6 with 2 wt% nanoclay and / or 5 wt% of diethyl aluminium phosphinate, Al-Phos, flame retardant was used to prepare samples with and without presence of ultrasound (90W) at the compounding stage. The compounded polymer pellets were extruded into tapes using the Lab-line extruder, but samples containing 1.3T clay failed to extrude into filaments due to their reactive nature of the clay and so was replaced by Cloisite 25A nanoclay (see Table 4.1). The samples with Cloisite 25A were successfully extruded into filaments and tapes. The tape samples were used for morphological studies and an SEM study showed the nanoclay dispersion in polyamide 6 is improved compared with that observed in polypropylene. No large aggregates or particle clusters were obtained both with and without exposure to ultrasound. This is because of the polar nature of this polymer and organically modified clays enable better dispersed in this polymer. EDS images showed that Si, P and Al elements are well dispersed and dispersion is enhanced after exposure to ultrasound. Thermal analysis was undertaken and the effects of ultrasonification had little affect on thermal properties. LOI testing was undertaken and the addition of both clays reduced LOI values and ultrasonification further reduced them. Nanoclay layers having dimensions similar to those of the surrounding polymer chains and significant anisotropy modify the polycrystalline morphology through the development of the so-called nanocomposite structure which will increase polymer melt viscosity and reduce the dripping tendency. This in turn prevents energy being removed from the flame zone and so causes the polymer to burn at a lower oxygen concentration and hence LOI decreased.

Addition of flame retardant at the 5 wt% level alone had no positive effect on the LOI even when the 1.3T clay is present. The PA6/25A(2 wt%)/Al-Phos(5 wt%) sample, however, showed a higher LOI value(24.3 vol%) than others and increased further (25.2 vol%) due to the ultrasound. UL-94 testing was carried out on horizontal and vertical orientations of the strands and yielded “fails” generally. The PA6/1.3T(2 wt%) sample with and without presence of flame retardant showed increases in rate of burning, which increases further after sonification. However, the PA6/25A(2 wt%)/Al-Phos(5 wt%)/90W sample showed a both reduced rate of flame spread and number of flaming drips in both horizontal and vertical modes.

The modified BS 5438 vertical flame spread test was used to assess burning fabric behaviour and the rate of flame spread increased and number of drops reduced for the PA6/25A(2 wt%) sample with and without presence of ultrasound (see Section 4.4.5) compared to a 100% PA6 knitted sample. The PA6/25A(2 wt%)/Al-Phos(5 wt%)/90W sample, however, is superior to the others in reducing the flammable properties, but an increase in level of the Al-Phos flame retardant would be necessary to achieve higher levels of flame retardancy in polyamide 6. To test this suggestion, aluminium phosphinate was added at 10 wt% level followed by 100 W ultrasonification at 90% amplitude for further study. The Lab-line extruder was not able to produce fine filaments, however, and the poor tensile results generally obtained coupled with this observation suggested that the newly acquired Fibre Extrusion Technology (FET) extruder should be used for further work.

8.1.3 Effects of ultrasound on the properties of Polyamide 6 filaments extruded using the FET extruder (Chapter 5)

PA6 with nanoclay (25A at 2 wt%) and / or flame retardant (Al-Phos at 10 wt%) was compounded into pellets with and without presence of ultrasonic power as explained above (90W) and then extruded into filaments and tapes using FET extruder (see Chapter 5). The tape surfaces were characterised for nanoparticle dispersion with the help of SEM and EDS images. Datacell software was used to map silicon-containing aggregates and elemental P and Al for the samples containing Al-Phos flame retardant. The number of Si dots in the PA6/25A(2 wt%) clay-only samples seems to be decreased after exposed of ultrasound and same was observed for P and Al elemental aggregations in the flame retarded samples. PA6 samples also showed some P and Al concentrations due to possible contamination. Filaments were tested for their tensile properties and it was seen that initial modulus slightly reduced changed in the presence of nanoclay or flame retardant with respect to the value of PA6, but increased with the presence of both nanoclay and flame retardant and slightly changed after exposure to ultrasound. Exposure to ultrasound has slightly increased the modulus for all the samples except PA6/Al-Phos(10 wt%)/90W. The elongation-at-break of the samples containing nanoclay with and without exposure of ultrasound fluctuate with respect to the value ($292.0 \pm 23\%$) for 100% PA6, but the presence of Al-Phos (10 wt%) shows a reduction of nearly 50%, although this has increased following exposure to ultrasound. Addition of nanoclay and flame retardant (PA6/Al-Phos(10 wt%)/25A(2 wt%)) decreased the elongation-at-break which slightly

decreased further after exposure to ultrasound. This might be due to the improvement of dispersion which has increased the nanocomposite character reflecting the increase in modulus.

Limiting oxygen index (see Chapter 5, Section 5.3.3) values of tapes were unchanged with and without exposure to ultrasound in the presence of nanoclay alone. Addition of the flame retardant Al-Phos has increased the LOI value to 23.9 vol% which further increased to 24.6 vol% after exposure to ultrasound. Also, the burning rate reduced in the presence of nanoclay and further reduced following exposure to ultrasound. While the PA / clay samples might have been well dispersed prior to ultrasonification, additional ultrasonification would not be expected to change the LOI values. However, that the addition of flame retardant increased the LOI values which further increased following exposure to ultrasound, suggests that the Al-Phos particle dispersion influences its effectiveness. Both clay and flame retardant together increased the sample LOI values which again increased further after exposure to ultrasound. The number of drops per second reduced in presence of clay and / or flame retardant with and without ultrasound and with the latter showing the greatest effect. In the case of PA6/25A(2 wt%)/Al-Phos(10 wt%) the burning rate and number of drops decreased with respect to 100% PA6 and both these values further decreased after the ultrasonification. The samples failed in the horizontal UL94 test result, but PA6/Al-Phos samples showed no burning after ignition flame removal. Presence of nanoclay and flame retardant together helped to reduce burning rate, but the effect of ultrasonification showing mixed results on the burning rate.

To examine the filament burning behaviour, fabrics were subjected to the vertical flame spread test. Area densities of fabrics were assumed to within an acceptable range for testing although values increased with the presence of nanoclay and / or flame retardant. Addition of nanoclay and flame retardant slightly increased the burning rate, but significantly decreased the number of drops per second with respect to 100% PA6 and further reduced in fabrics containing filaments compounded with exposure of ultrasound. According to the above test results, ultrasonification helped to improve the nanocomposite structure and flame retardant dispersion within the PA6 filaments containing nanoclay and flame retardant.

Effects of ultrasound on PA6 degradation of these samples were investigated by a relative viscosity study. An ASTM D 445 Ubbelohde viscometer was used and according to the results, relative viscosity values of unsonicated PA6 samples increase with addition of clay and / or flame retardant and the effect of ultrasound appears to have a marginal effect, suggesting that any accompanying chemical degradation is negligible or absent.

8.2 Effects of nanoparticles on the flame retardancy of the ammonium sulphamate (AS) and dipentaerythritol (DP) flame-retardant system in polyamide 6 (PA6).

PA6 with addition of AS (2.5 wt%)/DP(1 wt%) alone and 2 wt% of clay (clay 25A or 30B or 116 or fumed silica) samples were compounded into pellets and extruded into filaments, and then knitted into fabrics (see Chapter 6). Compounded pellets were examined by thermal analysis by using TGA / DTA. The major weight loss of the PA6 is in the temperature range of 375-485 °C (86% weight loss) and the rate of weight loss slows down at about 485 °C, because most of the material volatilises at this temperature range following random chain scission at the amide bonds. PA6 treated with AS and DP show different mass loss behaviours in the initial stages of degradation, where an additional DTG maximum peak is observed at 314 °C.

Compounded pellets were used for thermal analysis and cast plaques were used for LOI and UL 94 testing. Addition of AS(2.5 wt%)/DP(1 wt%) with PA6 increased LOI by 4.5 vol% for plaques and by 8 vol% for strands when compared with PA6 alone (20.5 vol % for plaques and 21.9 vol% for strands) In the case of plaques, nanoclay additives with PA6/AS(2.5 wt%)/DP(1 wt%) reduced LOI although the reductions were minimal for the addition of the unfunctionalised 116 clay and silica with respect to the PA6/AS(2.5 wt%)/DP(1 wt%) sample. In the case of strands, mixed results were observed. UL 94 testing of plaques in both for horizontal and vertical configurations showed that while in both, pure PA6 burned completely and was not rated, the addition of AS(2.5 wt%)/DP(1 wt%) with and without clay or silica showing an HB rating in the horizontal test and a V-2 rating in the vertical configuration.

Tensile properties of filaments both drawn and cold drawn with 1:2 draw ratio were evaluated separately. For undrawn filaments, addition of AS(2.5 wt%)/DP(1 wt%) showed an increase in modulus relative to the 100% PA6 yarn modulus value and addition of 25A(2 wt%) or 30B(2 wt%) show further increases in the modulus, but it is reduced with the addition of 116(2 wt%) to below that of the PA6/AS(2.5 wt%)/DP (1 wt%) sample.

The tenacity value of 100% PA6 decreased with addition of AS(2.5 wt%)/DP(1 wt%) and remained little changed with the addition of clay. This might be due to the degradation of AS and DP which offsets any potential advantage of the added clay.

After cold drawing, the modulus nearly doubled for 30B(2 wt%) and 116(2 wt%) samples in comparison with the 100% PA6 drawn yarn value. The trends of tenacities were the same as for the undrawn samples and breaking elongations hardly changed. All the undrawn filaments were knitted into fabrics and their flammable properties were characterised. Area densities of the samples were not much changed as a consequence of the presence of additives. Addition of flame retardants (AS+DP) decreased the burning time by about 40 % and number of drops by about 61 % with respect to pure PA6 and these are further reduced with the addition of 25A(2 wt%) organoclay, as well with the addition of 30B(2 wt%) and 116(2 wt%) clays. According to the test results of mass loss, burning time, number of drops and drops rate of the samples and as explained in the Chapter 5, the sample PA6/AS(2.5 wt%)/DP(1 wt%)/25A(2 wt%) is superior to all others in showing reduced flammability.

8.3 Effect of Dispersed Nanoclays and Flame Retardants in Bicomponent fibres (Chapter 6)

PA6 was selected as the polymer with addition of Cloisite 25A(2 wt%) and / or Al-Phos (10 wt%) with and without presence of ultrasound prior to formation of the initial starting pellets. Samples compounded with and without presence of ultrasound used in various locations of the core–sheath bicomponent fibres as explained in the Chapter 6. Uniform polymer distributions were observed from optical images of the cross section of the fibre and additive distribution was studied by using SEM and EDS. There was little evidence of mixing across the cross section of the fibre and mixing of the two components is negligible.

Small amounts of nanoclay or flame retardant in the core or sheath of the fibres slightly reduced the tensile modulus and elongation-at-break and did not affect the filament linear density values with respect to the control PA6-C/PA6-S filament yarn. The linear density, modulus and tenacity of yarns incorporating nanoclay or flame retardant in core or sheath when compounded under ultrasound are not significantly different from those of corresponding samples without ultrasound.

However, relative to a PA6-C/PA6-S control yarn, elongation-at-break values slightly improved when nanoclay or flame retardant were present in the core and again increased on exposure to ultrasound. When Al-Phos is present in either in sheath or core, the modulus, already less than for the control C-PA6/PA6-S yarn, is further reduced when compounded with ultrasound exposure. When clay is added to the non-flame retardant-containing component, the respective moduli (samples 5 and 6, Table 7.5) are partly restored. However, no further increase is observed when both clay and flame retardant components are together in either sheath or core.

Knitted, washed dried fabrics were used in the vertical flame spread test and according to their results, addition of Al-Phos either in core or sheath had little effect on burning time, but increased burn length and speed of flame spread and reduced mass loss and number of drops were observed. These effects might be due to the increase in PA6 viscosity due to the flame retardant. While single component filaments with addition of 2 wt% of clay level, increased burn length, number of drops and total mass loss but had no effect on the speed of flame spread with respect to the PA6, in the case of bicomponent, samples, addition of 2 wt% of nanoclay in to the sheath showed significantly lower values in all burning parameters than when the nanoclay is in the core. This effect might be due to the char forming character of the clay having a greater effect when it is the sheath. In the case of application of ultrasound, addition of nanoclay either in core or sheath have similar effects to their unsonicated analogues. When the clay and flame retardant together are either in the core or sheath, the number of drops were reduced further with respect to the sample containing Al-Phos only. According to the flammability test results the PA6-C / PA6/25A(2 wt%)/Al-Phos(10 wt%)/90W-S sample (reference 7, Table 7.7) is superior to all others in terms of their reduced flammable properties. This suggests that when the flame retardant and clay are present together in the sheath, there is greater flame retardancy than when in the core.

8.4 Suggestions for Future Work

The success of this series of studies detailed in this thesis addresses the aims stated and shows that improved flame retardancy of polypropylene and polyamide 6 may be achieved by combining a number of flame retardants and different nanoclays and that improved nanoclay dispersion obtained by used ultrasonic exposure during compounding may have a positive effect although some results are inconclusive. There are a number of additional issues and possibilities for further work which arise as a result of the study. These are outlined below

1. While ultrasonification has improved dispersion, comparisons with the effect on dispersion of selected nanoclays, in terms of other processing parameters such as shear rates, need to be examined in order to ascertain conditions for achieving successful exfoliation within each respective polymer matrix.
2. Visual examination in conjunction with microscopy techniques, as discussed in the Chapters 4 and 5 for PA6 samples, suggest the presence of a true nanocomposite structure within specific extruded films. Therefore, in-depth studies using x-ray diffraction (XRD) and transmission electron microscopy (TEM) require investigation in order to validate these findings.
3. PA6 with the combined flame retardant AS+DP present at low concentrations showed minimal levels of degradation and these filaments were extruded without drawing. While the addition of nanoclays slightly reduced the flame retardancy, tensile properties improved. The PA6/AS(2.5 wt%)/DP(1 wt%)/25A(2 wt%) sample in particular showed the best flame retardancy and this system is worthy of further investigation.
4. The bicomponent study suggests that the addition of flame retardant in the sheath showing improved level of flammability than when in the core. This observation should be confirmed and extended to other flame retardants so that a possible mechanistic model may be proposed.

References

1. Wei M, Murphy D, Barry C and Mead J. Halogen-Free flame retardants for wire and cable applications. *Rubber. Chem. Technol.* 2010; 83 : 282-302.
2. Chen X and Jiao C. Flame retardancy and thermal degradation of intumescent flame retardant polypropylene material. *Polym. Adv. Technol.* 2011; 22(6) : 817-821.
3. Zhao C S, Huang F L, Xiong W C and Wang Y Z. A novel halogen-free flame retardant for glass-fibre-reinforced poly(ethylene terephthalate). *Polym . Deg. Stab.* 2008; 93(6) : 1188-1193.
4. Liang S, Neisius N M and Gann S. Recent development in flame retardant polymeric coatings. *Prog. Org. Coat.* 2013; 76(11) : 1642-1665.
5. Sengwa R, Choudhary S and Sankhla S. Dielectric spectroscopy of hydrophilic polymers-montmorillonite clay nanocomposite aqueous colloidal suspension. *Colloids Surf.* 2009; 336(1-3) : 79-87.
6. Sun L, Boo W, Liu J, Clearfield A, Sue H, Verghese N, Pham H and Bicerano J. Effect of nanoplatelets on the rheological behaviour of epoxy monomers. *Mater. Corros.* 2009; 294(2) : 103-113.
7. Fu X and Qutubuddin S. Polymer-clay nanocomposites: exfoliation of organophilic montmorillonite nanolayers in polystyrene. *Polymer.* 2001; 42(2) : 807-813.
8. Litchfield D W and Baird D G. The role of nanoclay in the generation of poly(ethylene terephthalate) fibers with improved modulus and tenacity. *Polymer.* 2008; 49(23) : 5027-5036.
9. Maharsia R and Jerro H. Enhancing tensile strength and toughness in syntactic foams through nanoclay reinforcement. *Polymer.* 2007; 454-455 : 416-422.
10. Nyambo C and Wilkie CA. Layered double hydroxides intercalated with borate anions: Fire and thermal properties in ethylene vinyl acetate copolymer. *Polym. Deg. Stab.* 2009; 94(4) : 506-512.

11. Zhang J G, Jiang D D and Wilkie C A. Fire properties of styrenic polymer – clay nanocomposites based on an oligomerically – modified clay. *Polym. Deg. Stab.* 2006; 91(2) : 358-366.
12. Zhu J, Start P, Mauritz K and Wilkie C. Thermal stability and flame retardancy of poly(methylmethacrylate)-clay nanocomposites. *Polym. Deg. Stab.* 2002; 77(2) : 253-258.
13. Ma H, Zeng J, Realff M, Kumar S and Schiraldi D. Processing, structure, and properties of fibers from polyester / carbon nanofiber composites. *Compos. Sci. Technol.* 2003; 63 : 1617-1628.
14. Carneiro S, Covas J, Bernardo C, Caldeira G, Van Hattum F, Ting J and Alig L. Production and assessment of polypropylene fibres. *Compos. Sci. Technol.* 1998; 58 : 401-407.
15. Hammel E, Tang X, Trampert M, Schmitt T, Mauthner K, Eder A and Potschke P. Carbon nanofibers for composite applications . *Carbon.* 2004; 42 : 1153-1158.
16. Kuriger R J and Alam M K. Extrusion conditions and properties of vapour grown carbon fiber reinforced polypropylene. *Polym. Compos.* 2001; 22(5) : 604-612.
17. Kuriger R J, Alam M K, Anderson D P and Jacobsen R L. Processing and characterisation of aligned vapour grown carbon fibre reinforced polypropylene. *Compos. Part A: Appl. Sci. Manuf.* 2001; 33A : 53-62.
18. Hine P, Broome V and Ward I. The incorporation of carbon nanofibres to enhance the properties of self reinforced, single polymer composites. *Polymer.* 2005; 46 : 10936- 10944.
19. Zeng J, Saltysiak B, Johnson W S, Schiraldi D and Kumar S. Processing and properties of poly (methyl methacrylate) / carbon nanofiber. *Compos. Part B: Eng.* 2004; 35B : 245-249.

20. Lozano K and Barrera E V. Nanofiber-reinforced thermoplastic composites. I. Thermo analytical and mechanical analyses. *J. Appl. Polym. Sci.* 2000; 79 : 125-133.
21. Yang S, Lozano K, Lomeli A, Foltz HD and Jones R. Electromagnetic interference shielding effectiveness of carbon nanofiber / LCP composites. *Compos. Part A: Appl. Sci. Manuf.* 2005; 36A : 691-697.
22. Lozano K, Yang S and Zeng Q. Rheological analysis of vapour-grown carbon nanofiber. *J. Appl. Polym. Sci.* 2004; 93 : 155-162.
23. Lozano K, Bonilla-Rios J and Barrera E V. A study on nanofiber – reinforced thermoplastic composites (III): Investigation of the mixing rheology and conduction properties. *J. Appl. Polym. Sci.* 2001; 80 : 1162-1172.
24. Hegemann D. Plasma polymer deposition and coatings on polymer. *Compos. Eng.* 2014; 201-228.
25. Zhang P Y, Xu Z L, Yang H, Ming Y and Wu W Z. Fabrication and characterisation of PVDF membrane via an in situ free radical polymerisation. *Chem. Eng. Sci.* 2013; 97(28) : 293-308.
26. Quang T N and Baird D G. An improved technique for exfoliating and dispersing nanoclay particles into polymer matrices using super critical carbon dioxide. *Polymer.* 2007; 48 : 6923-6933.
27. Isayev A I, Hong C K and Kim K J. Continuous mixing and compounding of polymer / filler and polymer / polymer mixtures with the aid of ultrasound. *Rubber. Chem. Technol.* 2003; 76 : 923-947.
28. Lin H, Isayev A I. Ultrasonic treatment of polypropylene, polyamide 6, and their blends. *J. Appl. Polym. Sci.* 2006; 102(3) : 2643-2653.
29. Feng W, Isayev A I. In-situ compatibilization of PP / EPDM blends during ultrasound aided extrusion. *Polymer.* 2004; 45 : 1207-1216.

30. Ryu J G, Park S W, Kim H and Lee J W. Power ultrasound for in situ compatibilization of polymer-clay nanocomposites. *Mater. Sci. Eng.* 2004; 24(1-2) : 285-288.
31. Usuki A, Kojima Y, Kawasumi M, Okada A, Fukushima Y, Kurauchi T and Kamigaito O. Mechanical properties of nylon 6-clay hybrid. *J. Mater. Res.* 1993; 8 : 1185-89.
32. Luo H *et al.* Preparation and properties of polyamide 6 thermal conductive composites reinforced with fibers. *Mater. Design.* 2013; 5 : 257-261.
33. Kojima Y, Usuki A, Kawasumi M, Okada A, Kurauchi T and Kamigaito O. One-pot synthesis of nylon 6-clay hybrid. *J. Polym. Sci. Part A: Polym. Chem.* 1993; 31 : 1755-58.
34. Liu L, Qi Z and Zhu X. Studies on nylon 6 / clay nanocomposites by melt-intercalation process. *J. Appl. Polym. Sci.* 1999; 71 : 1133-38.
35. Lan T, Kaviratna D and Pinnavaia T. On the nature of polyimide-clay hybrid composites. *J. Chem. Mater.* 1994; 6(5) : 573-575.
36. Giannelis P. Polymer-layered silicate nanocomposites : Synthesis, properties and applications. *Appl. Organo. Met.Chem.* 1998; 12(10-11) : 675-680.
37. Araujo E M, Araujo K D, Paz R A, Gouveia T R, Barbosa R B and Ito E N. Polyamide 66 / brazilian clay nanocomposites. *J. Nano. Mater.* 2009 : 1-5.
38. Ravikumar B, Suresha B and Venkataramareddy M. Effect of particulate fillers on mechanical and abrasive wear behaviour of polyamide 66 / polypropylene nano composites. *J. Mater. Des.* 2009; 30 : 3852-8.
39. Reisse J *et al.* Quantitative sonochemistry. *Ultrason. Sonochem.* 1996; 3(3) : S147-S151
40. Turner-Jones A, Aizlewood J M and Beckett D R. Crystalline forms of isotactic Polypropylene. *J. Macromol. Chem.* 1964; 75 : 134-158.

41. Capiati N J and Porter R S. Tensile properties of ultra-drawn polyethylene. *J. Polym. Sci. Part B: Polym. Phys.*1975; 13 : 1177-1186.
42. Weeks N E and Porter P S. Mechanical properties of ultra-oriented polyethylene. *Polym. Sci. Part B: Polym. Phys.*1974; 12 : 635-643.
43. Hirschler M. Fire performance of organic polymers, thermal decomposition, and chemical composition, in: Nelson G L and Wilkie C A, Eds. Fire and Polymers: Materials and Solutions for Hazard Prevention. ACS Symposium Series. American Chemical Society, Washington, DC. 2001; 797 : 293-306.
44. Irvine D J, McCluskey J A and Robinson I M. Fire hazards and some common polymers. *J. Polym. Deg. Stabil.* 2000; 67(3) : 383-396.
45. Arvind V. Wallace Carothers: More than the inventor of Nylon and Neoprene. *World Pat. Info.* 2010; 32(4) : 300-305.
46. Horrocks A R. Flame-retardant finishing of textiles. *Rev. Prog. Color.* 1986; 16(1) : 62-101.
47. Wei M, Davis W, Urban B, Song Y, Porbeni E, Wang X, White L, Balik M, Rusa C, Fox J and Tonelli A. Manipulation of Nylon-6 Crystal Structures with Its α -Cyclodextrin Inclusion Complex. *J. Macromol.* 2002; 35(21) : 8039-8044.
48. McKeen L W. The effect of long term thermal exposure on plastics and elastomers, in: McKeen L W, Ed. Polyamides. William Andrew, Applied Science Publisher, USA. 2013 : 117-137.
49. Zhang M, June S M and Long T E. Principles of Step-Growth Polymerization (Poly condensation and Polyaddition). *J. Polym. Sci. Part A: Polym. Chem.* 2012; 5 : 7-47.
50. McMurry A. Fundamentals of Organic Chemistry, in: Solomons T W and Graham V, Eds. Organic Materials. John Wiley and Sons, New York.1996 (6).

51. Smith R L, Fang Z, Inomata H and Arai K. Phase behaviour and reaction of nylon 6 in water at high temperatures and pressures. *J. Appl. Polym. Sci.* 2000; 76(7) : 1062–1073.
52. Mukhopadhyay S. Thermodynamics of processing synthetic fibers. *J. Polym. Eng. Sci.* 1994; 34(4) : 371–376.
53. Hernandez J and Gavara R. Sorption and transport of water in nylon-6 films. *J. Polym. Sci. Part B: Polym. Phys.* 1994; 32(14) : 2367–2374.
54. Cannon C G. Infrared spectra and molecular configurations of polyamides. *Spectrochim. Acta: Part A.* 1960; 16 : 302-319.
55. Wilkie C A and Morgan A B. An introduction to polymeric flame retardancy, its role in materials science, and the current state of the field, in: Wilkie C A and Morgan A B, Eds. Fire retardancy of polymeric materials. CRC press Taylor & Francis Group, USA. 2010 : 1-10.
56. Dennett M F. Source of Ignition and Materials first ignited in: Dennett M F, Ed. Fire Investigation. Elsevier Ltd, USA. 1980 : 5-14.
57. Weil E D and Levchick S V. Flame retardant in Commercial Use or Development for Textile. *J. Fire. Sci.* 2008; 26(3) : 243-281.
58. Handermann A C. Flame resistant barriers for home furnishings. *J. Ind. Text.* 2004; 33(3) : 159-178.
59. Horrocks A R, Kandola B K, Davies P J, Zhang S and Padbury S A. Development in flame retardant textiles – a review. *Polym. Deg. Stab.* 2005; 88 : 3-12.
60. Lewin M. Unsolved problems and un answered questions in flame retardance of polymers. *Polym. Deg. Stab.* 2005; 88(1) : 13-19.
61. Perkins R M, Drake G L and Reeves W A. The effect of laundering variables on the flame retardancy of cotton fabrics. *J. Am. Oil. Chem. Soc.* 1971; 48(7) : 330-333

62. Parikh D V, Sachinvota N D, Sawney A S, Robert K Q, Graves E E and Clamari T A. Flame retardant cotton blend high lofts. *J. Fire. Sci.* 2003; 21 : 383-395.
63. Troitzsch J. International plastics flammability handbook, in: Troitzsch J, Ed. Principles, regulations, testing and approval. Hanser publishers, Munich. 1990(2) : 17, 43, 47.
64. Celebi F, Aras L, Gunduz G and Akhmedov I M. Synthesis and characterization of water-borne and phosphate flame retardant polyurethane coatings. *J. Coat. Tech.* 2003; 75 : 65 - 71.
65. Henry C A. Fire retardants, in: Xanthos M, Ed. Functional fillers for plastics. Wiley-VCH, USA. 2005 : 174, 290-293, 299, 339.
66. Lee T, Green J and Gilbilsco D. Recent developments using phosphorites - containing diol as a reactive combustion modifier for rigid polyurethane foams- Part ii. *J. Fire. Sci.* 1984; 2 : 439 - 453.
67. Jincheng W, Shenglin Y, Guang L and Jianming J. Synthesis of a new-type carbonific and its application in intumescent flame-retardant (IFR) / polyurethane coatings. *J. Fire. Sci.* 2003; 21 : 245-266.
68. Veen I V, Boer J D. Flame retardants: properties, production, environmental occurrence, toxicity and analysis. *Chemosphere.* 2012; 88 (10) : 1119-1153.
69. Gann S, Salimova V, Rupper P, Ritter A and Schmid H. Functional textiles for improved performance, protection and health, in: Pan N and Sun G, Eds. Flameretardant functional textiles. Woodhead, UK. 2011; 98-130.
70. Sain M, Park H and Suhara F. Flame retardant and mechanical properties of natural fibre-PP composites containing magnesium hydroxide. *J. Polym. Deg. Stabl.* 2004; 83(2) : 363-367.
71. Suppakarn N and Jarukumjorn K. Mechanical properties and flammability of sisal / PP composites: effect of flame retardant type and content. *J. Compos. Mater.* 2009; 40(7) : 613–618.

72. Abu Bakar M B, MohdIshak Z A and Mat Taib R B. Flammability and mechanical properties of wood flour filled polypropylene composites. *J. Appl. Polym. Sci.* 2010; 116(5) : 2714–22.
73. Schartel B, Braun U and Schwarz U. Fire retardancy of polypropylene / flax blends. *Polymer.* 2003; 44(20) : 6214–50.
74. Bourbigot S *et.al.* Effect of zinc borate on the thermal degradation of ammonium polyphosphate. *Thermochim.* 2007; 456(2) : 134–44.
75. Wang Y T *et al.* Flame retardant mechanism of an efficient flame-retardant polymeric synergist with ammonium polyphosphate for polypropylene. *Polym. Deg. Stab.* 2013; 10 : 2011-20.
76. Stoddard J W, Pickett O A, Cicero C J. Flame retarded nylon carpets. *Text. Res. J.* 1975; 45(6) : 474–83.
77. Horrocks A R and Zhang S. Char formation in polyamides (Nylons 6 and 6.6) and wool keratin phosphorylated by polyolphosphoryl chlorides. *Text. Res. J.* 2004; 74(5) : 433–41.
78. Wu W and Yang C. Comparison of different reactive organophosphorus flame retardant agents for cotton: Part I. The bonding of the flame retardant agents to cotton. *J. Polym. Sci.* 2006; 91(11) : 2541-2548.
79. Jeng R J, Shau S M, Lin J J, Su W C and Chiu Y S. Flame retardant epoxy polymers based on all phosphorus-containing components. *Eur. Polym. J.* 2002; 38(4) : 683-693.
80. Hui Y and Yang C Q. Durable flame retardant finishing of the nylon / cotton blend fabric using a hydroxyl-functional organophosphorus oligomer. *J. Polym. Deg. Stab.* 2005; 88 (3) : 363–70.
81. Liu J C and Zhau J. Synthesis, application and flame retardancy mechanism of a novel flame retardant containing silicon and caged bicyclic phosphate for polyamide 6. *Polym. Deg. Stab.* 2011; 96(8) : 1508-1515.

82. Weil E D and Levchik S V. Flame retardants for thermoplastic polyesters in commercial use or development. Flame retardants practical applications. 2009; 105-119.
83. Weil E D and Levchik S V. Current Practice and Recent Commercial Developments in flame retardancy of polyamides, in: Weil E D and Levchik S V, Eds. Flame retardants for plastics and textiles. Carl hanser verlag GmbH & Co, 2009 : 85-104.
84. Herwig W, Kleiner H J and Sabel H D. Flame-retarding agents and their use in the preparation of fire-proof thermoplastic polymers. European Patent 0006568, 1980.
85. Braun U and Schartel B. Flame retardancy mechanisms of aluminium phosphinate in combination with melamine cyanurate in glass-fibre Reinforced Poly(1,4-butylene terephthalate). *Macromol. Mater. Eng.* 2008; 293 : 206-217.
86. Doring M and Diederichs J. Non-reactive-fillers: In innovative flame retardants in E&E applications. *Pinfa.* 2009; (2) : 25-26.
87. Bourbigot S, Carpentier F and LeBras M. Mode of action of zinc borates in flame-retardant EVA-metal hydroxide system, in: Al-Malaika S, Golovoy A and Wilkie CA, Eds. Specialty polymer additives. principles and applications. Blackwell Science: UK, 2001; 259-269.
88. Lewin M, Brozek J and Martens M. The system polyamide / sulfamate / dipentaerythritol: flameretardancy and chemical reactions. *J. Polym. Adv. Technol.* 2003; 13(10-12) : 1091-1102.
89. Lewin M, Zhang J, Pearce E and Gilman J. Flammability of polyamide 6 using the sulfamate system and organo-layered silicate. *J. Polym. Adv. Technol.* 2007; 18(9) : 737-745.
90. Lewin M. Flame retarding polymer nanocomposites: Synergism, cooperation, antagonism. *J.Polym.Deg.Stab.* 2011; 96:256-269.
91. Levchik S V, Weil E D, Lewin M. Thermal decomposition of aliphatic nylons. *Polym. Intern.* 1999; 48(7):532-557.

92. Dahiya J B, Kandola B K, Sitpalan A and Horrocks A R. Effects of nanoparticles on the flame retardancy of the ammonium sulphamate-dipentaerythritol flame-retardant system in polyamide 6. *Polym. Adv. Technol.* 2013; 24(4) : 398-406.
93. Hu Y, Tang Y and Song L. Poly (propylene) / clay nanocomposites and their application in flame retardancy. *Polym. Adv. Technol.* 2006; 17(4) : 235-245.
94. Lu H D, Song L and Hu Y A. A review on flame retardant technology. Part II: flame retardant polymeric nanocomposites and coatings. *Polym. Adv. Technol.* 2011; 22(4) : 379-394.
95. Nyambo C, Chen D, Su S P and Wilkie C A. Does organic modification of layered double hydroxides improve the fire performance of PMMA?. *Polym. Deg. Stab.* 2009; 94(8) : 1298-1306.
96. Nyambo C and Wilkie A. Layered double hydroxides intercalated with borate anions: Fire and thermal properties in ethylene vinyl acetate copolymer. *Polym. Deg. Stab.* 2009; 94(4) : 506-512.
97. Costache M C, Heidecker M J, Manias E, Camino G, Frache A, Beyer G, Gupta R K and Wilkie C A. The influence of carbon nanotubes, organically modified montmorillonites and layered double hydroxides on the thermal degradation and fire retardancy of polyethylene, ethylene–vinyl acetate copolymer and polystyrene. *Polymer.* 2007; 48(22) : 6532-6545.
98. Noisong P, Danvirutai C, Srithanratana T and Boonchom B. Synthesis, characterization and non-isothermal decomposition kinetics of manganese hypophosphite monohydrate. *J. Solid State Sci.* 2008; 10(11) : 1598-1604.
99. Sue H J, Gam K T, Bestaoui N, Clearfield A, Miyamoto M and Miyatake N. Fracture behaviour of α -zirconium phosphate-based epoxy nanocomposites. *J. Acta. Mater.* 2004; 52(8) : 2239-2250.

100. Schartel B, Bartholmai M and Knoll U. Some comments on the main fire retardancy mechanisms in polymer nanocomposites. *Polym. Adv. Technol.* 2006; 17(9-10) : 772-777.
101. Chuang T H, Guo W J, Cheng K C, Chen S W, Wang H T and Yen Y Y. Thermal properties and flammability of ethylene-vinyl acetate copolymer / montmorillonite / polyethylene nanocomposites with flame retardants. *J. Polym. Res.* 2004; 11(3) : 169-174.
102. Chiu C W, Huang T K, Wang Y C, Alamani B G and Lin J J. Intercalation strategies in clay/ polymer hybrids. *Prog. Polym. Sci.* 2014; 39(3) : 443-485.
103. Xi Y, Frost R L, He H, Kloprogge T and Bostrom T. Modification of montmorillonite surfaces using a cationic surfactant. *Langmuir.* 2005; 21(19) : 8675–8680.
104. Huchins D A, Rakels J H, Tibbles P M and Mloazewski R. Characterisation of roll – drawn polypropylene using optical diffractometry. *J. Mater. Sci.* 1993; 28(3) : 789-794.
105. Pavlidou S. A review on polymer-layered silicate nanocomposites. *J. Polym. Sci.* 2008; 32 : 1119-1198.
106. Ahmad M B, Hoidy W H, Ibrahim N A and Al-Mulla E A. Modification of montmorillonite by new surfactants. *J. Eng. Appl. Sci.* 2009; 4(3) : 184-188.
107. Chigwada G, Wang D, Jiang D D and Wilkie C A. Styrenic nanocomposites prepared using novel biphenyl-containing modified clay. *Polym. Deg. Stab.* 2006; 91 : 755-762.
108. Ray S S and Okamoto M. Polymer / layered silicate nanocomposites: a review from preparation to processing. *J. Prog. Polym. Sci.* 2003; 28 : 1539-1641.
109. Rafiei B and Ahmadi F G. Preparation and characterisation of the Cloisite Na⁺ modified with cationic surfactants. *J. Cryst. Miner.* 2013; 21(2) : 25-32.

110. Paul D R and Robeson L M. Polymer nanotechnology: Nanocomposites. *Polymer*. 2008; 49 : 3187-3204.
111. Theng B K G. Polymer clay nanocomposites, In: Theng B K G, Ed. Developments in clay science. Elsevier Ltd, USA. 2012; 4 : 201-241.
112. Alexandre M and Dubois P. Polymer-layered silicate nanocomposites: preparation, properties and uses of a new class of materials. *J. Mater. Sci. Eng.* 2000; 28(1-2) : 1-63.
113. Pandey J K, Reddy K R, Kumar A P and Singh R P. An overview on the degradability of polymer nanocomposites. *Polym. Deg. Stab.* 2005; 88(2) : 234-250.
114. Lewin M. Some comments on the modes of action of nanocomposites in the flame retardancy of polymers. *J. Fire Mater.* 2003; 27(1) : 1-7.
115. Lewin M. Reflections on migration of clay and structural changes in nanocomposites. *Polym. Adv. Technol.* 2006; 17(9-10) : 758-763.
116. Ratna D, Becker O, Krishnamurthy R, Simon G P and Varley R J. Nanocomposites based on a combination of epoxy resin, hyper branched epoxy and a layered silicate. *Polymer*. 2003; 44(24) : 7449-7457.
117. Chen C, Khobai M and Curliss D. Epoxy layered-silicate nanocomposites. *J. Prog. Org. Coat.* 2003; 47(3-4) : 376-383.
118. Delozier D M, Orwoll R A, Cahoon J F, Ladislaw J S, Smith J G and Connell J W. Polyamide nanocomposites prepared from high-temperature, reduced charge organoclays. *Polymer*. 2003; 44(8) : 2231-2241.
119. Nah C, Han S, Lee J, Lee M, Lim S and Rhee J. Intercalation behaviour of polyamide / organoclay nanocomposites during thermal imidization. *J. Compos. PartB. Eng.* 2004; 35 : 125-131.

120. Kuila T. Polyolefin - based polymer nanocomposites, in: Fengge G, Ed. *Advances in polymer nanocomposites, types and applications*. Woodhead, UK. 2012; 181-215.
121. Sadiku E. Automotive components composed of polyolefins, in: Ugbolue S, Ed. *Polyolefin fibres*. Woodhead, UK. 2009:81-132.
122. Sephehr M, Utracki L A, Zheng X and Wilkie C A. Polystyrenes with macro-intercalated organoclay. Part II. Rheology and mechanical performance. *Polymer*. 2005; 46 (25) : 11569-581.
123. Houphouet B C, Plummer C J, Wakeman M D and Manson J A. Towards textile-based fiber-reinforced thermoplastic nanocomposites: Melt spun polypropylene-montmorillonite nanocomposite fibres. *J. Polym. Eng. Sci.* 2007; 47(7) : 1122–32.
124. Pavlikova S, Thomann R, Reichert P, Mulhaupt R, Marcincin A and Borsig E. Fiber spinning from poly(propylene)–organoclay nanocomposite. *J. Appl. Polym. Sci.* 2003; 89(3) : 604–611.
125. Giza E, Ito H, Kikutani T and Okui N. Fibre structure formation in high-speed melt spinning of polyamide 6 / clay hybrid nanocomposite. *J. Macromol. Sci. Phys.* 2000; 39 (4) : 545–559.
126. Ibanes C, David L, De Boissieu M, Seguela R, Epicier T and Robert G. Structure and mechanical behaviour of nylon-6 fibers filled with organic and mineral nanoparticles. I. Microstructure of spun and drawn fibres. *J. Polym. Sci: PartB. Polym. Phys.* 2004; 42 (21) : 3876–3892.
127. Lagaly G, Ogawa I and Dekany I. Clay mineral organic interactions, in: Bergaya F, Benny Theng B K G and Lagaly G, Eds. *Handbook of clay science*. Elsevier, USA. 2006; 1
128. Hasegawa N, Kawasumi M, Kato M, Usuki A and Okada A. Preparation and mechanical properties of polypropylene-clay hybrids using a maleic anhydride-modified polypropylene oligomer. *J. Appl. Polym. Sci.* 1998; 67(1) : 87-92.

129. Hasegawa N, Okamoto H, Kawasumi M, Kato M, Tsukigase A and Usuki A. Polyolefin-clay hybrids based on modified polyolefins and organophilic clay. *Macromol. Mater. Eng.* 2000; 280-281(1) : 76-79.
130. Li J, Xhou C, Wang G and Zhao D. Study on rheological behaviour of polypropylene / clay nanocomposites. *J. Appl. Polym. Sci.* 2003; 89 : 3609-3617.
131. Lee J W, Lim Y T and Park O. Thermal characteristics of organoclay and their effects upon the formation of polypropylene / organoclay nanocomposites. *Polym Bull.* 2000; 45(2) : 191-198.
132. Reichert P, Klinke S, Brandsch R, Thomann R and Ihaupt R. Poly(propylene) / organo clay nanocomposite formation: Influence of compatibilizer functionality and organoclay modification. *J. Macromol. Mater. Eng.* 2000; 275(1) : 8-17.
133. Manias E, Touny A, Wu L, Strawhecker K, Lu B and Chung T. Polypropylene / montmorillonite nanocomposites. Review of the synthetic routes and materials properties. *J. Chem. Mater.* 2001; 13(10) : 3516-3523.
134. Ryul J G, Lee P S, Kim H S and Lee J W. Mechanical and thermal behaviour of HDPE based polymer. *Spe. Antec. Techn. Pap.* 2001; 47 : 2135-39.
135. Usuki A, Kato M, Okada A and Kurauchi T. Synthesis of polypropylene-clay hybrid. *J. Appl. Polym. Sci.* 1997; 63 : 137-139.
136. Tang Y, Hu Y, Song L, Zong R, Gui Z, Chen Z and Fan W. Preparation and thermal stability of polypropylene / montmorillonite nanocomposites. *J. Polym. Deg. Stab.* 2003; 82 : 127-131.
137. Lee E C, Mielewski D F and Baird R J. Exfoliation and dispersion of enhancement in polypropylene nanocomposites by in-situ melt phase ultrasonication. *J. Polym. Eng. Sci.* 2004; 44(9) : 1773-1782.
138. Sharma S K and Nayak S K. Surface modified clay / polypropylene nanocomposites: effect on physico-mechanical, thermal and morphological properties. *J. Polym. Deg. Stab.* 2009; 94(1) : 132-138.

139. Shariatpanahi H, Sarabi F, Mirali M, Hemmati M and Mahdavi F. Polypropylene-organoclay nanocomposite: preparation, microstructure, and mechanical properties. *J. Appl. Polym. Sci.* 2009; 113(2) : 922-926.
140. Baniasadi H, Ramazani A S and Nikkhah S J. Investigation of in situ prepared polypropylene / clay nanocomposites properties and comparing to melt blending method. *J. Mater. Res.* 2010; 31(1) : 76–84.
141. Zhang X, Yang M, Zhao Y, Zhang S, Dong X, Liu X, Wang D and Xu D. Polypropylene / montmorillonite composites and their application in hybrid fibre preparation by melt-spinning. *J. Appl. Polym. Sci.* 2004; 92(1) : 552-558.
142. Wenyi W, Xiaofei Z, Guoquan W and Jianfeng C. Preparation and properties of polypropylene filled with organo- montmorillonite nanocomposites. *J. Appl. Polym. Sci.* 2006; 100(4) : 2875-2880.
143. Joshi M, Shaw M and Butola B. Studies on composite filaments from nanoclay reinforced polypropylene. *J. Fibers & Polym.* 2005; 5(1) : 59-67.
144. Horrocks A R, Kandola B K, Smart G, Zhang S and Hull T R. Polypropylene Fibres containing dispersed clays having improved fire performance. I. Effect of nanoclays on processing parameters and fibre properties. *J. Appl. Polym. Sci.* 2007; 106(3) : 1707–1717.
145. Smart G, Kandola B K, Horrocks A R and Nazare S. Polypropylene fibres containing dispersed clays having improved fire performance. Part II: characterization of fibres and fabrics from PP nanoclay blends. *J. Polym. Adv. Technol.* 2008; 19(6) : 658-670.
146. Song R, Wang Z, Meng X, Zhang B and Tang T. Influences of catalysis and dispersion of organically modified montmorillonite on flame retardancy of polypropylene nanocomposites. *J. Appl. Polym. Sci.* 2007; 106(5) : 3488-3494.

147. Marosi G, Marton A, Szep A, Csonto I, Keszei S, Zimonyi E, Toth A, Almeras X and Le- Bras M. Fire retardancy effect of migration in polypropylene nanocomposites induced by modified interlayer. *J. Polym. Deg. Stab.* 2003; 82 : 379–385.
148. Kojima Y, Usuki A, Kawasumi M, Okada A, Kurauchi T and Kamigaito O. Synthesis of nylon 6-clay hybrid by montmorillonite intercalated with ϵ -caprolactam. *J. Polym. Sci., Polym. Chem.* 1993; 34(4) : 983-986
149. Vlasveld D N, Groenewold J, Bersee H N and Picken S J. Moisture absorption in polyamide-6 silicate nanocomposites and its influence on the mechanical properties. *Polymer.* 2005; 46 : 12567–12576.
150. Maiti P and Okamoto M. Crystallization controlled by silicate surfaces in nylon 6-clay nanocomposites. *Macromol. Mater. Eng.* 2003; 288(5) : 440-445.
151. Morgan AB. Flame retarded polymer layered silicate nanocomposites: a review of commercial and open literature systems. *J. Polym. Adv. Technol.* 2006; 17(4) : 206–17.
152. Bourbigot S, Duquesne S and Jama C. Polymer Nanocomposites: How to reach low flammability?. *MacromolSymp.* 2006; 233 (1) : 180-90.
153. Horrocks A R, Kandola B K, Padbury S A. The effect of functional nanoclays in enhancing the fire performance of fibre-forming polymers. *J. Text. Inst.* 2003; 94 : 46-66.
154. Baniassadi M, Laachachi A and Hassouna F *et al.* Mechanical and thermal behaviour of nanoclay based polymer nanocomposites using statistical homogenisation approach. *J. Comp. Tech. Res.* 2011; 71(16) : 1930-1935.
155. Nazare S, Kandola B K and Horrocks A R. Flame-retardant unsaturated polyester resin incorporating nanoclays. *J. Polym. Adv. Tech.* 2006; 17(4) : 294–303.
156. Zanetti M, Camino G, Canavese D, Morgan A B, Lamelas F J and Wilkie C A. Fire retardant halogen-antimony-clay synergism in polypropylene layered silicate nanocomposites. *Chem. Mater.* 2002; 14(1) : 189–93.

157. Dasari A, Yu Z Z, Mai Y W and Liu S. Flame retardancy of highly filled polyamide 6 / clay nanocomposites. *Nanotech.* 2007; 18 : 445602 (1–10).
158. Kashiwagi T, Harris J, Zhang X, Briber R M, Cipriano BH and Raghavan SR, *et al.* Flame retardant mechanism of polyamide 6-clay nanocomposites. *Polymer.* 2004; 45 : 881–91.
159. Qin H, Zhang S, Zhao C, Hu G and Yang M. Flame retardant mechanism of polymer/clay nanocomposites based on polypropylene. *Polymer.* 2005; 46(8) : 8386-95.
160. Schartel B. Considerations regarding specific impacts of the principal fire retardancy mechanism in nanocomposites, In: Morgan A B and Wilkie C A, Eds. Flame retardant polymer nanocomposites. Hoboken New Jersey, USA: Wiley Inter science. 2007 : 107-29.
161. Giannelis P. Polymer layered silicate nanocomposites. *J. Adv. Mater.* 1996; 8(1) : 29-35.
162. Lam C K, Lau K T, Cheung H Y and Ling H Y. Effect of ultrasound sonication in nanoclay clusters of nanoclay / epoxy composites. *Mater. Lett.* 2005; 59(11) : 1369–1372.
163. Lakshminarayanan S, Lin B, Gelves G A and Sundararaj U. Effect of clay surfactant type and clay content on the rheology and morphology of uncured fluoro elastomer /clay nanocomposites prepared by melt-mixing. *J. Appl. Polym. Sci.* 2009; 112(6) : 3597–3604.
164. Wagner N J and Bender J B. The Role of nanoscale forces in colloid dispersion rheology. *MRS Bulletin.* 2004; 29 : 100-106.
165. Akira H, Taura J and Ogawa T. Heat conduction in nano-environment observed in cooling processes of colloidal silver nanoparticles in Water. *Jpn. J. Appl. Phys.* 2000; 39 : 2909-2912.

166. Uchida T, Sato T, Takeuchi S, Kuramochi N and Kawashima N. Basic study on dispersion and surface modification of diamond powders by sonochemical reaction. *Jpn. J. Appl. Phys.* 2003; 42 : 2967-2970.
167. Kawabata K, Sugita N, Yoshikawa H, Azuma T and Umemura A. Nanoparticles with multiple perfluorocarbons for controllable ultrasonically induced phase shifting. *Jpn. J. Appl. Phys.* 2005; 44 : 4548-4552.
168. Lorimer J P and Mason T J. Sonochemistry Part 1-The physical aspects. *Chem. Soc. Rev.* 1987; 16 : 239-274.
169. Kornet L, Hoeks A P, Janssen B J, Willigers J M and Reneman R S. Carotid diameter variations as a non-invasive tool to examine cardiac baroreceptor sensitivity. *J. Hypertens.* 2002; 20(6) : 1165-1173.
170. Suslick K S. Sonochemistry. *Science.* 1990; 247 : 1439-1445.
171. Ashokkumar M, Lee J, Kentish S and Grieser F. Bubbles in an ultrasonic field: an overview, *Ultrasound. Sonochem.* 2007; 14 : 470-475.
172. Kuijpers M, Kemmere M and Keurentjes J. Calorimetric study of the energy efficiency for ultrasound-induced radical formation. *Ultrasonics.* 2002; 40(1-8) : 675-678.
173. Loning J M, Horst C, Hoffmann U. Investigations on the energy conversion in sono chemical processes. *Ultrason. Sonochem.* 2002; 9(3) : 169-179.
174. Burnside S D and Giannelis E P. Synthesis and properties of new poly (dimethylsiloxane) nanocomposites. *Chem. Mater.* 1995; 7(9) : 1597-1600.
175. Park S S, Bernet N, Roche S and Hahn HT. Processing of iron oxide-epoxy vinyl ester nanocomposites. *J. Compos. Mater.* 2003; 37(5) : 465-476.
176. West R D and Malhotra V M. Rupture of nanoparticle agglomerates and formulation of Al₂O₃-epoxy nanocomposites using ultrasonic cavitation approach: effects on the structural and mechanical properties. *Poly. Eng. Sci.* 2006; 46(4) : 426-430.

177. Mahfuz H, Uddin M F, Rangari V K, Saha M C, Zainuddin S and Jeelani S. High strain rate response of sandwich composites with nano phased cores. *Appl. Compos. Mater.* 2005; 12(3-4) : 193–211.
178. Xia H and Wang Q. Preparation of conductive polyaniline / nanosilica particle composites through ultrasonic irradiation. *J. Appl. Polym. Sci.* 2003; 87(11) : 1811–1817.
179. Yasmin A, Luo J J and Daniel I M. Processing of expanded graphite reinforced polymer nanocomposites. *Compos. Sci. Tech.* 2006; 66(9) : 1182–1189.
180. Bittmann B, Hauptert F and Schlarb A K. Ultrasonic dispersion of inorganic nanoparticles in epoxy resin. *Ultrason. Sonochem.* 2009; 16(5) : 622–628.
181. Albdiry M T, Yousif B F, Ku H and Lau K T. A critical review on the manufacturing processes in relation to the properties of nanoclay / polymer composite. *J. Compos. Mater.* 2012; 47 : 1093-1115.
182. Erdik E. Organic synthetic reactions, in: Luche J L, Ed. Synthetic organic sonochemistry. Plenum Press, New York. 1998 : 202-208.
183. Cravotto G and Cintas P. Forcing and controlling chemical reactions with ultrasound. *Angew. Chemie. Int. Ed.* 2007; 46(29) : 5476-5478.
184. Price G J. Recent developments in sonochemical polymerization. *Ultrason. Sonochem.* 2003; 10 (4-5) : 277-283.
185. Gedanken A. Using sonochemistry for the fabrication of nanomaterials. *Ultrason. Sono chem.* 2004; 11(2) : 47-55.
186. Suslick K S and Price G. Applications of ultrasound to materials chemistry. *Annu. Rev. Mater. Sci.* 1999; (29) : 295-326.
187. Young F R. The acoustic bubble, in: Young F R, Ed. Cavitation. Imperial college press, London. 1999 : 200-215, 316-334.

188. Ibrahim K and Mahmut B. Various aspects of ultrasound assisted emulsion polymerization process. *Ultrason.Sonochem.* 2014; 21(4) : 1592-1599.
189. Price G J, Garland L, Comina J, Davis M, Snell D J and West P J. Investigation of radical intermediates in polymer sonochemistry. *Res. Chem. Intermed.* 2004; 30 : 807-827.
190. Price G J. Applications of high intensity ultrasound in polymer chemistry, in: Vaneldikand R and Hubbard C C, Eds. Chemistry under extreme or non-classical conditions. J. Wiley & Sons, New York. 1996 : 381-416.
191. Tjong S C. Structural and mechanical properties of polymer nanocomposites. *Mater. Sci. Eng. Rev.* 2006; 53(3-4) : 73-197.
192. Chen C and Curliss D. Processing and morphological development of montmorillonite epoxy nanocomposites. *Nanotechnology.* 2003; 14(6) : 643-648.
193. Liu T, Lim K P, Tjiu W C, Pramoda K P and Chen Z K. Preparation and characterization of nylon 11 / organoclay nanocomposites. *Polymer.* 2003; 44(12) : 3529-3535.
194. Zerda A S and Lesser A J. Intercalated clay nanocomposites: morphology, mechanics and fracture behavior. *J. Polym. Sci., Part B: Polym. Phys.* 2001; 39: 1137-1146.
195. Isik I, Yilmazer U and Bayram G. Impact modified epoxy / montmorillonite nanocomposites: synthesis and characterization. *Polymer.* 2003; 44(20) : 6371-6377.
196. Sanchez-Olivares G, Calderas F, Medina-Torres L, Herrera Valencia EE, Rivera-Gonzaga A and Manero O. Extrusion with ultrasound applied on intumescent flame-retardant polypropylene. *Polym. Eng. Sci.* 2013; 53(9) : 2018-2026.
197. Swain S K and Isayev A I. Effect of ultrasound on HDPE/clay nanocomposites: Rheology, structure and properties. *Polymer.* 2007; 48(1) : 281-289.

198. Lashin S, Swain S K and Isayev A I. Ultrasound aided extrusion for preparation of polyolefine clay nanocomposites. *Polym. Eng. Sci.* 2008; 48 : 1584-91.
199. Swain S K and Isayev A I. PA6 / clay nanocomposites by continuous sonification process. *J. Appl. Polym. Sci.* 2009; 114 : 2378-87.
200. Choi Y B and Kim S Y. Effects of interface on the dynamic mechanical properties of PET/ nylon 6 bicomponent fibers. *J. Appl. Polym. Sci.* 1999; 74(8) : 2083–2093.
201. Anantharamaiah N, Verenich S and Pourdeyhimi B. Durable Nonwoven Fabrics via Fracturing Bicomponent Islands-in-the-Sea Filaments. *J. Eng. Fibers.* 2008; 3(3) : 1–9.
202. Huang Z M, Zhang Y Z, Kotaki M and Ramakrishna S. A review on polymer nanofibers by electrospinning and their applications in nanocomposites. *Compos. Sci. Tech.* 2003; 63(15) : 2223–53.
203. Kikutani I, Radhakrishnan J, Arikawa S, Takaku A, Okui N, Jin N, Niwa F and Kudo Y. High-speed melt spinning of bicomponent fibers: mechanism of fiber structure development in poly (ethyleneterephthalate) / propylene system. *J. Appl. Pol. Sci.* 1996; 62 : 1913-24.
204. Lewin M and Preston J. Handbook of fiber science and technology, in. Marcel D P, Ed. High technology fibers, part A. J. Wiley & Sons, New York. 1985 : 56-102.
205. Morgan D. Bicomponent Fibers: Past, Present and Future. *Int. Mater. Rev.* 1992; 4(4) : 12-18.
206. Lund A, Jonasson C, Haagensen D and Hagstrom B. Piezoelectric polymeric bicomponent fibres produced by melt spinning. *J. Appl. Polym. Sci.* 2012; 126 : 490–500.
207. Perry H L. Polyamide sheath-core filaments with reduced staining by acid dyes and textile articles. US patent 5439364. Sep 5, 1995.
208. Campbell W L. Method for making bicomponent polyester yarns at high spinning rates. US patent 4217321. Aug 12, 1980.

209. Kane L J and Nadkarmi V M. Apparatus for producing Bicomponent filaments. US patent 4270888. June 2, 1981.
210. Kazutomo Ishizawa, Yoshio Sawa. Process for finishing textured knitted fabrics. US patent 3991449. June 09, 1971.
211. Gownder M R. Process of making a bicomponent fibre. US patent 6074590 A. July 28, 1987.
212. Davies S and Crosby D W. New developments in heterofil fibres and their application. *Macromol. Mater. Eng.* 1974; 40(1) : 125-138.
213. Smith C P. Process for preparing composite filamentary articles. US Patent 3316336. Apr 25, 1967.
214. Hansson C. Bicomponent super absorbent fibre. European Patent 2094322 A1. Sep 2, 2009.
215. Adrian R and Cecil R. Piece-dyeable carpet and yarns. Belgium Patent 3415051A. Apr 13, 1966.
216. West K. "Melded Fabrics", Paper presented at second Shirley International seminar, Manchester, 1970.
217. Marcher B. Tailor-made polypropylene and bicomponent fibers for the nonwovens industry. *Tappi J.* 1991; 74(12) : 103-107.
218. Seungun A J, Kwok W K, Molter J O and Tanny S R. Bicomponent binder fibres. European Patent 0366379 A2. May 2, 1990.
219. Sumio Kato. Process for producing electrically conductive synthetic fibers. US.4085182 A. Apr 18, 1978.
220. DR Hull. Synthetic filament having antistatic properties, US.3, 803, 453. April 9, 1974.
221. Lapshin S, Swain S K and Isayev. Ultrasound aided extrusion for preparation of polyolefin-clay nanocomposites. *Polym. Eng. Sci.* 2008; 48(8) : 1584-1591.

222. Bourbigot S, Devaux E, Rochery M, Flambard X. Nanocomposite textiles: new routes for flame retardancy. Proceedings from the 47th International SAMPE Symposium, 2000 May 12-16. 2002; 47 : 1108-1118.
223. J L Way, J R Atkinson and J Nutting. The effect of spherulite size on the fracture morphology of polypropylene. *J. Mater. Sci.* 1974; 9 (2) : 293- 299.
224. BS 2782-1: Method 140A: 1992, ISO 1210:1992, Plastics — Part 1: Thermal properties Method140A: Determination of the burning behaviour of horizontal and vertical specimens in contact with a small-flame ignition source.
225. Kandola B K, Smart G, Horrocks A R, Joseph P, Zhang S, Hull T R, Ebdon J, Hunt B and Cook A. Effect of different compatibilisers on nanoclay dispersion, thermal stability, and burning behaviour of poly propylene-nanoclay blends. *J. Appl. Polym. Sci.* 2008; 108(2) : 816-824.
226. Vijaya R V K, Koltypin Y, Palchik O and Gedanken A. Preparation and characterisation of nickel-polystyrene nanocomposite by ultrasound irradiation. *J. Appl. Polym. Sci.* 2002; 86(1) : 160-165.
227. Anantharamaiah N, Verenich N, and Pourdeyhimi B. Durable Nonwoven Fabrics via Fracturing Bicomponent Islands-in-the-Sea Filaments. *J. Eng. Fibres.* 2008; 3(3) : 1–9.
228. Choi Y B and Kim S Y. Effects of interface on the dynamic mechanical properties of PET/nylon 6 bicomponent fibres. *J. Appl. Polym. Sci.* 1999; 74(8) : 2083–2093.
229. Sun CQ, Zhang D, Liu YB, and Xiao R. Preliminary study on fibre splitting of bicomponent melt blown fibres. *J. Appl. Polym. Sci.* 2004; 93(5) : 2090–2094.